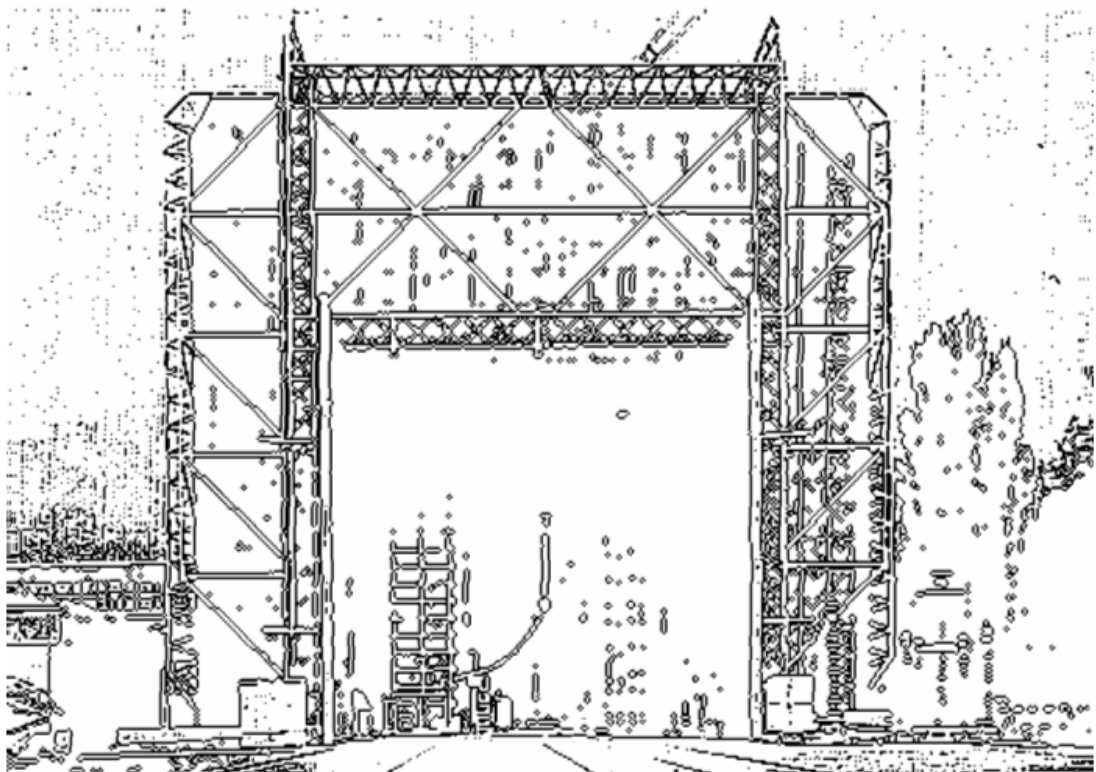


Technische Universität Graz

Diplomarbeit



Diplomarbeit

Insulation Coordination for Upgraded Overhead Lines

Michael HINTEREGGER

Institut für Hochspannungstechnik und Systemmanagement

Technische Universität Graz

Leiter: O. Univ.-Prof. Dipl.-Ing. Dr. Dr. h.c. Michael Muhr



Statnett

Betreuer: Dipl.-Ing. Thomas Judendorfer (TU Graz)

Dr. Sonja Berlijn (Statnett SF)

Begutachter: O. Univ.-Prof. Dipl.-Ing. Dr. Dr. h.c. Michael Muhr

Graz, Juni 2011

Statutory Declaration

I declare that I have authored this thesis independently, that I have not used other than the declared sources / resources, and that I have explicitly marked all material which has been quoted either literally or by content from the used sources.

Graz, _____
Place, Date

Signature

Eidesstattliche Erklärung

Ich erkläre an Eides statt, dass ich die vorliegende Arbeit selbstständig verfasst, andere als die angegebenen Quellen/Hilfsmittel nicht benutzt, und die den benutzten Quellen wörtlich und inhaltlich entnommenen Stellen als solche kenntlich gemacht habe.

Graz, _____
Ort, Datum

Unterschrift

Danksagung

Diese Diplomarbeit entstand aus einer Kooperation zwischen dem Institut für Hochspannungstechnik und Systemmanagement der TU Graz und dem norwegischen Übertragungsnetzbetreiber Statnett SF. Während der Entstehung dieser Diplomarbeit haben mich viele Menschen begleitet, bei denen ich mich auf diesem Wege bedanken möchte.

Mein besonderer Dank gilt dem Institut für Hochspannungstechnik und Systemmanagement, allen voran Herrn O.Univ.Prof. Dipl.-Ing. Dr.techn. Dr.h.c. Michael Muhr für die Ermöglichung einer praxisnahen Ausbildung im Laufe meiner mehrjährigen Tätigkeit am Institut. Weiters danke ich ihm herzlich für die wertvolle Unterstützung, sowie für die Durchsicht und die Begutachtung der Diplomarbeit. Ebenso möchte ich meinem Betreuer seitens des Instituts, Herrn Dipl.-Ing. Thomas Judendorfer, für die laufend engagierte Unterstützung, sowie die kritischen Anregungen und die Durchsicht der Diplomarbeit danken. Gleichermaßen gilt mein Dank meiner Betreuerin seitens Statnett SF, Frau Dr. Sonja Berlijn, für die ausgezeichnete Kooperation, ihre technische Unterstützung während der Diplomarbeit und für ihre Bereitschaft als Diplomprüferin zu fungieren. In diesem Zusammenhang möchte ich auch Herrn Ao. Univ.Prof. Dipl.-Ing. Dr.techn. Stephan Pack für sein Vertrauen und seine Unterstützung danken, die es mir ermöglicht haben, neben meinem Studium wertvolle praktische Erfahrungen in vielerlei Projekten zu sammeln. Diesbezüglich danke ich auch meinen Kollegen vom FM 1, welche dafür gesorgt haben, dass ich meine Tätigkeit am Institut immer in angenehmer Erinnerung behalten werde.

Weiters möchte ich auch den Mitarbeitern der Hochspannungshalle der TU Graz, allen voran Herrn Oberrat Dipl.-Ing. Dr.techn. Werner Lick und Herrn Gerald Muster, für die tatkräftige und hilfsbereite Unterstützung bei der Durchführung der Stoßspannungsversuche danken. Danken möchte ich auch der gesamten Werkstätte des Instituts für Hochspannungstechnik und Systemmanagement, unter der Leitung von Anton Schriebl, für die handwerkliche Unterstützung bei der Errichtung des Versuchsaufbaus.

An dieser Stelle möchte ich auch der Firma Lumpi-Berndorf, allen voran Herrn Norbert Hadinger, für die kostenlose Bereitstellung von Freileitungsseilen für den Versuchsaufbau, herzlich danken.

Ein außerordentliches Dankeschön gilt meiner Freundin Anna für die geduldige, verständnisvolle und tatkräftige Unterstützung bei der Diplomarbeit in jeglicher Hinsicht. Abschließend möchte ich mich bei meiner Familie, insbesondere meinen Eltern herzlich bedanken, die durch ihre Unterstützung und Ermutigungen meine Ausbildung erst ermöglicht haben.

Kurzfassung

Die Methode der Spannungserhöhung an Freileitungen, d.h. die Erhöhung der Betriebsspannung bei einer bestehenden Freileitung, stellt eine effiziente und günstige Möglichkeit zur Steigerung der Übertragungskapazität bzw. zur Erhöhung der Ausfallssicherheit von bestehenden Netzen dar. Vorteilhaft ist dabei einerseits die Nutzung der bestehenden Freileitungsmasten, wodurch der Neubau von selbigen vermieden werden kann. Andererseits führt diese Thematik zu Problemstellungen hinsichtlich Isolationskoordination. Das betrifft vor allem die Dimensionierung der Mindestabstände unter erhöhten Spannungsbedingungen. Norwegens Übertragungsnetzbetreiber Statnett SF plant auf einem größeren Teil des Übertragungsnetzes eine Erhöhung der Betriebsspannung von 300 kV auf 420 kV, indem die bestehenden Glaskappen-Isolatorstränge verlängert werden. Diese Diplomarbeit handelt von der Entwicklung und Konstruktion eines maßstabsgetreuen Modelles des obersten Bereiches eines betroffenen Tragmastens, wie er von Statnett SF unter spannungserhöhten Bedingungen verwendet wird. Mithilfe dieser Nachbildung ist es möglich, jeden beliebigen Ausschwingwinkel bzw. Abstand nachzubilden. Nach dem Entwurf und der Konstruktion des Modelles wurden praktische Stoßspannungsversuche in Form von Blitz- und Schaltstoßspannungstests für verschieden festgelegte Abstände durchgeführt, wobei letztere Tests unter trockenen und berechneten Bedingungen realisiert wurden. Zu diesem Zweck wurde ein spezieller Versuchsplan entwickelt, welcher Ausschwingwinkel und Abstände berücksichtigt, die vor Ort in Norwegen während des Betriebes der Freileitung auftreten können. Nach Beendigung der Stoßspannungsversuche wurden anhand der erhaltenen Ergebnisse die Funkenstreckenfaktoren (im Englischen gap factor genannt) errechnet und daraus resultierend die erforderlichen Mindestabstände unter spannungserhöhten Bedingungen ermittelt. Hauptziel dieser Arbeit ist die Ermittlung der Funkenstreckenfaktoren sowie der erforderlichen Mindestabstände. Abschließend erfolgte ein Vergleich der errechneten Werte mit Werten basierend auf internationalen Normen bzw. einschlägiger Literatur.

Schlüsselwörter: Spannungserhöhung, Freileitung, maßstäbliches Modell, praktische Stoßspannungsversuche, Funkenstreckenfaktor, Mindestabstände

Abstract

The method of upgrading overhead lines, which means an increased operating voltage by use of the existing line, is a fast and economic way to increase capacity and/or to improve the failure reliability of the system. On the one hand the circumstance that the existing towers are used and no new towers need to be constructed is an advantage, on the other hand this topic raises some issues in terms of insulation coordination concerning the exact dimensioning of the required clearances at the upgraded overhead line towers. Statnett SF (Norway's Transmission System Operator), in cooperation with the Institute of High Voltage Engineering and System Management of the Graz University of Technology is planning to upgrade a large part of its 300 kV overhead transmission line network to an operating voltage of 420 kV by lengthen the existing cap-and-pin insulator strings. This diploma thesis contains the development of a practical full-scale model composed of the highest tower section of an affected suspension tower of Statnett SF under upgraded conditions. It enables the simulation of several swing angles and distances. After design and construction of the model, it has been used to carry out lightning and switching impulse voltage tests for several defined distances, whereby the latter tests have been carried out under dry and raining conditions. Therefore a specific testing plan has been developed, which covers distances occurring on-site in Norway while the overhead line is in operation. After completing these impulse voltage tests, the determined results have been used to calculate the gap factors and arising thereof the minimum required distances under upgraded conditions. The main goal of this work is the determination of the gap factors as well as the minimum required distances. Finally, the calculated values have been compared with the values given in the international standards and the literature.

Keywords: voltage upgrading, overhead line, full-scale model, practical impulse voltage tests, gap factor, minimum required distances

Contents

1	Introduction	1
1.1	Background	1
1.2	Motivation	3
1.3	Scope	4
2	Insulation Design	5
2.1	Required gaps	5
2.1.1	Basics	5
2.1.2	Electric strength and characteristic values	5
2.1.3	Standard and calculations	8
2.2	Environmental influence on the gaps	14
2.2.1	Basics	14
2.2.2	Temperature	14
2.2.3	Ice load	14
2.2.4	Wind load	16
2.2.5	Concurrent activity of wind and ice	18
2.3	Swing angle and gap factor	20
2.3.1	Calculation of swing angle	21
2.3.2	Calculation of gap factor	24
2.3.3	Influence of the swing angle on the gap factor	26
3	Insulation coordination	29
3.1	Basics	29
3.2	Insulator	29
3.2.1	Types and materials	29
3.2.2	Types of arcing horns	31
3.3	Insulation level	34
3.3.1	Standard insulation level	34
3.3.2	Influence of different insulator materials	35
3.3.3	Influence of different arcing horns	35

4	Model development	39
4.1	Technical analysis of the affected tower	39
4.1.1	Basics	39
4.1.2	Technical description of the tower	39
4.2	Design of the model	41
4.2.1	Basics	41
4.2.2	Replication of the tower section	41
4.2.3	Dimensions of the model	41
5	Measurements	43
5.1	Basics	43
5.2	Testing setup	44
5.3	Tested insulators and corona rings	45
6	Measurements and calculations	50
6.1	Basics – Lightning impulse voltage Tests	50
6.2	Lightning impulse voltage Tests – Corona ring type 1	53
6.2.1	Lightning impulse voltage – Introduction Test I	56
6.2.2	Lightning impulse voltage – Test 1	59
6.2.3	Lightning impulse voltage – Test 2A	61
6.2.4	Lightning impulse voltage – Test 2B	62
6.2.5	Lightning impulse voltage – Test 2C	64
6.2.6	Lightning impulse voltage – Additional Test 1	65
6.2.7	Lightning impulse voltage – Additional Test 2	68
6.2.8	Lightning impulse voltage – Additional Test 3	70
6.2.9	Discussion of test results	72
6.3	Lightning impulse voltage Tests – Corona ring type 2	73
6.3.1	Lightning impulse voltage – Introduction Test II	75
6.3.2	Lightning impulse voltage – Test 1	77
6.3.3	Lightning impulse voltage – Test 2A	78
6.3.4	Lightning impulse voltage – Test 2B	79
6.3.5	Discussion of test results	81
6.4	Basics – Switching impulse voltage Tests	82
6.5	Switching impulse voltage Tests – Corona ring type 1	84
6.5.1	Switching impulse voltage – Introduction Test I	85
6.5.2	Switching impulse voltage – Test 1	88
6.5.3	Switching impulse voltage – Test 2A	90
6.5.4	Switching impulse voltage – Test 2B	92
6.5.5	Discussion of test results	94
6.6	Switching impulse voltage Tests – Corona ring type 2	95
6.6.1	Switching impulse voltage – Introduction Test II	95
6.6.2	Switching impulse voltage – Test 1	97

6.6.3	Discussion of test results	99
6.7	Switching impulse voltage Tests – Rain Tests	100
6.7.1	Switching impulse voltage – Rain Test 1	101
6.7.2	Switching impulse voltage – Rain Test 2	104
6.7.3	Discussion of test results	106
6.8	Switching impulse voltage Tests – Bare insulator string	107
6.8.1	Switching impulse voltage – Introduction Test I	108
6.8.2	Switching impulse voltage – Test 1	110
6.8.3	Discussion of test results	112
7	Results	113
7.1	Lightning impulse voltage	113
7.2	Switching impulse voltage	117
8	Conclusion	120
8.1	Survey	120
8.2	Summary	121
8.3	Relevance of the work	121
8.4	Outlook	121
9	Appendix	123
	Bibliography	132
	List of Figures	132
	List of Tables	134

Chapter 1

Introduction

1.1 Background

In the last decades a lot of changes concerning the topic of energy have arisen. Especially the rising electricity consumption in Europe as well as worldwide is mentioned particularly, as shown in Figure 1.1 and 1.2 [1][2]. In Europe the rate of growth is at 2 % per year [3]. In Austria it has risen between 1970 and 2001 from 74.4 PJ to 200.6 PJ which is a growth of 270 % [4]. During 2006 and 2007 the increase amounted to 1.2 % [5]. There are a lot of reasons for this progression. The rising standard of living and the technological progress are only two of the reasons for the growing demand of energy [6]. The rising electricity requirements lead to an increased power flow in the electrical lines. Also the renewables influence the energy flux, because they cause power fluctuation as a result of their unpredictable behaviour [6]. That is a matter of special importance, because for example the wind power output in the European Union has risen more than 150 % since 2000 (see also Figure 1.3). Furthermore, one of their general target is the rise of renewables onto 20 % until year 2020 [3][7]. In Europe also the deregulation of the electrical sector and the consequent changes in the generation sector affect the power flow across transmission lines.

In consequence of these considerations some lines are operated close to the ampacity limit, which is the allowed maximum in terms of design, security and safety criteria. A consequence of the excessive conductor temperature is an increased elongation of the conductor which results in a reduction of clearance to ground. Moreover, annealing and high temperature creep of the conductor as well as a decreased suitability of compression joints could be possible. All these effects caused by excessive current flow pose a risk for public safety and must be avoided [6].

Therefore one solution of this problem would be the installation of a new line, which is problematical concerning social obstacles, environmental protection issues and long project durations. For example in Austria the environmental impact assessment of a transmission line with a length of 97.8 km continued about three and a half years. In this context also other aspects that limit the projection of new transmission lines must be mentioned: difficulties with obtaining right-of-way and way-leave, possible effects of electromagnetic fields on human health, visual influences,

ecological impacts and environmental doubts. Certainly, the financial component especially the lack of financial furtherance is an important factor [8][9].

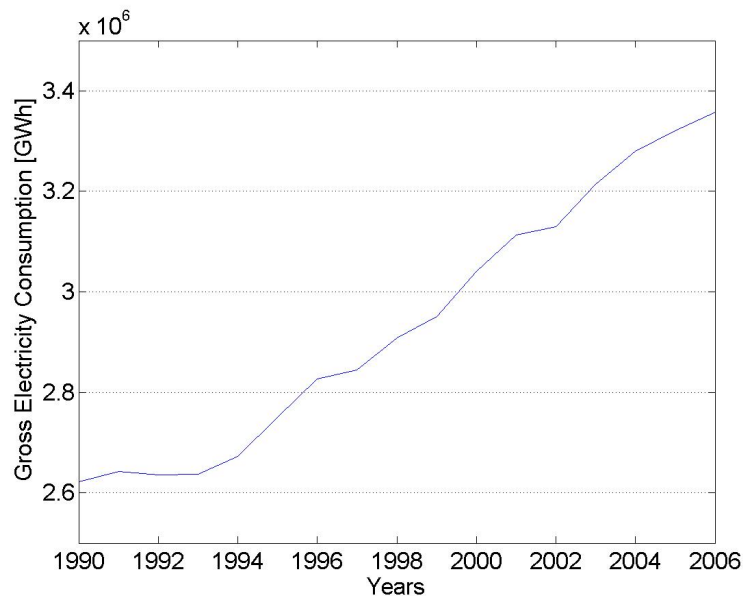


Figure 1.1: Gross Electricity Consumption 1990 – 2006 (adapted from [1])

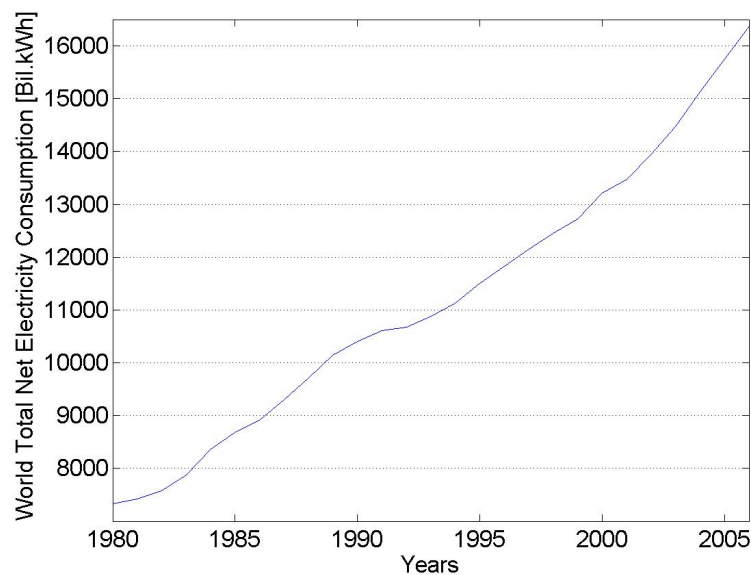


Figure 1.2: World Total Net Electricity Consumption 1980 – 2006 (adapted from [2])

Therefore power supply companies attempt to increase the transmission capacity by upgrading the existing transmission lines. There are several methods for increasing the power rating: increasing the ampacity or increasing the voltage [6][8]. Increasing the ampacity takes place through increasing the number of conductors and/or increasing the conductor section. The increasing of the conductor section causes a decrease of the Joule effect. It is also possible to replace the existing conductors by conductors with a high temperature resistance and low thermal

expansion. Increasing the value of the line voltage leads to a decreased value of current for the same transmitted power [6][10]. Another method of upgrading, which Statnett SF is applying currently in several projects, is called temperature upgrading. Thereby the basic consideration is to increase the maximum rated temperature of the conductor (in practice from 50°C up to 80°C), if that is possible due to the construction of the existing conductors. The occurring value of current for the increased value of the temperature must be calculated. In the next step, the corresponding occurring sag of the conductors and the distances to the surrounding area have to be determined. After that, these values are compared with the required distances in the standards to evaluate if upgrading is permitted or not [11].

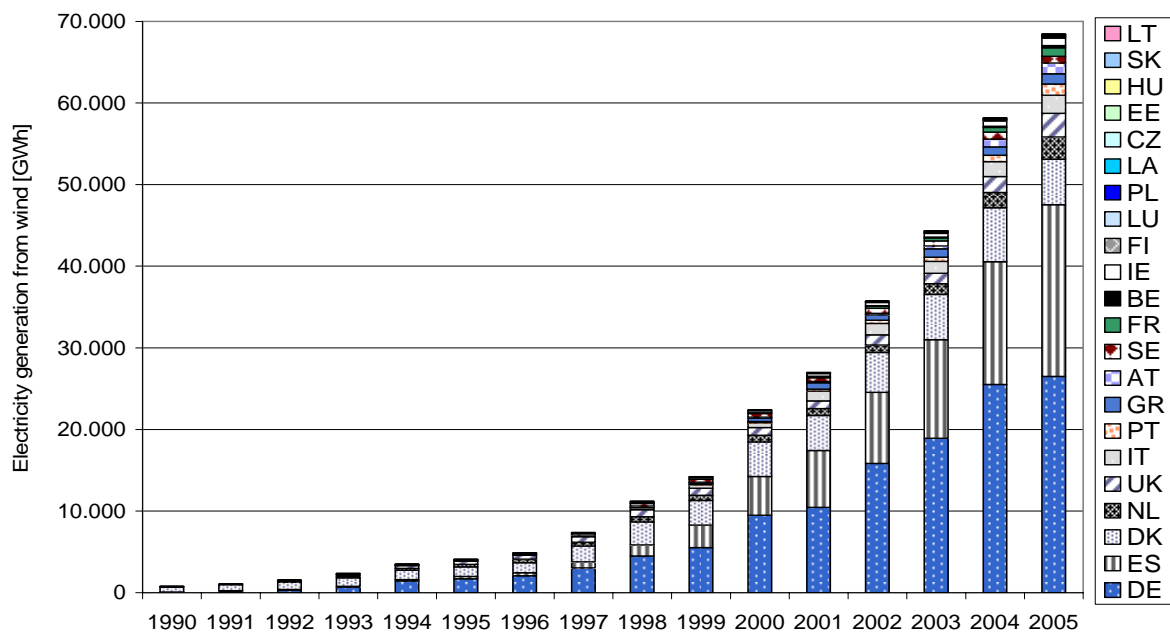


Figure 1.3: Electricity generation from wind 1990 – 2005 [3]

1.2 Motivation

The method of upgrading an existing overhead line involves advantages but also disadvantages. The major advantage is the fact that it is a fast and economic way to increase capacity and/or improve the reliability of the system. This reduction of costs is due to the fact, that the existing towers are used and no new towers need to be constructed. This is of particular importance in areas where it is not environmentally possible or economically feasible to acquire a new right of way. Also the lengthy and cost intensive environmental processes are observable reduced in time and scope [12]. On the other hand, several projects in the last years have shown that upgrading an existing line is not necessarily better regarding to the structural electrical opinion [6]. Especially the observance of the required clearance levels for the uprated structure is often problematic. One possibility to tackle this problem is to use line arresters for controlling overvoltages. The required distances in terms of insulation design and coordination can be reduced in that case. Nevertheless the required clearances for safety operating are given [13]

and must be maintained. Furthermore, this topic raises issues in terms of insulation coordination concerning the exact dimensioning of the required clearances at the upgraded overhead line towers. These distances are influenced by the lengthened insulator string as well as environmental influences. In this context the correct determination of the gap factor which influences the withstand voltages and arising thereby the required distances is of particular interest.

1.3 Scope

Statnett SF (Norway's Transmission System Operator), with the support of the Institute of High Voltage Engineering and System Management of the Graz University of Technology (TU Graz) and the NTNU Trondheim, would like to upgrade approximately 5000 km of its 300 kV overhead transmission line network to an operating voltage of 420 kV by lengthen the existing cap-and-pin insulator strings. This thesis contains the development of a practical full-scale model of the upper tower section of an affected suspension tower of Statnett SF under upgraded conditions, which means an operating voltage of 420 kV. Using this model it is possible to simulate several swing angles and distances. After the design and construction phase, impulse voltage tests including lightning and switching impulse voltage (dry and rain) have been carried out for several defined swing angles and clearances, respectively. For the impulse voltage tests a specific testing plan has been developed. It covers swing angles respectively distances occurring on-site in Norway during operation of the overhead line on the one hand and considers and efficient design and realization of the experiments during the testing procedure on the other hand. The impulse voltage tests took place at the test High Voltage Laboratory of the Institute of High Voltage Engineering and System Management at the Graz University of Technology. After completing the impulse voltage tests, the determined results have been used to calculate the gap factors and arising thereby the minimum required distances under upgraded conditions. The main goal of this work is the determination of the gap factors and the minimum required distances as well as the comparison of the calculated values with the values given in the international standards and the literature.

Chapter 2

Insulation Design

2.1 Required gaps

2.1.1 Basics

For the upgrading of overhead lines by increasing the value of the operating voltage it is necessary to observe the required tower air clearances in order to the higher voltage level. The increased clearance due to the higher voltage rating as they are specified in IEC 60071-Part 1 and 2 and EN 50341-1 must be achieved uncompromisingly. Based on this demand the tower structure is influenced by this higher operating voltages [13]. Due to the increased operating voltage, the use of longer insulators is necessary. As a result of this retrofitting the vertical distances between conductor and ground are reduced. Also the distances between the phases as well as phase and tower construction may not be enough to guarantee the safety. In the case of the reduced vertical gap it is possible to raise the point of connection of the conductor, which perhaps leads to changes in the structure. To better handle the distance between the phases or phase and tower, the use of an I-strut or V-string is a possible solution [6]. Another method is the limitation of switching overvoltages especially when used in conjunction with surge arrester or reducing switching overvoltages by using circuit breakers equipped with pre-insertion resistors [13] [14].

2.1.2 Electric strength and characteristic values

The behaviour of an overhead line under electrical and mechanical stress is an important factor for a reliable and safe electrical grid, especially for the construction and the involved costs but also for the time of failure. Due to this fact the dimensioning of the gaps at the towers has to be considered carefully. That means that the insulation level must constitute a compromise between the electrical behaviour and sustainable costs.

There are three types of voltages that must be taken into account for calculation of the required gaps:

- Fast front overvoltages

- Slow front overvoltages
- Permanent operating frequent voltage

1. Fast front overvoltages:

- lightning strokes hitting a conductor
- overvoltages due of the back-flashover

The calculation of the clearance depends on the distance d_{i5} of the insulation chain and the type of spark gap.

2. Slow front overvoltages:

Slow front overvoltages occur due to switching actions in an electrical grid, which leads to a transient overvoltage. There are two methods for the insulation coordination of slow front overvoltages:

- Deterministic or conventional method:

In this method an established maximum overvoltage U_{max} and a minimum withstand voltage U_w , which is called basic surge insulation level (BSIL) is given. The insulation is dimensioned for the case that the U_w exceed U_{max} considering a collateral security margin. This method is conservative, because it is based on the highest overvoltages and it is unusual, that the insulation strength reaches the minimum rating. Nevertheless, there is a slight probability of coexisting of both occurrences [15].

- Statistical method for calculation of flashover probability:

At this method, a probability of exceeding a certain value of overvoltage instead of a defined overvoltage due to a switching action is described. The overvoltage is described completely by a density or distribution function. The capability (probability of flashover or the probability of failure) is defined as the integrated probability for combining of the two properties (overvoltage and strength of the spark gap) as shown in Figure 2.1.

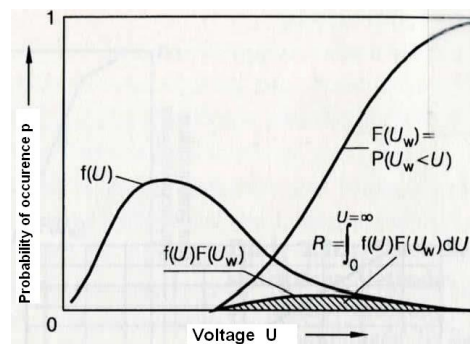


Figure 2.1: Statistical method [15]

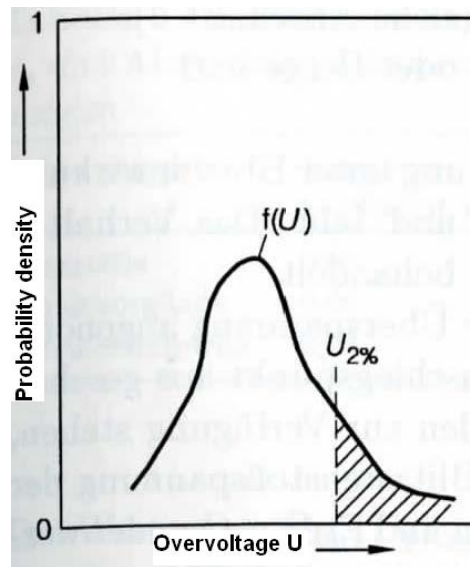


Figure 2.2: Density function of overvoltage [15]

$$U_{50\%real} = U_{50\%} \cdot \left(\frac{\rho'}{H}\right)^n = U_{50\%} \cdot RIS \quad (2.1)$$

- ρ ... relative humidity
- H ... correction factor
- n ... exponent depending on air gap
- $\left(\frac{\rho'}{H}\right)^n$... relative insulation strength (RIS)
- $U_{50\%}$... value of voltage, that withstand in 50 % of cases

If the distribution of overvoltages and strengths is unknown, it is possible to calculate an approximate value of risk by using the simplified statistical method. For this method the real distribution is replaced by a Gaussian distribution which is defined by standard deviation and the statistical overvoltage $U_{2\%}$. $U_{2\%}$ is the overvoltage that exceeded with a probability of 2 % (Figure 2.2). The distribution of withstand voltage is marked by the statistical withstand voltage $U_{W90\%}$, which means a probability of withstand of 90 % and a probability of breakdown of 10 % (Figure 2.3). The distribution of slow front overvoltages and the distribution of withstand voltage need to be brought in relation to get the forced reliability [15].

3. Operating frequent voltage:

In that case the representative permanent operating voltage is equal to the peak value of the highest operating voltage [15].

There are 4 kinds of electrical gaps in air which depend on the possible stresses [15][16]:

- (a) Avoidance of flashovers between outer conductor and objects on earth potential for slow and fast front overvoltage. The minimum air gap, which is necessary, is called

- D_{el} . It can be either an inner distance (distance between conductor and tower) or an outer distance (distance between conductor and surrounding object).
- Avoidance of flashovers between outer conductors for slow and fast front overvoltage. The minimum air gap is called D_{pp} and is an inner distance.
 - Avoidance of flashovers between outer conductor and objects on earth potential during operating frequency voltage. The minimum air gap is called $D_{50Hz_p_e}$ and is an inner distance.
 - Avoidance of flashovers between outer conductors during operating frequency voltage. The minimum air gap is called $D_{50Hz_p_p}$ and is an inner distance.

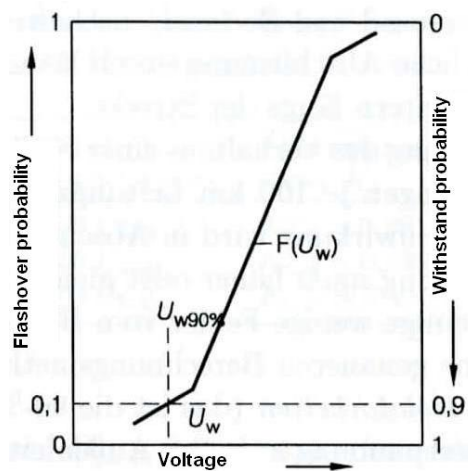


Figure 2.3: Cumulative frequency of impulse withstand voltage [15]

To ensure that flashovers occur to parts of the overhead line and not to obstacles or crossing objects, a minimum distance has to be determined which is larger than the shortest distance between conductor and objects on earth potential [15].

2.1.3 Standard and calculations

The property of an air gap to be able to resist the electric stress resulting of overvoltages can be described by statistical methods. Therefore the required withstand voltage of air gaps can be determined as shown in DIN EN 50341-1. Therein for a given insulation system, altitude and surge in defined form, the probability of a breakdown can be calculated for every voltage value. For assessment of gaps the proper withstand voltage of spark gap must sustain with probability $x\%$. There are three parameters which describe this voltage:

- 50%-withstand voltage of the spark gap ($U_{50\%}$)
- standard deviation σ_u
- number of standard variance N_x (difference between 50 and $x\%$)

$$U_{rw} = U_x = U_{50\%} - N_x \cdot \sigma_u \quad (2.2)$$

In case of transient overvoltages (fast front, slow front) the 90 %-withstand voltage of the air gap will be consulted.

$$U_{rw} = U_{90\%} = U_{50\%} - 1.3 \cdot \sigma_u \quad (2.3)$$

In case of operating frequency the withstand voltage is considered deterministic:

$$U_{rw} = U_{100\%} = U_{50\%} - 3 \cdot \sigma_u \quad (2.4)$$

The withstand voltage can be described by use of the variation coefficient ν_u and variation factor K_z . Table 2.1 shows typical values of ν_u and K_z for different types of stress.

$$U_{rw} = (1 - \nu_u \cdot N) \cdot U_{50\%} = K_z \cdot U_{50\%} \quad (2.5)$$

Table 2.1: Typical values for ν_u and K_z [15][16]

Types of stress	Variance coefficient	Standard deviation	Variation factor
	ν_u	σ_u	K_z
lightning impulse	0.03	$0.03 \cdot U_{50\%}$	$K_{z_ff} = 0.961$
switching impulse	0.06	$0.06 \cdot U_{50\%}$	$K_{z_sf} = 0.922$
operating frequency	0.03	$0.03 \cdot U_{50\%}$	$K_{z_pf} = 0.910$

The withstand voltage $U_{50\%}$ of a spark gap of an arrangement can be described as a function of the 50%-withstand voltage of a rod-plate-arrangement (RP).

$$U_{50\%} = K_g \cdot U_{50\%rp} \quad (2.6)$$

The factor K_g is called the gap factor and depends on the type of stress (see also section 2.3). Using Equation (2.5) in combination with Equation (2.6) it follows [15]:

$$U_{rw} = K_z \cdot K_g \cdot U_{50\%rp} \quad (2.7)$$

The flashover voltage also depends on the altitude above sea level, which is considered in Equation (2.8) by the altitude factor K_a [15].

$$U_{rw} = K_z \cdot K_g \cdot K_a \cdot U_{50\%rp} \quad (2.8)$$

Table 2.2 shows typical values of K_a for different altitudes [15][16][17][18].

Table 2.2: Typical values for K_a depending on the coordination withstand voltage [15][16][17][18]

Altitude [m]	Altitude factor K_a				
	<200 kV	201 - 400 kV	401 - 700 kV	701 - 1100 kV	>1100 kV
0	1.000	1.000	1.000	1.000	1.000
100	0.994	0.995	0.997	0.998	0.999
300	0.982	0.985	0.990	0.993	0.996
500	0.970	0.975	0.982	0.987	0.992
1000	0.938	0.946	0.959	0.970	0.978
1500	0.904	0.915	0.934	0.948	0.960
2000	0.870	0.883	0.906	0.923	0.938
2500	0.834	0.849	0.875	0.896	0.913
3000	0.798	0.815	0.844	0.867	0.885

For the three types of voltage that must be taken into account for the calculation of the electrical gaps the following relations can be applied:

1. Fast front overvoltage:

For standard lightning surge (1.2/50 μs) the calculation of the 50%-withstand voltage of a sparking distance in form of a rod-plane configuration can be described as follows [15][16]:

$$U_{50\%rp_ff} = 530 \cdot d \quad (2.9)$$

$U_{50\%rp_ff}$... peak value of voltage impulse (lightning impulse voltage)
 d ... striking distance in [m]

This equation is applicable for a striking distance of 10 m and impulses with positive polarity.

2. Slow front overvoltage:

Similar to the fast front overvoltage the 50%-withstand voltage in case of standard switching impulse voltage with a front time of 250 μs for a rod-plane configuration up to a striking distance of 25 m can be calculated as follows [15][16]:

$$U_{50\%rp_sf} = 1080 \cdot \ln(0.46 \cdot d + 1) \quad (2.10)$$

$U_{50\%rp_sf}$... peak value of voltage impulse (switching impulse voltage)
 d ... striking distance in [m]

3. Operating frequent voltage:

Similar to the fast and slow front overvoltage the 50%-withstand voltage in case of operating frequent voltage for a rod-plane configuration can be calculated as follows [15][16]:

$$U_{50\%rp_pf} = 750 \cdot \sqrt{2} \cdot \ln(1 + 0.55 \cdot d^{1.2}) \quad (2.11)$$

$U_{50\%rp_pf}$... peak value of voltage
 d ... striking distance in [m]

For the four types of electrical gaps that depend on the electrical stress the following equations can be applied:

1. Minimum air gap D_{el} for the avoidance of flashovers between outer conductor and objects on earth potential during slow and fast front overvoltage, whereby Equation (2.12) is applied for fast front overvoltage and Equation (2.13) for slow front overvoltage [15][16][17][18]:

$$D_{el} = \frac{U_{90\%_ff_is}}{530 \cdot K_a \cdot K_{z_ff} \cdot K_{g_ff}} = \frac{1}{K_a} \cdot \frac{K_{g_ff_is}}{K_{g_ff}} \cdot d_{is} \quad (2.12)$$

D_{el} ... minimum air gap between outer conductor and earth potential
 d_{is} ... distance between the outer part of insulation chain
 K_a ... altitude factor
 K_{g_ff} ... lightning impulse gap factor (expressed by switching impulse gap factor K_g , see also Equation (2.32))
 $K_{g_ff_is}$... lightning impulse gap factor of the insulation chain
 K_{z_ff} ... variation factor of the withstand voltage distribution for the spark gap for fast front overvoltage (see also Table 2.1)
 $U_{90\%_ff_is}$... highest value of the 90%-LI-voltage of the insulation chain

$$D_{el} = \frac{1}{0.46} \cdot \left(e^{\frac{K_{cs} \cdot U_{e2\%_sf}}{1080 \cdot K_a \cdot K_{z_sf} \cdot K_{g_sf}}} - 1 \right) \quad (2.13)$$

D_{el} ... minimum air gap between outer conductor and earth potential
 K_a ... altitude factor
 K_{cs} ... statistical coordination coefficient
 K_{g_sf} ... SI - gap factor, $K_{g_sf} = K_g$ (see also Equation (2.31))
 K_{z_sf} ... variation factor of the withstand voltage distribution for the spark distance for slow front overvoltage (see also Table 2.1)
 $U_{e2\%_sf}$... slow front 2%-overvoltage between outer conductor and earth potential (the overvoltage that is exceeded with a probability of 2 %)

2. The minimum air gap D_{pp} for avoidance of flashovers between outer conductors during slow and fast front overvoltage whereby Equation (2.14) is applied for fast front overvoltage and Equation (2.15) for slow front overvoltage [15][16][17][18]:

$$D_{pp} = \frac{1.2 \cdot U_{90\%_ff_is}}{530 \cdot K_a \cdot K_{z_ff} \cdot K_{g_ff}} \quad (2.14)$$

D_{pp}	...	minimum air gap between outer conductors
K_a	...	altitude factor
K_{g_ff}	...	lightning impulse gap factor (expressed by switching impulse gap factor K_g , see also Equation (2.32))
K_{z_ff}	...	variation factor of the withstand voltage distribution for the spark gap for fast front overvoltage (see also Table 2.1)
$U_{90\%_ff_is}$...	highest value of the 90%-LI-voltage of the insulation chain

$$D_{pp} = \frac{1}{0.46} \left(e^{\frac{1.4 K_{CS} \cdot U_{e2\%_sf}}{1080 \cdot K_a \cdot K_{z_sf} \cdot K_{g_sf}}} - 1 \right) \quad (2.15)$$

D_{pp}	...	minimum air gap between outer conductors
K_a	...	altitude factor
K_{CS}	...	statistical coordination coefficient
K_{g_sf}	...	SI - gap factor , $K_{g_sf} = K_g$ (see also Equation (2.31))
K_{z_sf}	...	variation factor of the withstand voltage distribution for the air distance for slow front overvoltage (see also Table 2.1)
$U_{e2\%_sf}$...	slow front 2%-overvoltage between outer conductor and earth potential (the overvoltage that is exceeded with a probability of 2%)

Table 2.3 and 2.4 show typical values of D_{el} and D_{pp} for slow and fast front overvoltage (altitude 1000 m above sea level) [15]:

Table 2.3: Typical values for D_{el} and D_{pp} for fast front overvoltages [15]

D_{el} and D_{pp} for fast front overvoltages (altitude 1000 m above sea level)		
LI withstand voltage [kV]	D_{el} [m]	D_{pp} [m]
400	0.77	0.85
600	1.14	1.26
800	1.50	1.68
1000	1.88	2.08
1200	2.23	2.50
1400	2.61	2.92
1600	2.98	3.33
1800	3.35	3.75
2000	3.72	4.17
2050	3.82	4.27
2100	3.91	4.38
2150	4.00	4.48

Table 2.5 shows empirical values of D_{el} and D_{pp} for common voltage levels, which are based on an analysis of values used in Europe to guarantee the public safety of people [15][16].

Table 2.4: Typical values for D_{el} and D_{pp} for slow front overvoltages [15]

D_{el} and D_{pp} for slow front overvoltages (altitude 1000 m above sea level)		
SI withstand voltage [kV]	D_{el}[m]	D_{pp}[m]
400	0.88	1.02
600	1.44	1.67
800	2.07	2.45
1000	2.84	3.41
1200	3.71	4.57
1400	4.77	5.97
1600	6.02	7.66
1800	7.50	9.70

Table 2.5: Empirical values of D_{el} and D_{pp} [15][16]

Empirical values of D_{el} and D_{pp}		
Highest operating voltage U_s [kV]	D_{el} [m]	D_{pp} [m]
52	0.60	0.70
72.5	0.70	0.85
82.5	0.75	0.85
100	0.90	1.05
123	1.00	1.15
145	1.20	1.40
170	1.30	1.50
245	1.70	2.00
300	2.10	2.40
420	2.80	3.20
525	3.50	4.00
765	4.90	5.60

3. The minimum air gap $D_{50Hz_p_e}$ for avoidance of flashovers between outer conductor and objects on earth potential during operating frequency voltage [16][17][18]:

$$D_{50Hz_p_e} = \left(\frac{e^{\frac{U_s}{750 \cdot \sqrt{3} \cdot K_a \cdot K_{z_pf} \cdot K_{g_pf}} - 1}}{0.55} \right)^{0.83} \quad (2.16)$$

- $D_{50Hz_p_e}$... minimum air gap between outer conductor and earth potential during permanent operating frequency voltage
- K_a ... altitude factor
- K_{cs} ... statistical coordination coefficient
- K_{g_pf} ... gap factor for operating voltage (see also Equation (2.31))
- K_{z_pf} ... variation factor of the withstand voltage distribution for operating voltage (see also Table 2.1)
- U_s ... highest operating frequent voltage (root mean square in [kV])

4. The minimum air gap $D_{50Hz_p_p}$ for avoidance of flashovers between outer conductors during operating frequency voltage [16][17][18]:

$$D_{50Hz_p_e} = \left(\frac{e^{\frac{U_s}{750 \cdot K_a \cdot K_{z_pf} \cdot K_{g_pf}} - 1}}{0.55} \right)^{0.83} \quad (2.17)$$

- K_a ... altitude factor
 K_{cs} ... statistical coordination coefficient
 K_{g_pf} ... gap factor for operating voltage (see also Equation (2.31))
 K_{z_pf} ... variation factor of the withstand voltage distribution for the air distance operating voltage (see also Table 2.1)
 U_s ... highest operating frequent voltage (root mean square in [kV])

2.2 Environmental influence on the gaps

2.2.1 Basics

Environmental influences, especially lightning strokes, temperature as well as wind and ice load represent the uppermost threat to the performance of overhead lines and lead to faults, failures and voltage drops. Therefore it is necessary to operate the overhead line with focus on continuity of supply to the load as well as the quality of power supply.

2.2.2 Temperature

The vertical distances of the conductors must be dimensioned sufficiently for the highest temperature specification of the conductors [15]. The standard DIN EN 50341-part 1 describes five different situations of temperature influence, which are also depending on other climate influences.

1. lowest temperature (must be mentioned without climate influences)
2. usual ambient temperature for extreme wind speed
3. if applicable a lowest temperature in combination with reduced wind speed
4. temperature that occur with ice accretion
5. temperature (must be mentioned for combination of wind and ice effect)

The decisive temperatures and situations are appointed in the national normative aspects (NNA) [16].

2.2.3 Ice load

There are two different types of ice on conductors corresponding the origin:

1. formation of ice in fact of humidity
2. formation of ice in fog or aqueous air (consequences thereof are soft and hard hoarfrost)

Ice load in form of hoarfrost is unimportant, because it does not lead to essential loads. Formation of ice due to humidity occur in three types:

1. clear ice due to frozen rain
2. approach of dry snow
3. approach of wet snow

In this case the approach of ice depends on the magnitude and duration of precipitation, the wind speed and the temperature. The ice load referring to length that must be chosen for a specific place, called I_K (in N/m), means ice load regarding the different regions of the country, called I_R , which is specified in the NNA or other project specification. For the ice load of conductors it must be distinguished between normal ice load and raised ice load, which must be mentioned when occurring at regular intervals. The national demands are defined in the NNA [15][16]. The ice load of conductors causes vertical forces as well as tensile forces inside the conductors. By the use of the two adjacent spans the ice load of every conductor in one support point can be calculated as [16]:

$$Q_I = I \cdot (L_{W1} + L_{W2}) \quad (2.18)$$

I ... ice load on the conductors referring to length
 L_{W1}, L_{W2} ... parts of the two adjacent weight spans

Ice load model according to IEC 60826 [15]: In this standard the annual maximum values of ice load are described with a Gumbel-distribution. Employing a statistical analysis of existing information of ice load a reference ice load g_{IR} can be calculated, which depends on the construction of the line. For the case of ice approach there are defined 4 requirements for the load of the towers:

1. Similar approach of ice on the conductors:

All conductors and the guard wire are burdened with the reference ice load g_{IR}

2. Dissimilar approach of ice at one of the outer conductors or guard wire:

This case occur in fact of ice drop or disparate growth and leads to a longitudinal load at the support structure. In IEC 60826 the ice load on the conductors is $0.7 \cdot g_{IR}$ and on the outer conductor and guard wire is $0.28 \cdot g_{IR}$.

3. Dissimilar approach of ice at all of the outer conductors in adjacent spans :

In this case the ice load on all conductors in the span on one side of the tower is $0.28 \cdot g_{IR}$ whether on the other side it is $0.7 \cdot g_{IR}$.

4. Dissimilar approach of ice at one of the current circuits:

In this case the ice load on all conductors of one of the current circuit is $0.28 \cdot g_{IR}$ whether on the conductor of the other current circuit it is $0.7 \cdot g_{IR}$.

Specific national ice load models are also defined in the according NNA.

2.2.4 Wind load

There are three requirements that must be mentioned for the electrical gaps concerning the wind [16][17]:

1. No wind
2. wind load with recurrence of 3 years
3. wind load with recurrence of 50 years for gusts of wind, but the probability that a transient overvoltage appears at the same time can be regarded as acceptable small.

The following points must be mentioned when the electrical gaps are considered [18]:

1. The inner distances must be equal or greater than D_{el} and D_{pp} when there is no wind
2. The inner distances for the recurrence of 3 years can be reduced, because there is a minimal probability of concurring of an overvoltage that leads to a flashover. The factor of reducing must be defined by the national committees.
3. The inner distances for the recurrence of 50 years must withstand the highest conductor-earth-voltage for direct grounded neutral point with an earth-failure-factor of 1.3 or smaller. For higher earth-failure-factor, especially in grids with insulated neutral point or earth fault compensation, it is necessary to have a look at the temporary overvoltage.

Wind load model according to IEC 60826 [15]:

This model is based on the wind speed measurement, whereby the 10-minute-averages of the wind speeds, which are measured 10 metres above the ground in open country, are used as reference. The reference dynamic pressure for all types of terrain can be specified as [15]:

$$q_0 = 0.612 \cdot (k_R \cdot V_R)^2 \quad (2.19)$$

q_0 ... reference dynamic pressure

k_R ... depends on type of terrain

V_R ... reference wind speed

Furthermore the wind load on the conductor can be calculated as [15]:

$$Q_{WC} = q_0 \cdot G_L \cdot C_C \cdot G_C \cdot d \cdot a_w \cos^2 \Delta \quad (2.20)$$

Q_{WC}	...	wind load on conductor
q_0	...	reference dynamic pressure (see also Equation (2.19))
G_C	...	combined wind factor (considered height dependence and speed of gusts)
C_C	...	wind resistance coefficient (value=1.0 can be chosen)
G_L	...	span length factor (considered variability of wind pressure due to span length)
Δ	...	angle between wind direction and vertical of the conductor

The wind load on the insulators can be calculated as [15]:

$$Q_{WI} = q_0 \cdot C_{is} \cdot G_{is} \cdot A_{is} \quad (2.21)$$

Q_{WI}	...	wind load on insulator
q_0	...	reference dynamic pressure (see also Equation (2.19))
C_{is}	...	wind resistance coefficient (value=1.2 can be chosen)
G_{is}	...	combined wind factor
A_{is}	...	area which the wind is flowing against

The wind load on towers can be calculated as [15]:

$$Q_{WM} = q_0 \cdot G_M \cdot (1 + 0.2 \cdot \sin^2 2\Omega) \cdot (C_{M1} \cdot A_{M1} \cdot \cos^2 \Omega + C_{M2} \cdot A_{M2} \cdot \sin^2 \Omega) \quad (2.22)$$

Q_{WM}	...	wind load on tower
q_0	...	reference dynamic pressure (see also Equation (2.19))
A_{M1}, A_{M2}	...	area of the tower shape
C_{M1}, C_{M2}	...	wind resistance coefficient
G_M	...	gust factor
Ω	...	angle of wind to axis of crossmember

Wind load model according to European standard DIN EN 50341-1 [15][16]:

With the help of this model it is possible to derive the wind load from the wind speed. Equally to the model in the standard IEC 60826 it is based on the 10-minutes-averages of the wind speeds, which are measured 10 metres above the ground in open country. The dependency on the altitude can be described as follows [15][16]:

$$V_z = k_T \cdot V_R \cdot \ln \left(\frac{z}{z_0} \right) \quad (2.23)$$

k_T	...	coefficient depending on the type of terrain (values are given in [16])
z	...	altitude above the terrain
z_0	...	roughness length (values are given in [16])
V_R	...	reference wind speed of the terrain II in an altitude of 10 m and 10-min-average (values are given in the NNA)

The dynamic pressure (in $[N/m^2]$) of the altitude z can be written as [15][16]:

$$q_z = \frac{1}{2} \cdot \rho \cdot V_z^2 \quad (2.24)$$

ρ ... air density ($=1.225 \text{ kg/m}^3$)
 V_z ... wind speed in $[m/s]$ in altitude z

Furthermore the wind load on the conductor can be calculated as [15][16]:

$$Q_{WC} = q_z \cdot G_q \cdot C_C \cdot G_L \cdot d \cdot a_w \cos^2 \Delta \quad (2.25)$$

q_z ... dynamic pressure (see also Equation (2.24))
 G_q ... gust factor $G_q = [1 + 2.28/(\ln z/z_0)]^2$
 C_C ... wind resistance coefficient (value = 1 can be chosen)
 G_L ... span length factor (values and calculation are given in [16])
 d ... diameter of the conductor
 a_w ... $(L_1 + L_2)/2 \Rightarrow L_1, L_2$... length of the two adjacent spans (average is called wind span length)
 Δ ... angle between wind direction and vertical of the conductor

The wind load on towers can be calculated as [15][16]:

$$Q_{WM} = q_z \cdot G_q \cdot G_x \cdot (1 + 0.2 \cdot \sin^2 2\Omega) \cdot (C_{M1} \cdot A_{M1} \cos^2 \Omega + C_{M2} \cdot A_{M2} \cdot \sin^2 \Omega) \quad (2.26)$$

q_z ... dynamic pressure (see also Equation (2.24))
 G_q ... gust factor $G_q = [1 + 2.28/(\ln z/z_0)]^2$ (see also Equation (2.25))
 G_x ... building reaction coefficient (for buildings lower than 60 m, value=1.05 can be chosen)
 A_{M1}, A_{M2} ... area of the tower shape
 C_{M1}, C_{M2} ... wind resistance coefficient
 Ω ... angle of wind to axis of crossmember

2.2.5 Concurrent activity of wind and ice

The effect of wind on conductors with approach of ice depends on three parameters [15]:

1. Wind speed during the approach of ice
2. Ice weight
3. Shape of approach and appropriate wind resistance coefficient

Statistics concerning the concurrent activity of the both parameters are very often unavailable and also difficult to determine. Therefore variables of observation are combined in such a kind, that the probability of occurrence corresponds with the target recurrence T . Therefore the parameter with low probability, which is denoted with the index L , is combined with a parameter with high probability with the index H . Practically the highest values of a parameter are joined with the averages of the annual maximums to define a loading case. For the wind loads only the values during the presence of ice must be mentioned, but the annual peak values can be neglected. Determination of the parameters [15]:

1. Ice load: If no stats are available the ice load with low probability can be equated with the reference ice load. The average of the annual maximum ice loads can be assumed by the ice load with a recurrence of 50 years multiplied with 0.45. The corresponding temperature is -5°C .
2. Wind load: If stats of the wind speed during approach of ice are available, they can be evaluated statistically [15]. Otherwise the reference wind speed with low probability of occurrence can be derived from the wind speed without approach.

Wind-ice load model according to IEC 60826 [15]: In the standard IEC 60826 only the concurrent activity of wind and ice of conductors is taken into account. Two load cases are treated in the model:

1. Ice with the recurrence T in combination with average of the annual maximum values of wind load on the conductors
2. Ice concerning average of the annual extreme value together with one wind load with approach and recurrence T

Regarding the ice load it is equal to the reference ice load g_{IR} . The ice load with a low probability of occurrence is equal g_{IR} , whereby g_{IR} is the reference ice load from the ice load model in IEC 60826. For ice load with a high probability of occurrence, g_{IR} must be multiplied with 0.4. The corresponding temperature is -5°C . The wind load with a low probability of occurrence is equal $0.6 \dots 0.85 \cdot V_R$, whereby V_R is the reference wind load from the wind load model in IEC 60826. For wind load with a high probability of occurrence, g_{IR} must be multiplied with $0.4 \dots 0.5$ [15]. Model for concurrent activity of wind and ice according to European standard DIN EN 50341-1[16]: There are two main combination mentioned in the standard:

1. Extreme ice load in combination with moderate wind load
2. High wind speed in combination with moderate ice load

Load combination and combination coefficient are given in the NNA. The dynamic pressure is equal to the model of wind load (see also Equation (2.24) [16]).

The equivalent radius D of conductors with approach of ice can be calculated as [16]:

$$D = \sqrt{d^2 + \frac{4 \cdot l}{9.81 \cdot \pi \cdot \rho}} \quad (2.27)$$

d ... diameter of conductor in [m]

l ... ice load in [N/m] corresponding to combination of wind

ρ ... density of ice in [kg/m^3] corresponding to type of ice and wind resistance coefficient

Wind verdures in suspension points due to conductors with approach of ice can be written as [16]:

$$Q_{WC} = q_z \cdot G_q \cdot G_c \cdot C_{cl} \cdot D \cdot a_w \cos^2 \Delta \quad (2.28)$$

- q_z ... dynamic pressure (see also Equation (2.24))
 G_q ... gust factor $G_q = [1 + 2.28/(\ln z/z_0)]^2$ (see also Equation (2.25))
 G_c ... span length factor (values and calculation are given in [16])
 C_{cl} ... wind resistance coefficient (values are given in [16])
 D ... equivalent radius (see also Equation (2.27))
 a_w ... $(L_1 + L_2)/2 \Rightarrow L_1, L_2$... length of the two adjacent spans
 Δ ... angle of wind for critical direction of wind

2.3 Swing angle and gap factor

The swing angle ϕ is defined by the wind load Q_{WC} and the own weight Q_K of the conductor and can be calculated as follows [17]:

$$\phi = \arctan \left(\frac{Q_{WC}}{Q_K} \right) \quad (2.29)$$

Therefore the required wind load Q_{WC} can be written as [17]:

$$Q_{WC} = q_c \cdot G_{XC} \cdot C_{XC} \cdot d \cdot L \quad (2.30)$$

- q_c ... 58 % of dynamic pressure
 G_{XC} ... reaction coefficient of conductor ($G_{XC} = 0.75$... span length < 200 m; $G_{XC} = 0.45 + 60/L$... span length > 200 m)
 C_{XC} ... wind resistance coefficient
 d ... diameter of the conductor in [m]
 L ... wind span length in [m] $\Rightarrow (L_1 + L_2)/2$

For a long time duration and constant wind speed the calculation would not be difficult. The variation of the wind speed effects the behaviour of the swing angle enormously. Peak values of wind speeds do not lead to a statically equivalent swing angle corresponding to the swing angle of the local maximum wind speed. Due to the inertia of the conductors, wind with short duration effects neither the swing angle nor the verdures occurring in the tower. Only winds speed which are averaged over a longer duration lead to a movement in form of swinging. For that purpose it can be shown, that the measured values of swing angle are smaller than the theoretically calculated ones. The time distribution of the swing angle can be described by the Weibull-distribution. The parameters are derived by the wind distribution with a recurrence of two years. Another possibility of calculating the swing angle is to derive it from measured wind speeds. Therefore an often used method is described by measurements in Hornisgrinde in Germany [15].

The gap factor k of an air gap is defined as the ratio between the flashover voltage of the air gap to the positive rod-plane air gap flashover voltage with air gaps of identical spacings and submitted to the same switching impulse. The gap factor is practically independent of the length of the air gap [19]. The different gap factors are expressed by the gap factor for switching impulses for [15]:

- slow front overvoltages:

$$K_{g_sf} = K_g \quad (2.31)$$

- fast front overvoltages:

$$K_{g_ff} = 0.74 + 0.26K_g \quad (2.32)$$

- operating frequent voltages:

$$K_{g_pf} = 1.35 - 0.35K_g^2 \quad (2.33)$$

2.3.1 Calculation of swing angle

The swing angle of an insulator chain can be calculated from the wind speed as follows [15]:

$$\bar{\phi}_I = \tan^{-1} \left[\frac{\left(\frac{\rho}{2}\right) \cdot C_C \cdot V_R^2 \cdot G_L \cdot D \cdot a_W + \left(\frac{F_{WI}}{2}\right)}{W_C + \left(\frac{W_I}{2}\right)} \right] \quad (2.34)$$

- ρ ... air density, depending on temperature and sea level
- V_R ... reference wind speed
- C_C ... wind resistance coefficient (can be chosen with 1.0)
- D ... diameter of the conductor
- G_L ... correction factor of span length
- a_W ... wind span width
- F_{WI} ... wind on the insulator chain
- W_C ... conductor weight corresponding the height difference at the suspension points
- W_I ... weight of the insulator chain

The swing angle of conductor can be calculated from the wind speed as follows [15]:

$$\bar{\phi}_C = \tan^{-1} \left[\frac{\left(\frac{\rho}{2}\right) \cdot C_C \cdot V_R^2 \cdot G_L \cdot D \cdot a}{m_C g \cdot a} \right] \quad (2.35)$$

- ρ ... air density, depending on temperature and sea level
- V_R ... reference wind speed
- C_C ... wind resistance coefficient (can be chosen with 1.0)
- D ... diameter of the conductor
- G_L ... correction factor of span length
- a ... span length
- $m_C g$... linear weight of conductor

The standard deviation of swing angle (in [°]) can be described with following equation [15]:

$$\sigma_{\phi} = 2.25 \cdot \left[1 - e^{(-V_R^2/230)} \right] \quad (2.36)$$

V_R ... reference wind speed

Swing angle and distances in the span middle

The required gaps should be dimensioned in such a way that flashovers for middle wind speeds and overvoltage as well as for highest wind speeds and permanent operating frequent voltage are prevented. For getting the most unfavorable positions of 2 conductors, the swing angle is calculated as follows [15]:

$$\phi_c = \overline{\phi_c} \pm 2 \cdot \sigma_{\phi} \quad (2.37)$$

$\overline{\phi_c}$... average of swing angle of conductor (see also Equation (2.35))

σ_{ϕ} ... standard deviation (see also Equation (2.36))

The minimum distance c (in [m]) of the static conductors in the middle of the span must be [15] [17]:

$$c = k \cdot \sqrt{f_c + l_k} + 0.75 \cdot D_{pp} \quad (2.38)$$

f ... sag of the conductor in [m] for a temperature of 40 °C

l_k ... length of the conductor part (in [m]) which swings rectangular

k ... coefficient (see Table 2.6)

D_{pp} ... minimum air gap between the outer conductors depending on the type of voltage (see also Equation (2.14), Equation (2.15) and Table 2.4, 2.6)

but not less than k . The minimum distance c (in [m]) between the conductor and the guard wire in static case must be [15] [17]:

$$c = k \cdot \sqrt{f_c + l_k} + 0.75 \cdot D_{el} \quad (2.39)$$

f ... sag of the conductor in [m] for a temperature of 40 °C

l_k ... length of the conductor part (in [m]) which swings rectangular

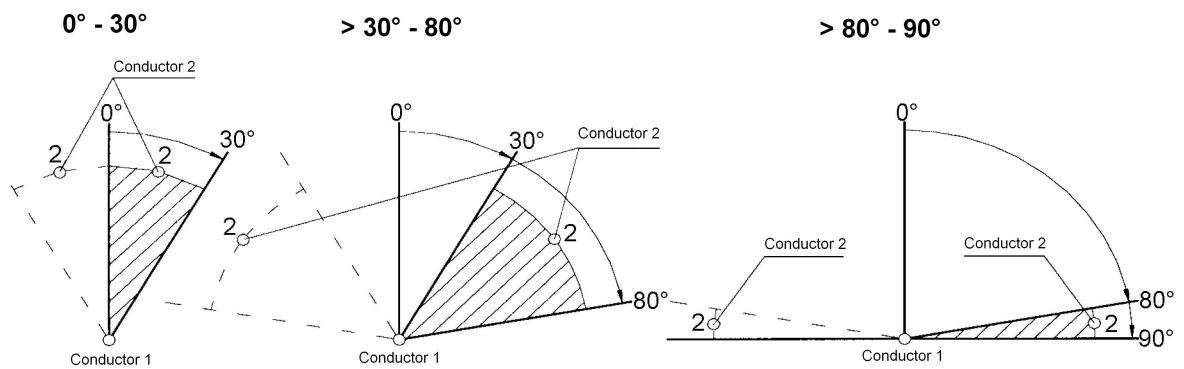
k ... coefficient (see Table 2.6)

D_{el} ... minimum air gap between the outer conductor and earth wire depending on the type of voltage (see also Equation (2.12), Equation (2.13) and Table 2.4, 2.6)

but not less than k . Table 2.6 shows typical values of coefficient k [17]:

Table 2.6: Typical values for coefficient k [17]

Swing angle ϕ in $^\circ$	Factor k		
	$0^\circ - 30^\circ$	$>30^\circ - 80^\circ$	$>80^\circ - 90^\circ$
≥ 65.1	0.95	0.75	0.70
55.1 – 65.0	0.85	0.70	0.65
40.1 – 55.0	0.75	0.65	0.62
≤ 40.0	0.70	0.62	0.60

**Figure 2.4:** Position of conductor 2 to vertical conductor 1 regarding Table 2.6 [17]

The minimum distance D of static conductors in the middle of the span can be calculated, regarding to the Austrian Standard, with [18]

$$D = k \cdot \sqrt{f + l} + Z. \quad (2.40)$$

- f ... sag of the conductor in [m] for the loading case that leads to the biggest value
- l ... length of the insulator chain (in [m])
- k ... coefficient (see Table 2.7)
- Z ... Addition (in [m]) depending on the rated insulation of the line (see also [18])

Table 2.7 shows typical values of coefficient k as they are defined in Austrian standard [18].

Table 2.7: Typical values for coefficient k [18]

Swing angle ϕ in $^\circ$	Factor k		
	$0^\circ - 25^\circ$ ¹	$>25^\circ - 60^\circ$ ²	$>60^\circ - 90^\circ$ ³
≥ 65	0.70	0.75	0.95
55 – 65	0.65	0.70	0.85
40 – 55	0.62	0.65	0.75
≤ 40	0.60	0.62	0.70

¹ Conductors arranged parallel

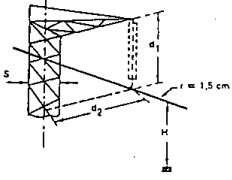
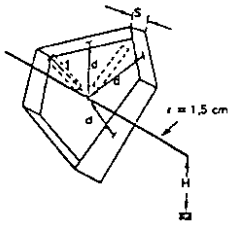
² Conductors arranged slanting

³ Conductors arranged above each other

2.3.2 Calculation of gap factor

Table 2.8 shows equations and values of typical configuration [19][20][21]:

Table 2.8: Equations and value of typical configurations [19][20][21]

Configuration	Figure	Equation	Typical value
conductor-cross arm		$k = 1.45 \cdot 0.015 \left(\frac{H}{d_1} - 6 \right) 0.35 e^{\left(\frac{-8S}{d_1} - 0.2 \right)} \cdot 0.135 \left(\frac{d_2}{d_1} - 1.5 \right)$ <p>Applicable in the range:</p> $d_1 = 2 - 10 \text{ m}$ $d_2/d_1 = 1 - 2$ $S/d_1 = 0.1 - 1$ $H/d_1 = 2 - 10$	1.45
conductor-tower window		$k = 1.25 + 0.005 \left(\frac{H}{d} - 6 \right) 0.25 e^{\left(\frac{-8S}{d} - 0.2 \right)}$ <p>Applicable in the range:</p> $d = 2 - 10 \text{ m}$ $S/d = 0.1 - 1$ $H/d = 2 - 10$	1.25

Continued on next page

Table 2.8 – continued from previous page

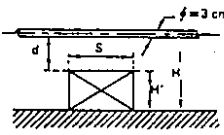
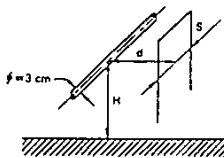
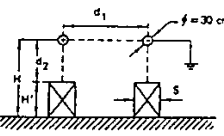
Configuration	Figure	Equation	Typical value
conductor-lower structure		$k = 1.15 \cdot 0.81 \left(\frac{H'}{H}\right)^{1.167} 0.02 \frac{H'}{d} - A[1.209 \left(\frac{H'}{H}\right)^{1.167} \cdot 0.03 \left(\frac{H'}{H}\right)](0.67 - e^{\frac{-2S}{d}})$ <p>where A is 0 if $S/d < 0.2$ and A is 1 if $S/d > 0.2$</p> <p>Applicable in the range: $d = 2 - 10$ m $H'/H = 0 - 1$</p>	1.15 for cond.-plane to 1.5 or more
conductor-lateral structure		$k = 1.45 + 0.024 \left(\frac{H'}{H}\right) - 6 \cdot 0.35 \cdot e^{\left(\frac{-8S}{d} - 0.2\right)}$ <p>Applicable in the range: $d = 2 - 10$ m $S/d = 0.1 - 1$ $H/d = 2 - 10$</p>	1.45
rod-rod-structure (open switchgear)		<p>Horizontal rod-rod-structure: $k_1 = 1.35 - 0.1 \left(\frac{H'}{H}\right) - \left(\frac{d_1}{H} - 0.5\right)$</p> <p>Rod-lower-structure: $k_2 = 1 \cdot 0.6 \left(\frac{H'}{H}\right) - A 1.093 \frac{H'}{H} \left[\left(0.549 - e^{\left(\frac{-3S}{d_2}\right)}\right) \right]$</p> <p>where A is 0 if $S/d_2 < 0.2$ and A is 1 if $S/d_2 > 0.2$</p> <p>Applicable in the range: $(k_1)d_1 = 2 - 10$ m $d_1/H = 0.1 - 0.8$ if $d_1 < d_2$ $(k_2)d_2 = 2 - 10$ m</p>	$k_1 = 1.3k_2 = 1 \cdot 0.6 \left(\frac{H'}{H}\right)$

Table 2.9 shows typical values of K_g for different types of arrangements [15][16][18][21].

The values of gap factor for the insulator string given in the standard [21][16] are ambiguous, because in contrast to the value for the air gap, where the factor for the configuration conductor - tower window can be chosen, for the insulator string two values are possible. On the one hand the value for the configuration conductor - tower window ($K_g = 1.25$) and on the other hand

for the conductor - tower construction ($K_g = 1.45$) can be chosen. In [22] the typical value of the gap factor of insulator string is defined with $K_g = 0.96$ (1.30) and in [23] with $K_g = 1.10$.

Table 2.9: Typical values for K_g [15][16][18][21]

Arrangement	sf-ov ⁴	ff-ov ⁵	of-ov ⁶
	$K_{g_sf} = K_g$	K_{g_ff}	K_{g_pf}
Rod - plate	1.00	1.00	1.00
Outer conductor - obstacle	1.30	1.08	1.16
Conductor - plate	1.15	1.04	1.09
Outer conductor - tower window	1.25	1.07	1.14
Outer conductor - tower construction	1.45	1.12	1.22
Conductor - guy wire	1.40	1.10	1.2
Outer conductor - conductor	1.60	1.16	1.26

⁴ slow front overvoltage

⁵ fast front overvoltage

⁶ operating frequent voltage

2.3.3 Influence of the swing angle on the gap factor

In Figure 2.5 the typical construction of a suspension insulator string assembly including the arcing horns is shown [24].

The gap factor K_s for the assembly in Figure 2.5 in case of switching overvoltage can be described by the following equation [24]:

$$K_s = 1.68 \cdot e^{\left(\frac{-0.34}{d}\right)} \quad (2.41)$$

K_s ... gap factor of the arcing horn

D ... clearance between line side horn and tower [m]

d ... horn gap length [m]

As can be seen from Figure 2.5 the distance D can be expressed as:

$$D = \cos \phi \cdot (d + l_a + x) \quad (2.42)$$

D ... clearance between line side horn and tower [m]

d ... horn gap length [m]

ϕ ... swing angle

l_a ... length of the arcing horn [m]

As can be seen from the circuit in Figure 2.5 the variable x can be calculated according to the following equations:

$$x = l_s - y \quad (2.43)$$

x ... variable
 l_s ... length of the suspension of the arcing horn [m]

$$\tan(\beta) = \tan(90^\circ - \phi) = \frac{w_a}{y} \rightarrow y = \frac{w_a}{\tan(90^\circ - \phi)} \quad (2.44)$$

y ... variable
 β ... angle $\beta = 90^\circ - \phi$
 w_a ... width of the arcing horn [m]

$$x = l_s - \frac{w_a}{\tan(\beta)} = l_s - \frac{w_a}{\tan(90^\circ - \phi)} \quad (2.45)$$

x ... variable
 β ... angle $\beta = 90^\circ - \phi$
 w_a ... width of the arcing horn [m]
 l_s ... length of the suspension of the arcing horn [m]

Therefore the distance D can be expressed as:

$$D = \cos \phi \cdot \left[d + l_a + l_s - \left(\frac{w_a}{\tan(90^\circ - \phi)} \right) \right] = \cos \phi \cdot [d + l_a + l_s - (w_a \cdot \tan(\phi))] \quad (2.46)$$

D ... clearance between line side horn and tower [m]
 d ... horn gap length [m]
 ϕ ... swing angle
 l_a ... length of the arcing horn [m]
 l_s ... length of the suspension of the arcing horn [m]
 w_a ... width of the arcing horn [m]

Finally the gap factor K_S can be written as:

$$K_S = 1.68 \cdot e^{\left(\frac{-0.34}{\cos \phi [d + l_a + l_s - (w_a \cdot \tan(\phi))]} \right)} \quad (2.47)$$

K_S ... gap factor of the arcing horn
 D ... clearance between line side horn and tower [m]
 d ... horn gap length [m]
 ϕ ... swing angle
 l_a ... length of the arcing horn [m]
 w_a ... width of the arcing horn [m]

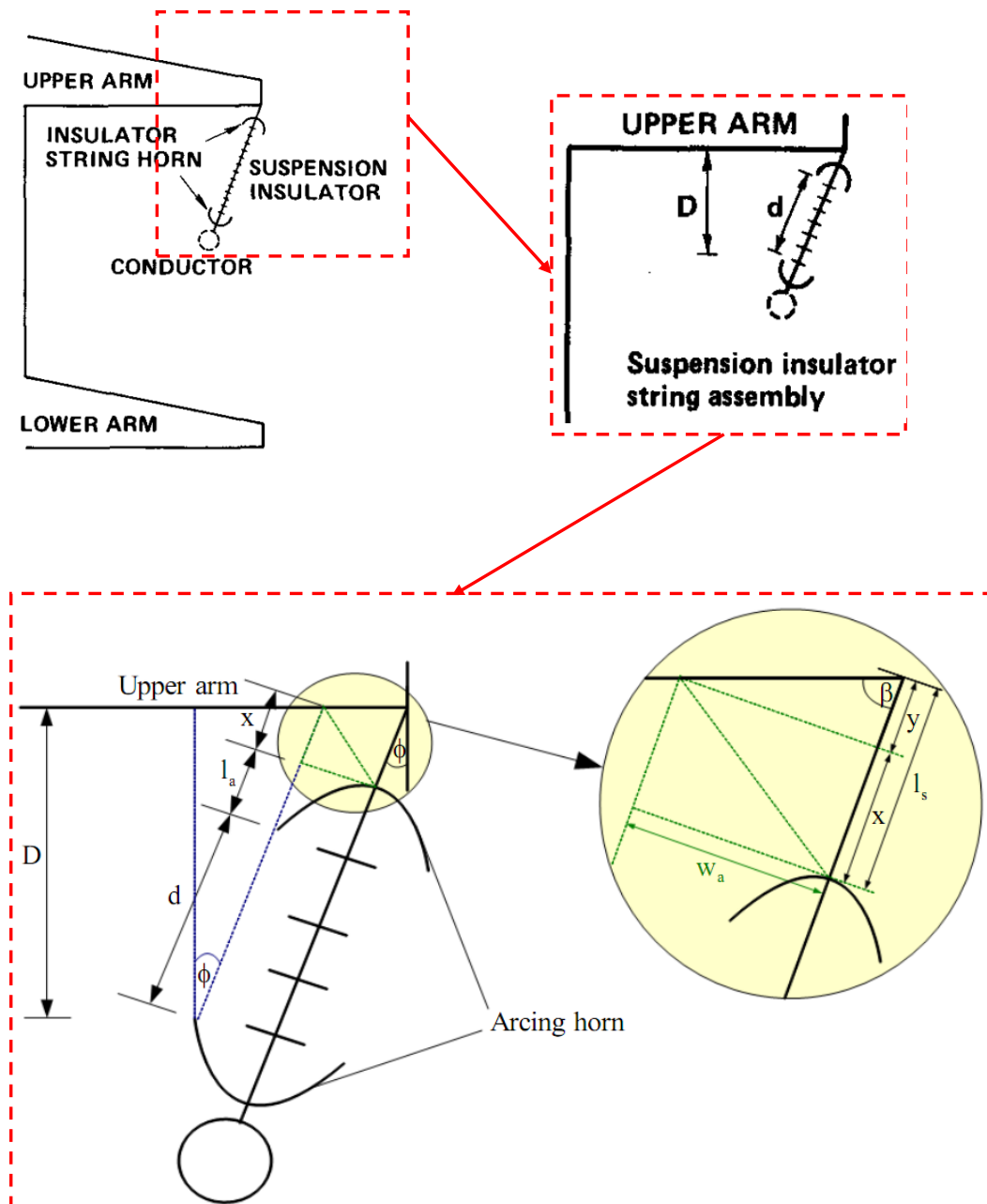


Figure 2.5: Typical Construction of a suspension insulator string assembly and detailed figure of suspension insulator assembly (adapted from [24])

Chapter 3

Insulation coordination

3.1 Basics

Insulation coordination is defined as the selection of the dielectric strength of equipment in relation to the voltages which can appear on the system for which the equipment is intended. Furthermore, the service environment and the characteristics of the available protective devices [25] must be taken into account. For the insulation level it must be differentiated between the stress due to the operating voltage and the stress due to overvoltages. The reason is that overvoltages are less common and of short duration, whereas the operating frequent voltage has a comparable amplitude, but is applied to the equipment as long as the line is operating [15].

3.2 Insulator

3.2.1 Types and materials

The materials of an insulation system have to meet different requirements. On the one hand it has to be an excellence dielectric, capable of accommodating high electrical stress over long time duration and on the other hand it has to withstand the environmental effects such as lightning strokes. Hereinafter, the most common insulating materials used at overhead lines are described [26]:

1. Porcelain:

This material is produced from clays and inorganic materials. After firing in a kiln, they consist of various oxides and silicon in their glassy matrix. Due to the firing process it is completely impervious to moisture, as well as highly resistant against degradation by environmental factors and damage by surface electrical discharge and leakage current activity. They are usually glazed for inhibiting the adherence of contaminants, facilitating the natural washing by the rain and increasing the compressive strength. The greatest disadvantage of this material is its brittle nature, which leads to breakage, chipping and cracking [26].

2. Toughened glass:

Most of the appointed glass units are of the toughened type instead of the annealed type in order to achieve the mechanical requirements. The process of hardening occurs due to an accelerated cooling of the insulator surface whereas the inner regions are cooling more slowly. These differential rate of solidification leads to a permanent compressive pre-stressing of the outer layers, which prevents the material from surface microcracks and crack propagation. The advantages of glass are its unusual resistance against environmental effects and electrical puncture, its high dielectric strength and the good compressive strength. The disadvantages are its mechanical characteristics (limitation of certain applications) and its the tendency to shatter (target of vandals) [26].

3. Epoxy resin:

Epoxy resin belongs to the group of casting resins, which are composite systems consisting of resin, hardener, accelerator, flexibilization, filler and colorant. The single components are all stable and storable for a certain time duration, but they are reactive and the processing time (so called pot life) is limited. First the components are mixed up and homogenized, after that the resin compound is filled in forms for hardening. The positive features of this material are the possibility of suiting a variety of applications due to its ability of mouldeling in many different forms. A further advantage is that integral metal ware can be supplied whereby external fittings are not necessary anymore. The possibility of erosion due to leakage current leads to a disadvantageous impact on the applicability. General the use of resin for overhead lines is limited to medium voltage [26][27].

4. Polymer composite:

A polymer composite insulator consists of a fiberglass core for providing the mechanical strength, covered by a housing to protect the core from environmental influences and to ensure the required electrical characteristics. Nowadays, materials used for housing are either based on ethylene propylene diene monomers (EPDM) or on silicone. EPDM has a high mechanical strength whereas silicones have a higher resistance to ultraviolet degradation. The advantages of composites are its high tensile strength-to-weight ratio and an improved performance in highly polluted areas when compared to glass or porcelain. The disadvantages are erosion owing to leakage current, if the material is incorrectly used or dimensioned [26].

General these are two class of overhead insulators [26]:

1. Class A:

They are characterized by the fact, that the puncture distance through the solid insulating material is at least equal to the half arcing distance. Class A insulators are considered to be unpuncturable (e.g. long rod insulator) [26][28].

2. Class B:

They are characterized by the fact, that the puncture distance through the solid insulating material is less than the half arcing distance. Class B insulator types are considered to be puncturable (e.g. cap-and-pin insulator made of glass, base insulator) [26][28].

The type of insulator, Statnett SF is using currently at the affected overhead lines, are cap-and-pin disc insulator, which are made of glass (see also section 5.3).

This insulator of class B consisting of an insulating part (glass, porcelain) in form of a disc or bell and the fixing device formed as an outside cap and inside pin. Typical applications of this insulator type are suspension and strain positions of overhead lines (see also Figure 3.1) [26].

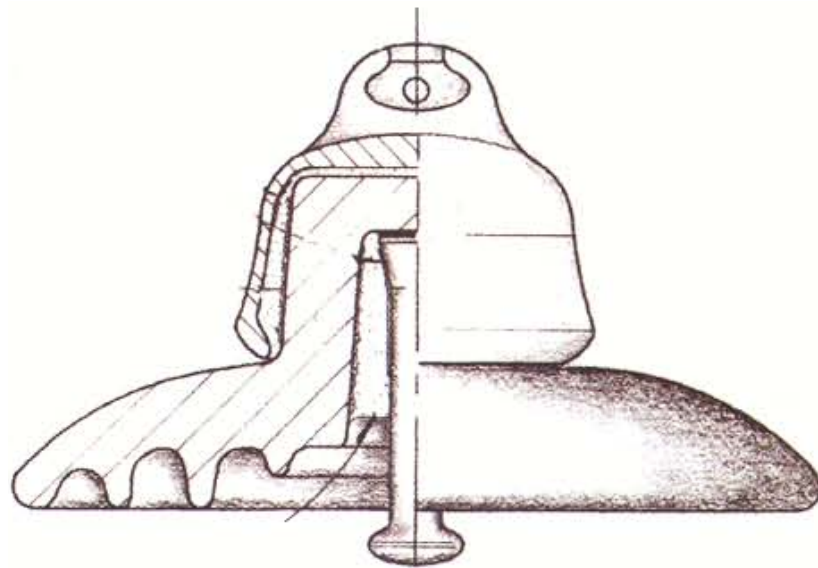


Figure 3.1: Cap-and-pin disc insulator [26]

3.2.2 Types of arcing horns

Arcing horns are used to provide a predetermined air gap of the discharge current in case of a phase-to-earth-fault. Practically they are usually only used for porcelain insulators as they are prone to insulation puncturing or cracking [29]. Arcing horns are also installed to protect the conductor and insulator from possible damages caused by lightning flashovers and arc currents arising thereby [24]. In general there are two different types of insulator assemblies with different positions and implementation of arcing horns [24]:

1. Suspension insulator assembly: In this case the arcing horns are installed conductor-sided and tower-sided on the insulator string. In Figure 3.2 the suspension insulator assembly of a 1000 kV AC UHV transmission line is shown.
2. Tension insulator assembly: Thereby the arcing horns are installed on the upper part of the jumper and vertically above on the cross arm. In Figure 3.3 the tension insulator assembly of a 1000 kV AC UHV transmission line is shown [24].

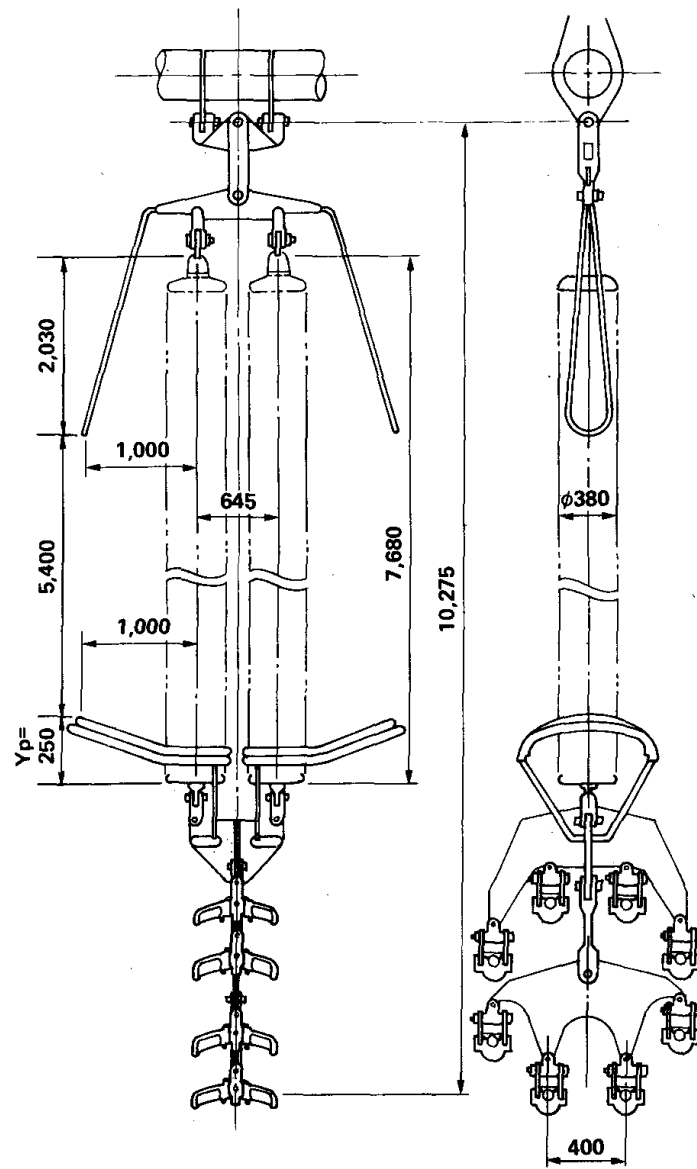


Figure 3.2: Suspension insulator assembly of a 1000 kV AC UHV transmission line [24]

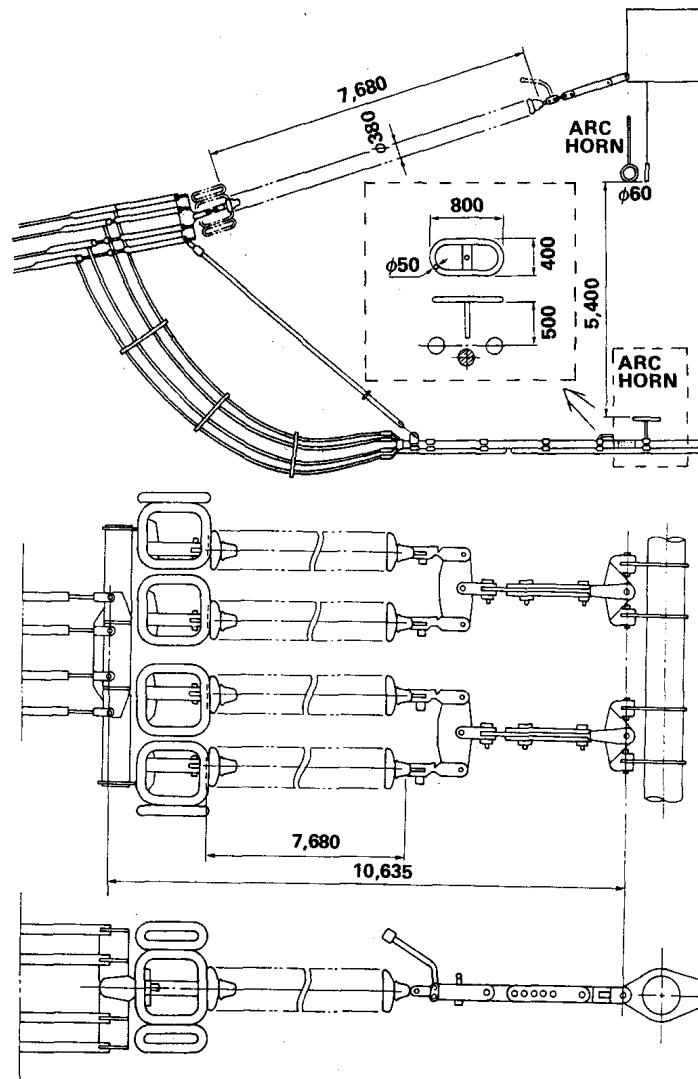


Figure 3.3: Tension insulator assembly of a 1000 kV AC UHV transmission line [24]

3.3 Insulation level

3.3.1 Standard insulation level

The insulation level for the different voltage levels are defined in the standard IEC 60071 - part 1 [25] and can be seen in Table 3.1.

Table 3.1: Standard insulation level for range II ($U_m > 245$ kV) [25]

Highest voltage for equipment U_m	Standard switching impulse withstand voltage			Standard lightning impulse withstand voltage
	Longitudinal insulation	Phase-to- earth	Phase-to- phase (ratio to the phase- to-earth peak value)	
kV (r.m.s value)	kV (peak value)	kV (peak value)		kV (peak value)
300	750	750	1.50	850
				950
	750	850	1.50	950
				1050
362	850	850	1.50	950
				1050
	850	950	1.50	1050
				1175
420	850	850	1.60	1050
				1175
	950	950	1.60	1300
				1425
950	1050	1.60	1300	
			1425	
525	950	950	1.70	1175
				1300
	950	1050	1.60	1300
				1425
950	1175	1.50	1425	
			1550	
765	1175	1300	1.70	1675
				1800
	1175	1425	1.70	1800
				1950
1175	1550	1.60	1950	
			2100	

3.3.2 Influence of different insulator materials

The voltage distribution along a glass and ceramic insulator string or a composite insulator is not linear, which leads to an increased electrical field at the high voltage end and the ground end [30]. This is due to the fact, that the insulator chain is a system built of several materials in which the end fittings have a fixed potential whereas the area in between has a floating potential [31]. In case of a 400-kV insulator string or composite insulator, voltages greater 10 % of the phase to ground line voltage can occur at the last insulator on high voltage end. This effect is influenced by the type of end fitting as well as the conductor bundle configuration. However, the insulator located in the middle has to absorb only 2 % of this voltage. In dry conditions the maximum of electrical field is always located near the high voltage end of insulator, whereby corona or electrical discharge can appear in air, if the electrical field is not controlled. Corona and electrical discharge at the surface can generate radio interference noise and radio interference voltage (RIV). In case of composite insulators a frequent or permanent existence of corona and electrical discharge can influence the aging and can lead to a reduced lifetime. That is the reason why, in case of composite insulator, the electrical field at the end of the insulator must be controlled. At wet composite insulators, water is dropping on the housing, which leads to an increasing of the electrical field whereby corona can appear around a water drop or between adjacent water drops. In case of insulator with silicone rubber housing the hydrophobicity of the housing surface can be reduced due to this effect which does not significantly damage the insulator. The field distribution is significantly different for different type of insulator depending on some critical insulator factors as they are [30]:

- Type and shape of the end fittings
- Shed profile
- Location of the shed nearest to the end fitting
- Shape of the ring if existent
- Location of the ring if existing

Figure 3.4 and Figure 3.5 show the calculated field distribution of two different insulator profile of a 400 kV insulator (applied voltage 243 kV_{rms} phase to ground). In Profile 1 the first shed is located over the collar of the end fitting, whereas in profile 2 the first shed is situated 53 mm above the end fitting [30].

3.3.3 Influence of different arcing horns

As described in section 2.1.3 the withstand voltage U_{rw} depends on the 50%-withstand voltage of a rod-plate-arrangement (RP) U_{rp} , the variation factor K_z , the altitude above sea level and the gap factor K_g (see also Equation (2.8)[15]).

$$U_{rw} = K_z \cdot K_g \cdot K_a \cdot U_{50\%rp} \quad (3.1)$$

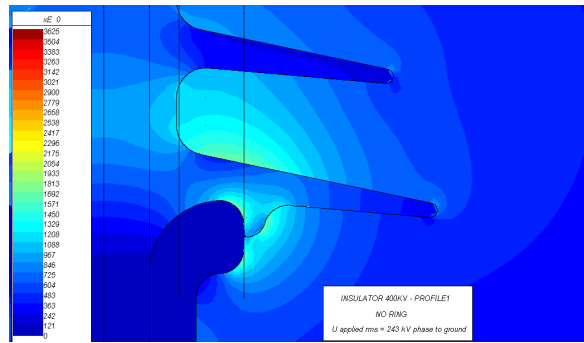


Figure 3.4: Field distribution of insulator profile 1

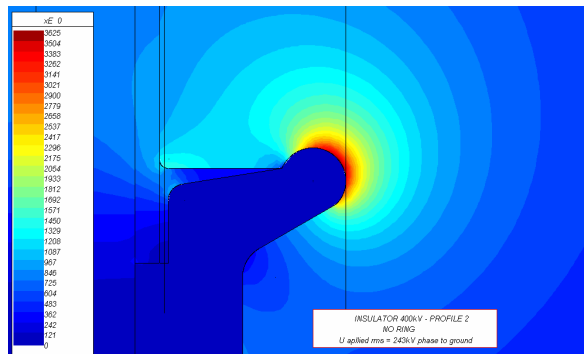


Figure 3.5: Field distribution of insulator profile 2

Furthermore, the gap factor K_S for arcing horns in case of switching impulse voltage depends on the swing angle and the dimensions is described in section 2.3.3 and can be written as (see also Equation (2.47)):

$$K_S = 1.68 \cdot e^{\left(\frac{-0.34}{\cos \phi [d + l_a + l_s - (w_a \tan(\phi))]} \right)} \quad (3.2)$$

- K_S gap factor of the arcing horn
- D clearance between line side horn and tower [m]
- d horn gap length [m]
- ϕ swing angle
- l_a length of the arcing horn [m]
- w_a width of the arcing horn [m]

In [19] it is defined that the gap factor for switching impulse voltage (slow front overvoltage) is equal to the gap factor of lightning impulse voltage (fast front overvoltage), but there is no evidence mentioned.

Example of calculation: Table 3.2 shows calculated values by use of Equation (3.1) and Equation (3.2), whereas the following values were assumed:

- $d = 2.89$ m
- $l_a = 0.30$ m
- $w_a = 0.35$ m
- $l_S = 0.355$ m
- $K_Z = 0.922$ (see also Table 2.1)
- $K_a = 0.922$ (Altitude 1000 m above sea level, 201 - 400 kV, see also Table 2.2)
- withstand voltage $U_{50\%rp} = 340$ kV

Table 3.2: Example of calculation

Swing angle ϕ [°]	Clearance D [m]	Gap factor K_S	Withstand voltage U_{RW} [kV]
5	3.5	1.27	376.29
10	3.43	1.26	374.12
15	3.33	1.25	371.02
20	3.21	1.24	366.89
25	3.06	1.22	361.56
30	2.90	1.20	354.82
35	2.70	1.17	346.37
40	2.49	1.13	335.80
45	2.26	1.10	322.49

In Figure 3.6 and Figure 3.7 the clearance D as well as the gap factor K_S is shown as a function of the swing angle ϕ .

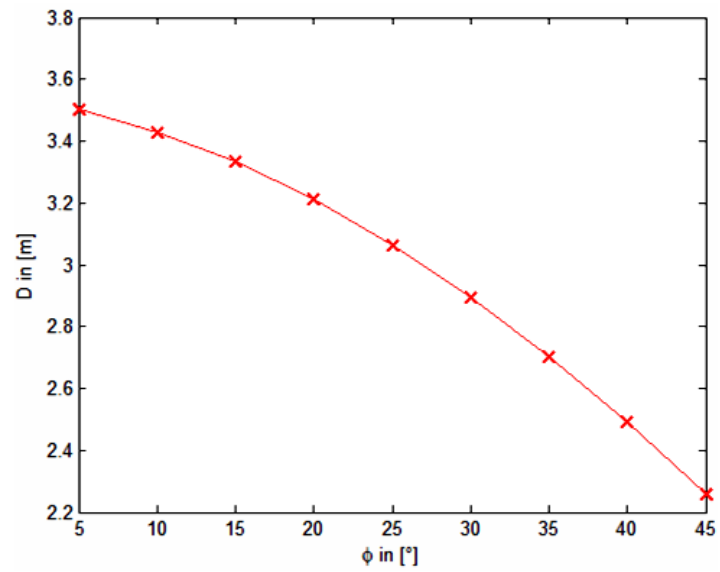


Figure 3.6: Plot – Clearance D as a function of the swing angle ϕ

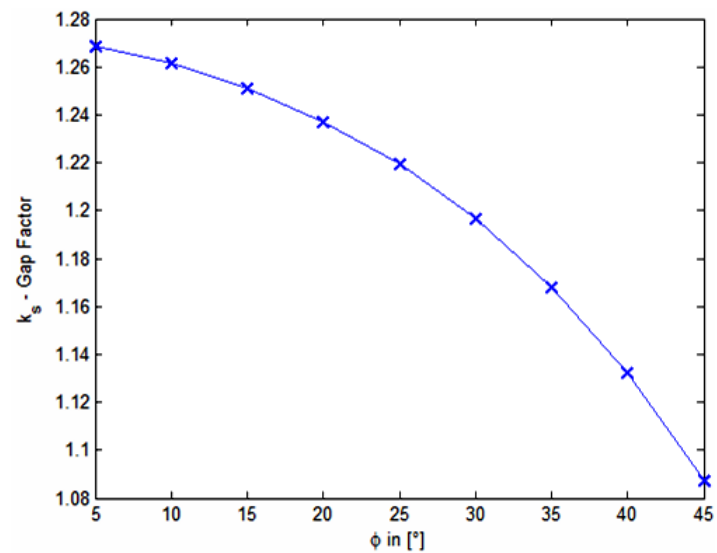


Figure 3.7: Plot – Gap factor K_S as a function of the swing angle ϕ

Chapter 4

Model development

The practical full-scale model of an affected overhead line suspension tower, which has been designed and constructed in the course of this work is a realistic replication of an affected suspension tower, which Statnett SF is using currently. Therefore several towers with different dimensions have been evaluated to choose the tower with the slightest clearances to ensure a simulation of a "worst-case-scenario" of clearances (see also section 4.1.2).

4.1 Technical analysis of the affected tower

4.1.1 Basics

The affected suspension towers, which Statnett SF is using currently, are arranged in mono layer design, whereby the middle phase is mounted inside and the remaining two phases are fixed sideways of the tower window (see also Figure 4.1).



Figure 4.1: Affected tower of Statnett SF

4.1.2 Technical description of the tower

The affected towers consist of three tower sections, whereby the tower window including the middle phase is in the upper part of the tower. Inside the tower window of the highest tower section there are two short guy wires in the upper corners and two longer guy wires in the lower

corners. The short guy wires are carried out in steel in form of a L-profile and the lower guy wires are made of steel ropes with a diameter of 15 mm. Figure 4.2 shows a picture of the guy wires inside the tower window. The affected towers, which Statnett SF is using currently are all the same design, but have different dimensions to ensure the required distances between the overhead line and the surrounding area. Figure 4.3 shows a drawing of an affected suspension tower of the overhead line between Ogdal and Namsos. It is the affected tower with the lowest dimensions concerning the tower window and the dimensions between the centre phase and the tower. Therefore it was taken as a basis for designing of the model to guarantee a simulation of a "worst-case-scenario" of clearances.

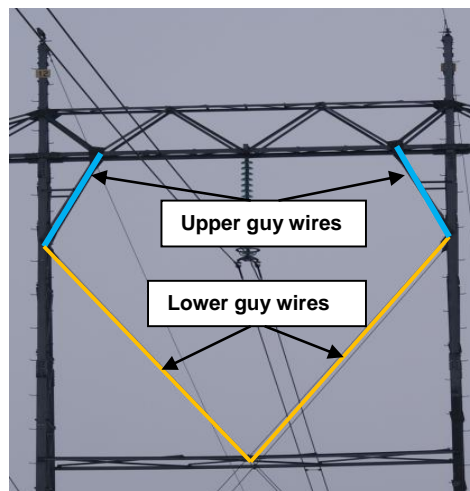


Figure 4.2: Tower window with guy wires

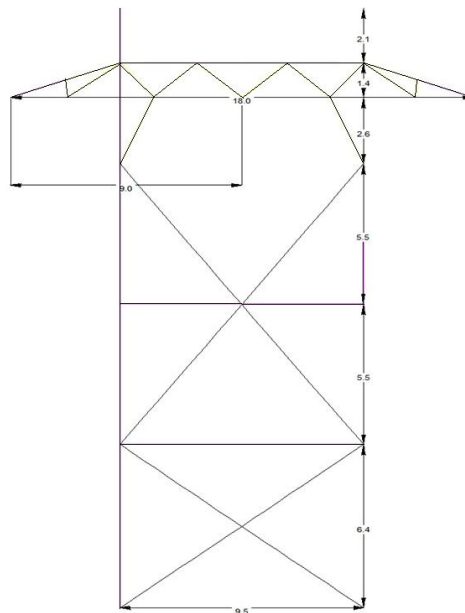


Figure 4.3: Drawing of an affected suspension tower

4.2 Design of the model

4.2.1 Basics

Preliminary investigations on side of Statnett SF have shown that most of the problems concerning insulation coordination concern the middle phase of the suspension towers and the two lateral conductors can be seen as uncritical. This is largely because the distance between the centre phase and the tower window are comparable shorter than the distance between the conductors sidewise and the tower. Due to the small diameter of the steel ropes, the lower guy wires of the tower window could be damaged by a flashover caused by an impulse overvoltage due to a lightning stroke or switching operation.

4.2.2 Replication of the tower section

Based on the previous considerations in section 4.2.1, a replication of the upper part of the suspension tower including the tower window and the middle phase is appropriate and was therefore chosen. Figure 4.4 shows the replication of the upper tower section including the tower window and the centre phase.

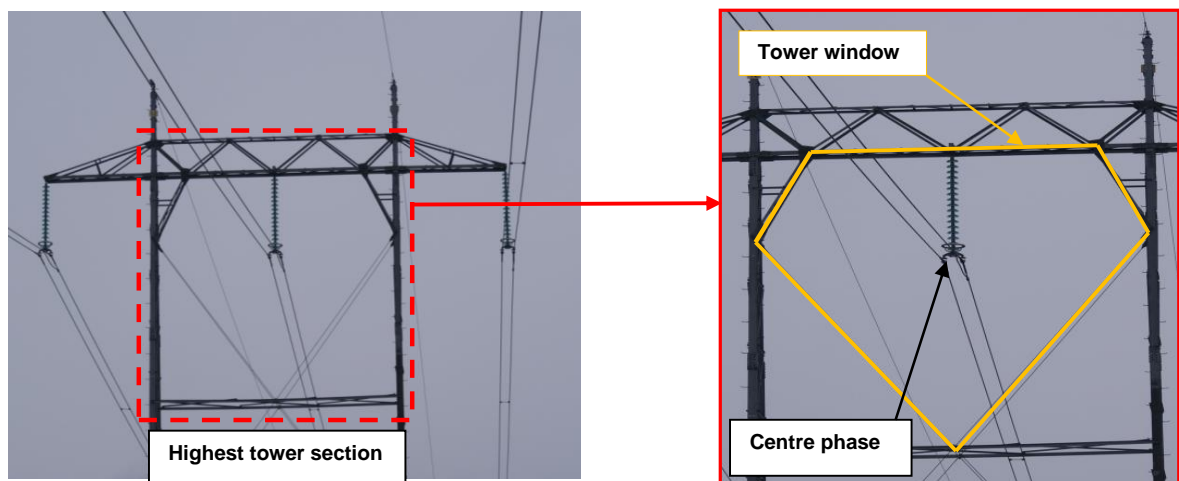


Figure 4.4: Replication of the upper tower section including tower window and centre phase

4.2.3 Dimensions of the model

As mentioned in section 4.1.2, the tower, which is shown in Figure 4.3, is the affected suspension tower with the lowest dimensions and was therefore taken as a basis for model design. Based on the dimensions of this tower the outer dimensions of the whole model are 9308 x 8650 x 1048 mm and the inner dimensions are 9260 x 8100 x 952 mm. The most important demand was a strictly adherence of the given actual dimensions to ensure a realistic replication of the tower section. Regarding to the maximum hoisting capacity of the cranes used in the testing setup (see section 5.2) an important requirement was to reduce weight for the model. Therefore it was made of aluminum and the total weight including the insulator was approximately 700 kg.

It was built by the company JUST LEITERN AG in Zeiselmauer in Lower Austria. Due to the large dimensions, the model was not built in one piece, because that would have led to high transportation costs. Therefore, the model was delivered in sub-groups, which have been put together on-site. Detailed drawings of the model are given in the Appendix (see chapter 9).

Chapter 5

Measurements

Using the practical full-scale model in combination with the testing setup a method has been developed to simulate several swing angles and distances, respectively (see also section 5.2). They have been required in the following impulse voltage tests which are covered below. Furthermore, for these impulse voltage tests a specific testing plan covering swing angles respectively distances occurring on-site in Norway has been scheduled (see also sections 6.2, 6.3, 6.5, 6.6, 6.7, 6.8). In the testing plans lightning impulse voltage tests and switching impulse voltage tests as well as two types of corona rings (see also section 5.3) are included.

5.1 Basics

The tests took place at the open air testing area of the High Voltage Laboratory of the Institute of High Voltage Engineering and System Management at the Graz University of Technology. The normative shape forms for lightning and switching impulse voltage stress as defined in [32] were used for the tests (see also Figure 5.1).

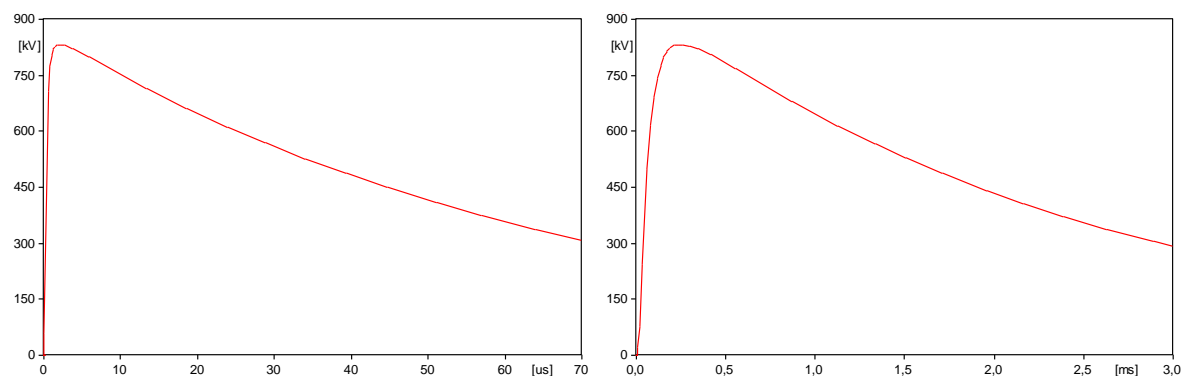


Figure 5.1: Normative shape form 1.2/50 μs (left) and 250/2500 μs (right)

The appropriate tolerances for lightning impulse voltage for normative shape form (1.2/50 μs) are also defined in [32]:

Peak value: $\pm 3\%$
Front time: $\pm 30\%$
Time to halve: $\pm 20\%$

In case of switching impulse voltage the tolerances for normative shape form ($250/2500 \mu s$) are defined as [32]:

Peak value: $\pm 3\%$
Front time: $\pm 20\%$
Time to halve: $\pm 60\%$

5.2 Testing setup

The tests took place at the open air testing area of the High Voltage Laboratory of the Graz University of Technology, whereby the model was hung up on the two cranes of the testing portal (see also Figure 5.2).

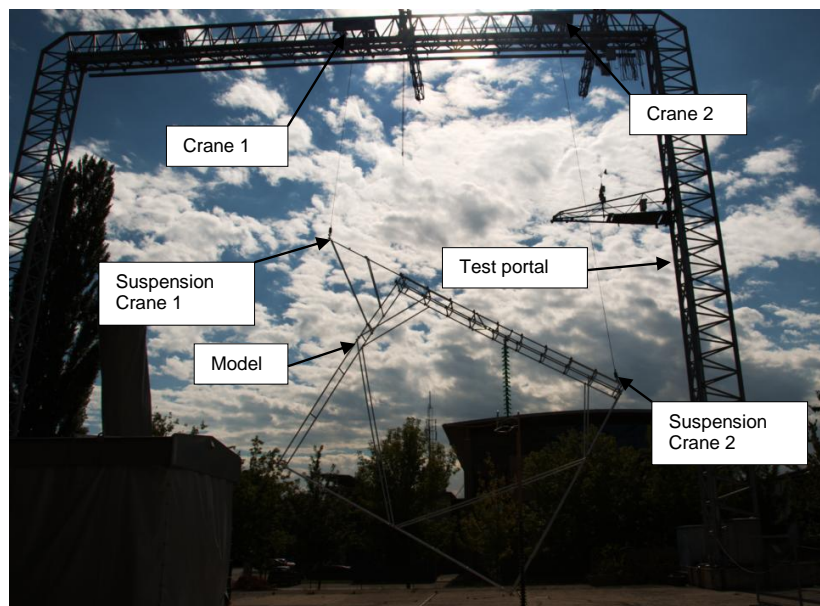


Figure 5.2: Testing setup with testing portal

Figure 5.3 shows a schematic of the whole testing setup with the High Voltage Laboratory Hall and the testing open air area. The impulse voltage generator, which is located inside the Laboratory Hall, was connected with the model hanging on the testing portal by use of a stranded wire. The stranded wire led from the generator to the voltage divider, which was necessary for measurement, and from there via two post insulator to the model.

The conductor wires mounted at the bottom of the corona ring were replicated by use of two metal tubes with the diameter of the wires (34.5 mm) and spacers on both ends to ensure the exact distance between the tubes (see also Figure 5.4). The stranded wire was connected with one of the tubes.

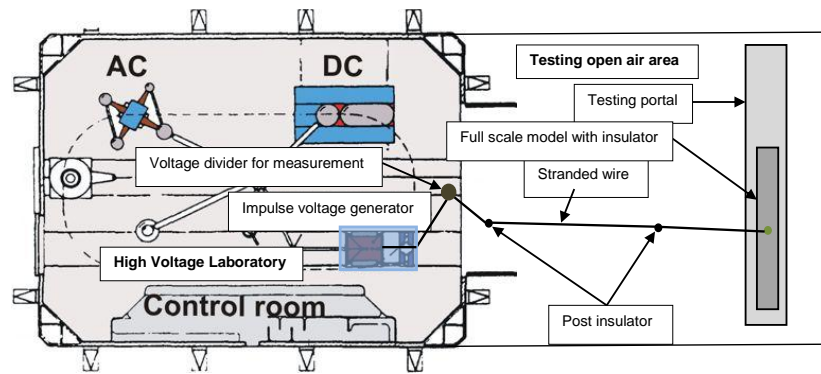


Figure 5.3: Schematic of the testing setup

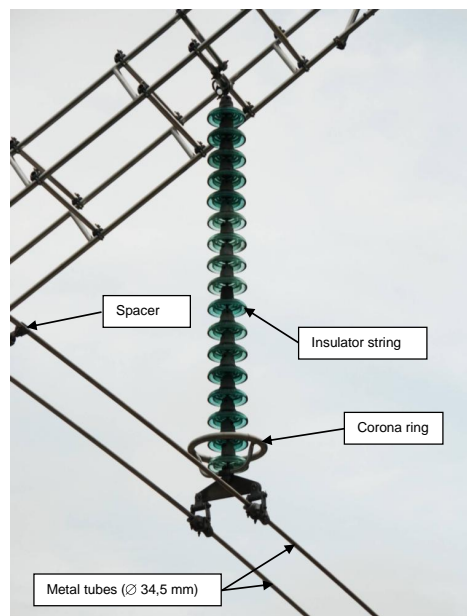


Figure 5.4: Insulator, corona ring and metal tubes (replication of conductor wire)

To simulate specified swing angles respectively distances between conductor/ corona ring and the guy wire the two cranes were used. Therefore the model was raised up one-sided whereas the other side was left in place (see also Figure 5.5, Figure 5.6 and Figure 5.7).

5.3 Tested insulators and corona rings

The insulators Statnett SF is using currently on the affected lines are glass insulators of the cap-and-pin disc type, whereby the insulator string for the 300-kV-Level consists of 14 to 15 insulator discs and for the 420-kV-Level it is planned to lengthen it up to 16 - 17 discs. For the tests two different numbers of discs have been chosen, depending on the used type of corona ring. Figure 5.8 shows a drawing of the used cap-and-pin glass insulator including one type of corona ring and the conductors. The total height of one cap is 170 mm and the total weight of one cap is approximately 6.9 kg. That implies, that the total weight of the whole insulator string for the 420-kV-Level in case of 17 insulators is approximately 117 kg.

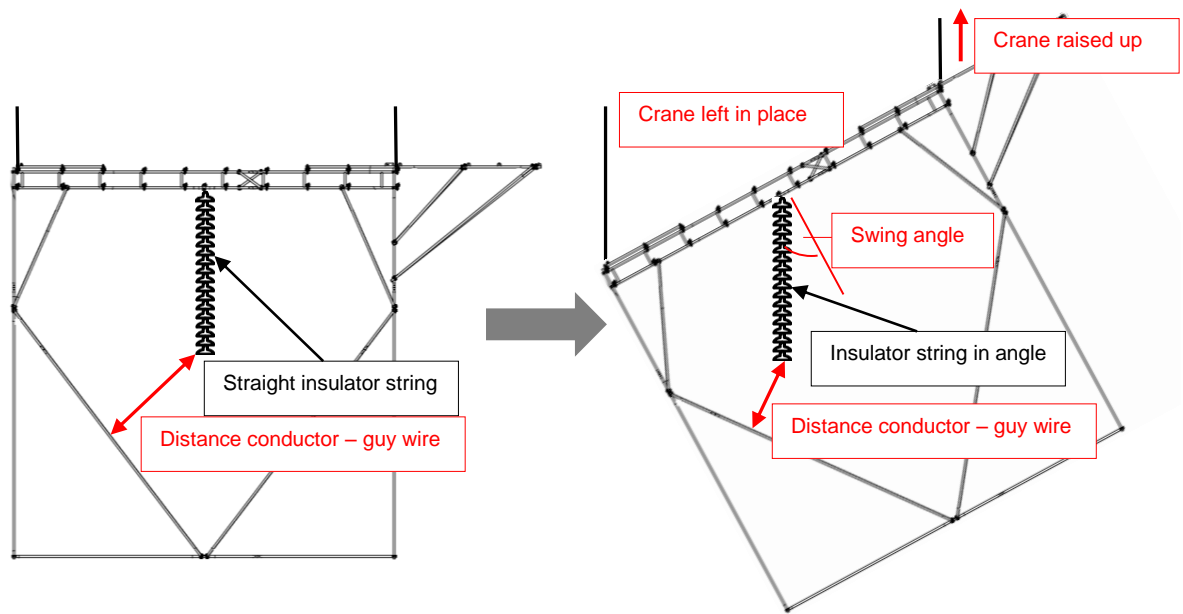


Figure 5.5: Simulation of swing angle and distances, respectively

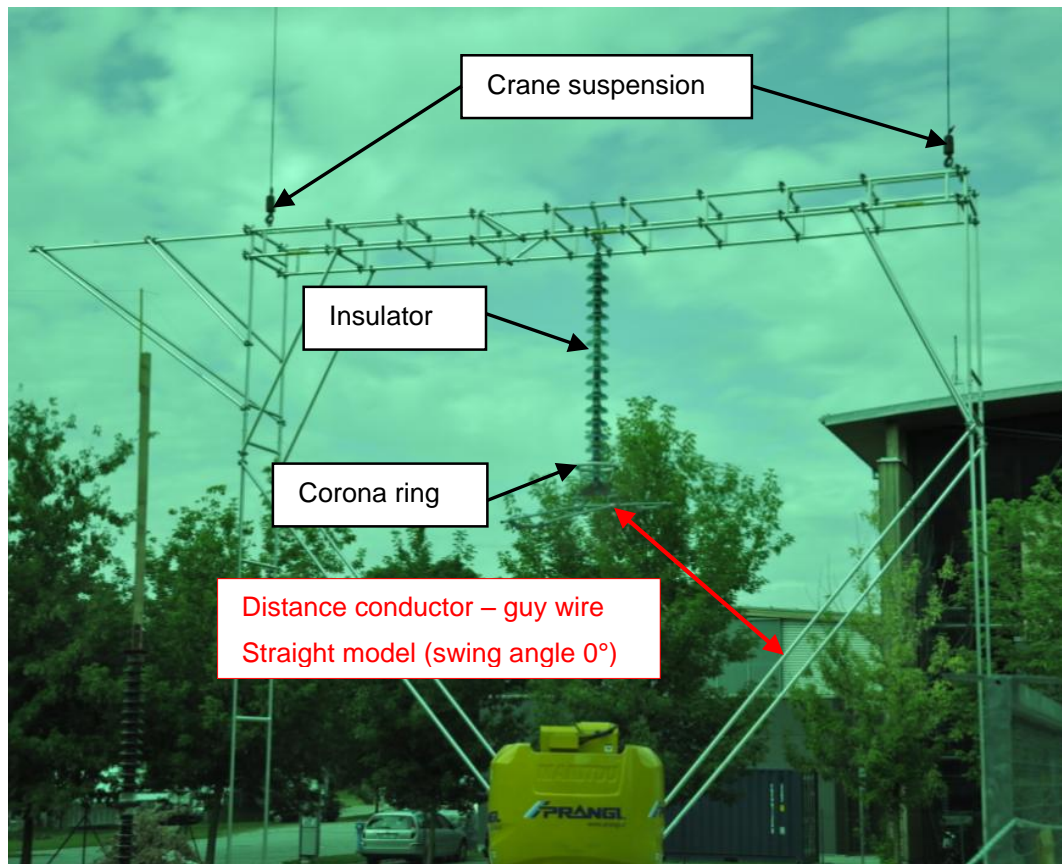


Figure 5.6: Straight model

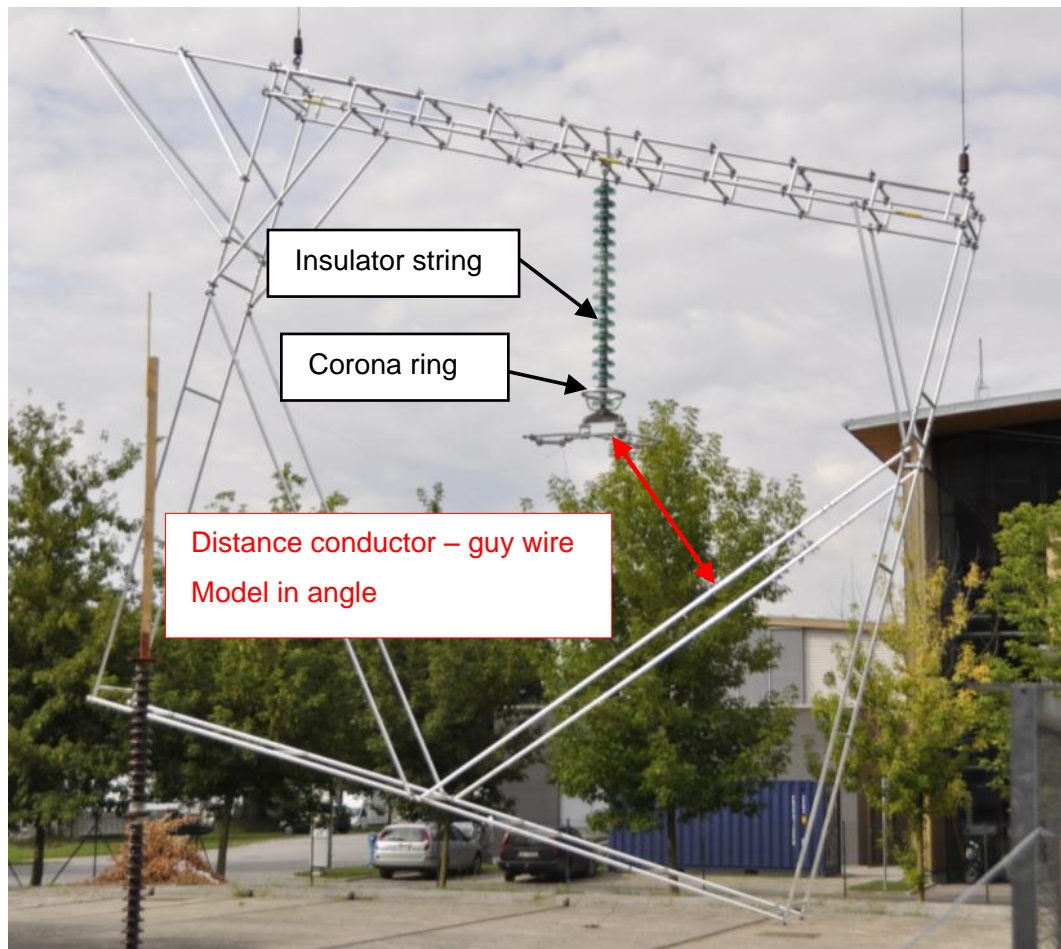


Figure 5.7: Model in angle

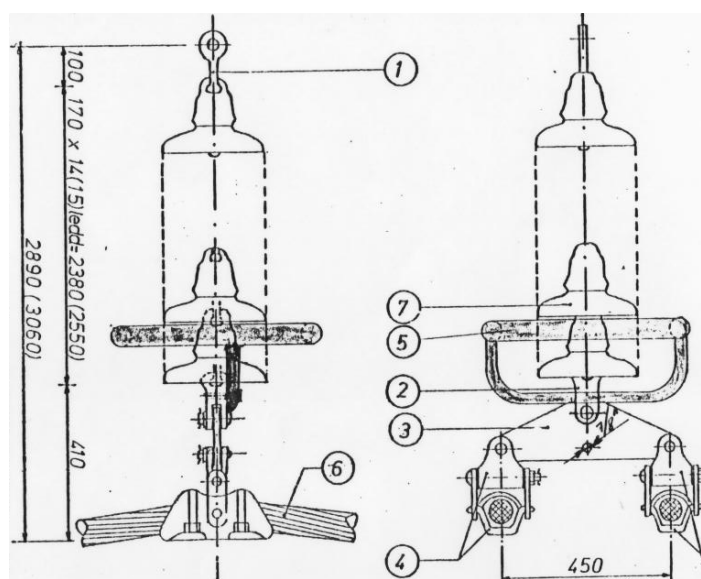


Figure 5.8: Drawing of insulators

In the tests two different types of corona rings have been tested, which Statnett SF is using at the affected overhead line towers.

1. Corona ring type 1:

This type of corona ring consists of one ring, which is mounted horizontally at the end of the insulator string and the conductor wires are fixed below the ring on the mounting device. All the impulse voltage tests have been carried out with 17 insulator discs by use of this type of corona ring, because this type is covering one whole insulator cap (see also Figure 5.9 and Figure 5.10).

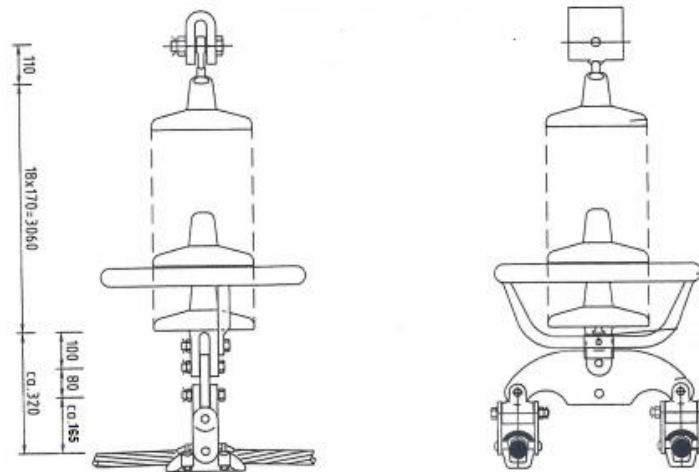


Figure 5.9: Drawing of corona ring type 1

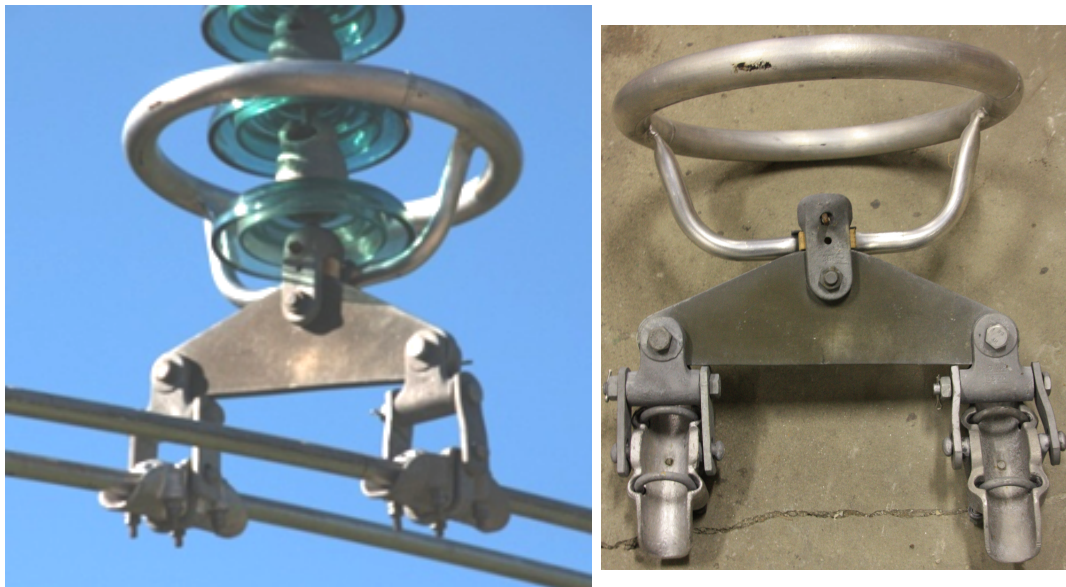


Figure 5.10: Corona ring type 1

2. Corona ring type 2:

The second type of corona ring consists of two rings, which are mounted vertical on the left and the right side of the conductor wires. All the impulse voltage tests have been

carried out only with 16 insulator discs by use of this ring, because this type of corona ring is not covering an insulator cap totally (see also Figure 5.11 and Figure 5.12).

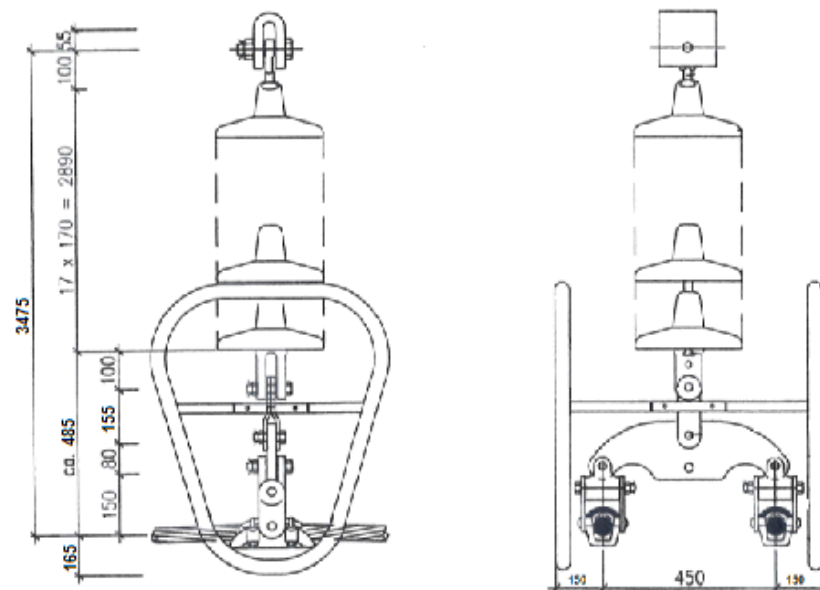


Figure 5.11: Drawing of corona ring type 2

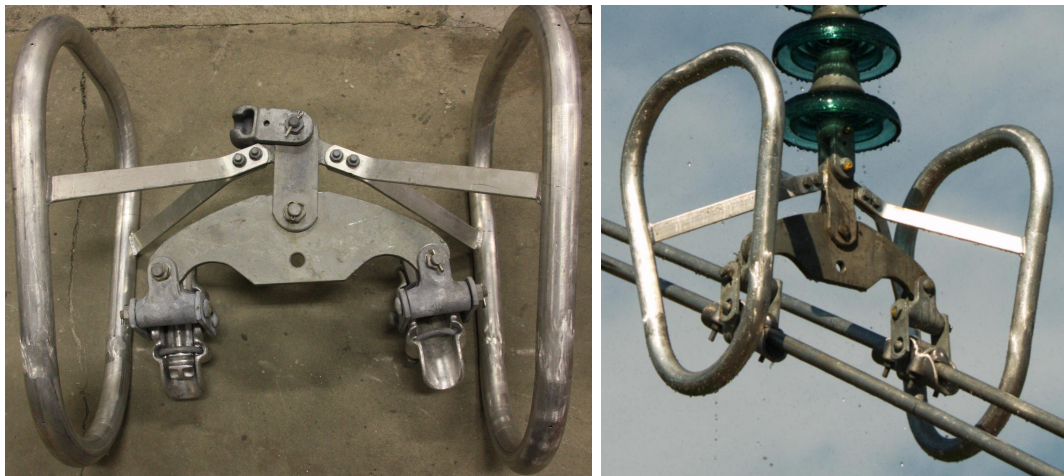


Figure 5.12: Corona ring type 2

Chapter 6

Measurements and calculations

In this chapter the implementation and results of all realized experiments are explained in more detail. In general, the following types of experiments have been carried out:

- Lightning impulse voltage tests with corona ring type 1 (see section 6.2)
- Lightning impulse voltage tests with corona ring type 1 using a damper loop (see section 6.2)
- Lightning impulse voltage tests with corona ring type 2 (see section 6.3)
- Switching impulse voltage tests with corona ring type 1 (see section 6.5)
- Switching impulse voltage tests with corona ring type 2 (see section 6.6)
- Rain test with switching impulse voltage and corona ring type 2 (see section 6.7)
- Switching impulse voltage tests with bare insulator string (see section 6.8)

6.1 Basics – Lightning impulse voltage Tests

In case of lightning impulse voltage tests the main goal of the tests was to find out where the flashover occur. This is due to the fact that for the calculation of the gap factor for the air gap the percentages of the flashover occurrence inside the tower window are necessary, which is explained in more detail in section 7.1. The lightning impulse voltage tests have been carried out with the two different types of corona rings as they are described in section 5.3. To generate enough flashovers it was necessary to choose an appropriate high value of impulse voltage. Therefore the $U_{90\%}$ -voltage, which is defined as the value of influenced voltage, which leads with a probability of 90 % to a flashover [32], fits very well. The $U_{90\%}$ -voltage in case of lightning impulse voltage is defined as following, whereby $z = 0.03$ in case of lightning impulse voltage [32]:

$$U_{90} = U_{50} \cdot (1 + 1.3 \cdot z) \quad (6.1)$$

In section 2.1.3 the determination of the 90 %-withstand voltage ($=U_{10\%}$ -voltage) of the air gap using the $U_{50\%}$ -voltage and the standard deviation σ_u is described. Similar to Equation (2.3)

the $U_{10\%}$, which is described as the value of influenced voltage which leads with a probability of 10 % to a flashover [32] can be calculated by use of Equation (6.2).

$$U_{10} = U_{50} \cdot (1 - 1.3 \cdot z) \quad (6.2)$$

As it can be seen in Equation (6.1) and Equation (6.2) the estimation of the $U_{50\%}$ -voltage is necessary for the calculation of the $U_{90\%}$ -voltage and the $U_{10\%}$ -voltage, respectively. In general the estimation of the U_p -voltage, whereby p defines the probability of a voltage breakdown, is also defined in [32]. Therefore the up-and-down method can be used, where the testing object is tested with m -equal voltage stresses for similar defined voltage levels. Depending on the result of the previous voltage stress, the voltage is either increased or decreased by a step of ΔU . In case of $m = 1$, the $U_{50\%}$ -voltage can be calculated as shown in Equation (6.3), whereby k_i is the number of stresses for a voltage level and $n = \sum k_i$ [32].

$$U_p^* = \sum \frac{k_i \cdot U_i}{n} \quad (6.3)$$

Due to the previous considerations an introduction test has been carried out at the beginning of the lightning impulse voltage tests for both types of corona rings to determine the $U_{50\%}$ -voltage (see also testing plans – Figure 6.3 and Figure 6.14). Based on this value the $U_{90\%}$ -voltage has been calculated and used for the following lightning impulse voltage tests to evaluate where the flashovers occur. To convert the determined values under testing conditions in values under standard basic reference atmosphere conditions correction factors are used. The conversion is necessary, because the flashover for an outer insulation depends on the atmosphere conditions. The atmospheric correction factor K_t is the product of the factor of air density and of the factor for air humidity and can be calculated as following [32]:

$$K_t = k_1 \cdot k_2 \quad (6.4)$$

The detailed calculation of the two factors k_1 and k_2 are also described in [32]. The given flashover voltage U can be converted to standard basic reference atmosphere by dividing through the factor K_t [32]:

$$U_0 = U / K_t \quad (6.5)$$

To calculate the atmospheric correction factor respectively the given flashover voltage under standard basic reference atmosphere, the atmospheric outdoor conditions have been measured during the tests by use of the measuring device mounted at the High Voltage Laboratory. Specifically, the following three values of atmospheric outdoor conditions have been measured:

1. Temperature in [°C]
2. Air pressure in [mbar]
3. Air humidity in [%] and [g/m^3]

The correction factor K_t arising from this measured atmospheric outdoor conditions have been calculated. As mentioned before - especially in case of lightning impulse voltage - the occurrence of the flashover inside the tower window was of particular interest. To evaluate, where the flashovers occur inside the model, the tower window has been classified into 6 areas (see also Figure 6.1) and all flashovers had been photographed to assign them to the appropriate area.



Figure 6.1: Classification of tower window for evaluation of flashover occurrence

Concerning the results of the tests it must be mentioned that the impulse voltage generator of the High Voltage Laboratory consists of 13 stages, which are charged in parallel and discharged in series by use of spark gaps. The leftmost column of the voltage level in all tables of results is the charging voltage (per stage) and the second value of the measured load voltage which arise from the series connection of the capacitances. The variation of the voltage level has been accomplished by variation of the charging voltage of the capacitances, whereby a ΔU of 3 kV was chosen. Between the impulses an waiting time of 1 minute was chosen in all tests. The value in the column "area of flashover in tower window" of the tables in case of flashover denotes the area of the tower window in which the flashover occur according to Figure 6.1.

6.2 Lightning impulse voltage Tests – Corona ring type 1

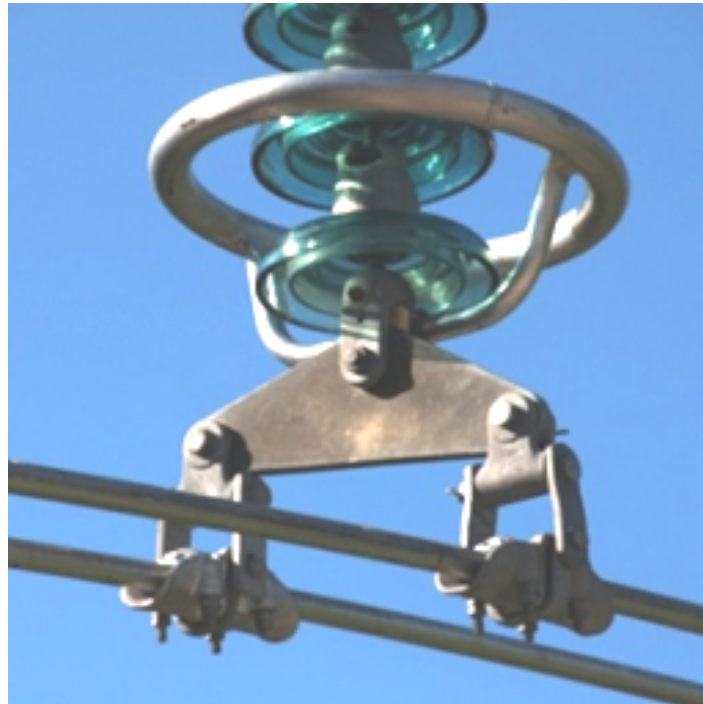


Figure 6.2: Corona ring type 1

Figure 6.3 shows the total testing plan for the lightning impulse voltage tests in case of the corona ring type 1 (1-ring corona ring, see also Figure 6.2). In the additional tests a damper loop has been used in the same configuration (see section 6.2.6, section 6.2.7, section 6.2.8).

INTRODUCTION TEST I

- # insulators = 17
- corona ring type 1
- Swing angle = 0°
- Distance to guy wire $a = 2.87$ m
- Up-and-down-method (44 enhancement, 21 flashovers)
- Determination $U_{50\%}$
- Classification of tower window in 6 areas
- Photography of flashover (where does flashover occur?)



TEST 1

- # insulators = 17
- corona ring type 1
- Distance to guy wire $a = 2.6$ m
- 20 shots with flashover
- Test voltage $U_{90\%} = U_{50\%} + 1.3 \cdot z = 1476$ kV
- Classification of tower window in 6 areas
- Photography of flashover (where does flashover occur?)



TEST 2A

- # insulators = 17
- corona ring type 1
- Distance to guy wire $a = 2.35$ m
- 20 shots with flashover
- Test voltage $U_{90\%} = U_{50\%} + 1.3 \cdot z = 1476$ kV
- Classification of tower window in 6 areas
- Photography of flashover (where does flashover occur?)



TEST 2B

- # insulators = 17
- corona ring type 1
- Distance to guy wire $a = 2.44$ m
- 20 shots with flashover
- Test voltage $U_{90\%} = U_{50\%} + 1.3 \cdot z = 1476$ kV
- Classification of tower window in 6 areas
- Photography of flashover (where does flashover occur?)



TEST 2C

- # insulators = 17
- corona ring type 1
- Distance to guy wire $a = 2.5$ m
- 20 shots with flashover
- Test voltage $U_{90\%} = U_{50\%} + 1.3 \cdot z = 1476$ kV
- Classification of tower window in 6 areas
- Photography of flashover (where does flashover occur?)



Additional TEST 1

- # insulators = 17
- corona ring type 1
- Distance to damper loop – guy wire $a = 2.45$ m
- Distance to conductor tube – guy wire $a = 2.63$ m
- 20 shots with flashover
- Test voltage $U_{90\%} = U_{50\%} + 1.3 \cdot z = 1476$ kV
- Classification of tower window in 6 areas
- Photography of flashover (where does flashover occur?)



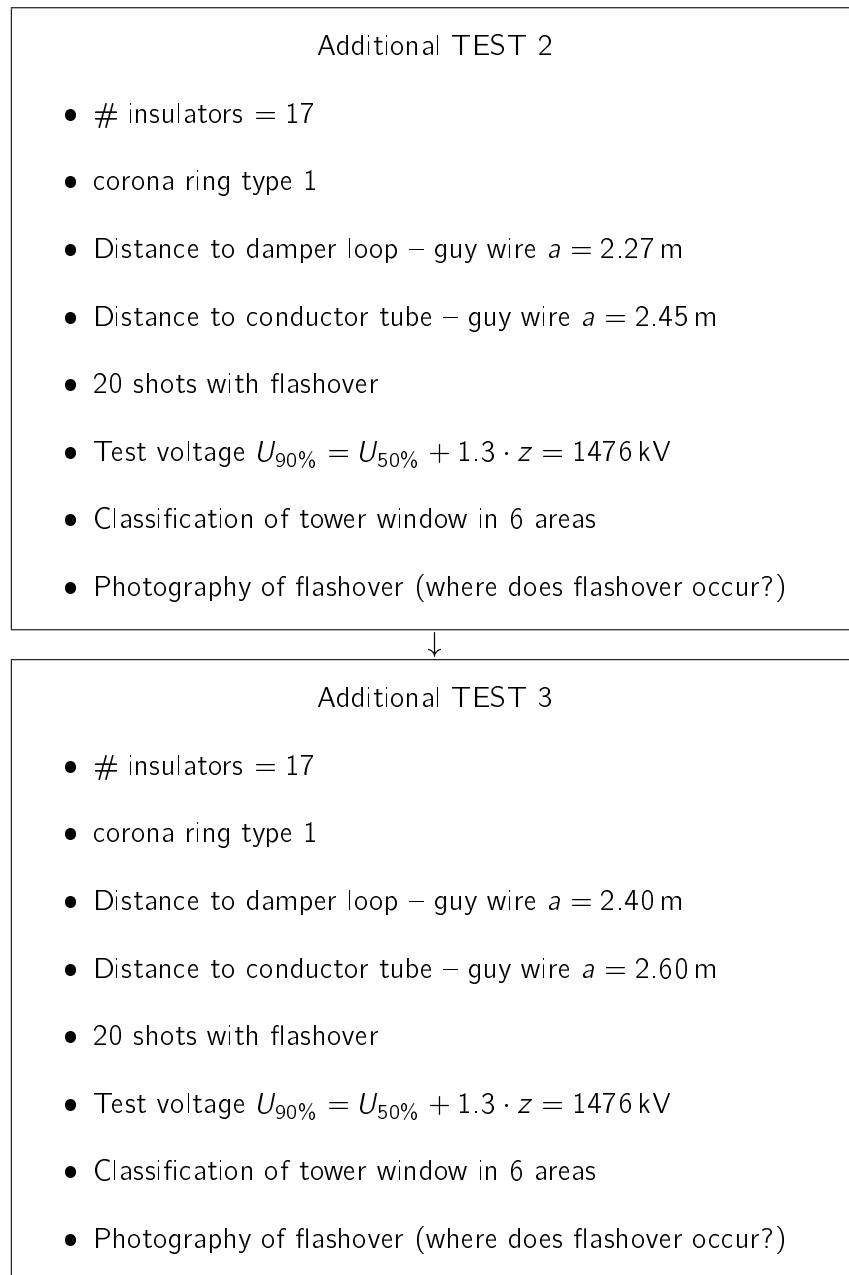


Figure 6.3: Testing plan: Lightning impulse voltage Tests – Corona ring type 1

6.2.1 Lightning impulse voltage – Introduction Test I (Corona ring type 1)

Thereby a *swing angle* of 0° has been simulated and a *distance* of 2.87 m between conductor and the lower guy wire has been measured. As mentioned in section 6.1 the main target of this test was to determine the $U_{50\%}$ -voltage and the calculation of the $U_{90\%}$ -voltage.

Results

Table 6.1 shows a summary of the results of the Introduction Test I for corona ring type 1 using the up-and-down method.

Table 6.1: Summary of results: LI – Introduction Test I (Corona ring type 1)

Lightning impulse voltage – Introduction Test I (Corona ring type 1)				
Voltage level		flashover	Area of flashover in tower window	No flashover
Charging voltage [kV]	Load voltage [kV]			
121	1399			✓
124	1431	✓	2	
121	1397			✓
124	1429	✓	2	
121	1398			✓
124	1434	✓	2	
121	1399			✓
124	1434	✓	2	
121	1398			✓
124	1433	✓	2	
121	1398			✓
124	1434	✓	2	
121	1398			✓
124	1434	✓	2	
121	1399			✓
124	1434	✓	2	
121	1399			✓
124	1435	✓	2	
121	1399			✓
124	1434	✓	2	
121	1401			✓
124	1436	✓	2	
121	1401			✓
124	1435	✓	2	
121	1401			✓
124	1437	✓	2	
121	1404			✓
124	1435	✓	2	
121	1403			✓
124	1437	✓	2	
121	1402			✓
124	1437	✓	2	
121	1402			✓

Continued on next page

Table 6.1 – continued from previous page

124	1438	✓	2	
121	1403			✓
124	1438			✓
127	1469	✓	2	
124	1435	✓	2	
121	1402			✓
124	1438			✓
127	1469	✓	2	
124	1437	✓	2	
121	1403			✓

Table 6.2 shows the measured values of atmospheric conditions at the time of the Introduction Test I for corona ring type 1 using the up-and-down method.

Table 6.2: Atmospheric conditions at the time of LI – Introduction Test I (Corona ring type 1)

Atmospheric conditions: LI – Introduction Test I (Corona ring type 1)	
Temperature [°C]	26.0
Air pressure [mbar]	968.9
Air humidity [%]	44.2
Air humidity [g/m^3]	10.3

Calculation

$U_{50\%}$ under testing conditions:

$$U_p^* = \sum \frac{k_i \cdot U_i}{n} \Rightarrow U_{50\%test} = \sum \frac{U_i}{n} = \frac{61079}{43} = 1420 \text{ kV}$$

Conversion to $U_{50\%}$ under standard basic reference atmosphere:

$$K_t = 0.9372 \Rightarrow U_{50\%basicref} = 1516 \text{ kV}$$

Calculation of $U_{90\%}$ under testing condition:

$$U_{90\%test} = U_{50\%test} \cdot (1 + 1.3 \cdot 0.03) = 1420 \text{ kV} \cdot (1 + 1.3 \cdot 0.03) = 1476 \text{ kV}$$

Conversion to $U_{90\%}$ under standard basic reference atmosphere:

$$K_t = 0.9372 \Rightarrow U_{90\%basicref} = 1575 \text{ kV}$$

Calculation of $U_{10\%}$ under testing condition:

$$U_{10\%test} = U_{50\%test} \cdot (1 - 1.3 \cdot 0.03) = 1420 \text{ kV} \cdot (1 - 1.3 \cdot 0.03) = 1365 \text{ kV}$$

Conversion to $U_{10\%}$ under standard basic reference atmosphere:

$$K_t = 0.9372 \Rightarrow U_{10\%basicref} = 1457 \text{ kV}$$

Representing result

Figure 6.4 shows a plot of a voltage breakdown due to a flashover during Introduction Test I.

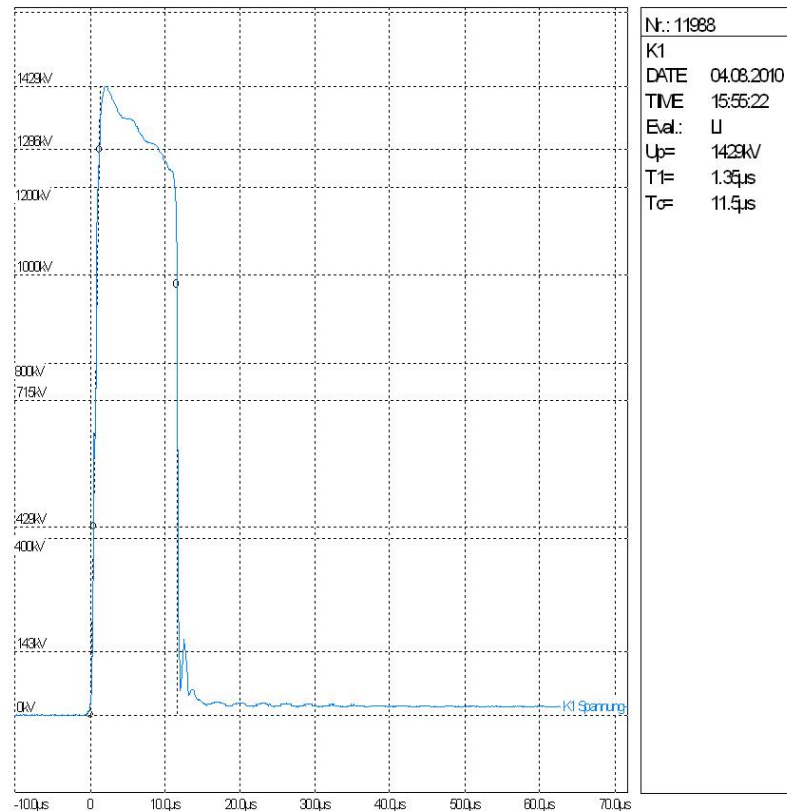


Figure 6.4: Voltage breakdown in case of flashover - Introduction Test I

6.2.2 Lightning impulse voltage – Test 1 (Corona ring type 1)

For this experiment a *distance between the conductor and the lower guy wire of 2.60 m* has been simulated. Thereby the $U_{90\%}$ -voltage with a value of 1476 kV under testing conditions was chosen as testing voltage. The calculation of this $U_{90\%}$ -value is described in section 6.1. The main target of this test was to determine in which sector of the tower window the flashover occur.

Results

Table 6.3 shows the summary of the results of the Lightning impulse voltage – Test 1 for corona ring type 1.

Table 6.3: Summary of results: LI – Test 1 (Corona ring type 1)

Lightning impulse voltage – Test 1 (Corona ring type 1)				
Voltage level		flashover	Area of flashover in tower window	No flashover
Charging voltage [kV]	Load voltage [kV]			
127.2	1471	✓	2	
	1472	✓	2	
	1473	✓	2	
	1473	✓	2	
	1474	✓	2	
	1474	✓	2	
	1473	✓	2	
	1472	✓	2	
	1472	✓	2	
	1472	✓	2	
	1474	✓	2	
	1472	✓	2	
	1472	✓	2	
	1472	✓	2	
	1473	✓	2	
	1473	✓	2	
	1473	✓	2	
	1473	✓	2	
	1471	✓	2	
	1473	✓	2	

Table 6.4 shows the measured values of atmospheric conditions at the time of the Lightning impulse voltage – Test 1 for corona ring type 1.

Table 6.4: Atmospheric conditions at the time of LI – Test 1 (Corona ring type 1)

Atmospheric conditions: LI – Test 1 (Corona ring type 1)	
Temperature [°C]	26.0
Air pressure [mbar]	968.9
Air humidity [%]	44.2
Air humidity [g/m^3]	10.3

As it can be seen in Table 6.3 all the flashovers occur in area 2, which means that they occur along the insulator.

6.2.3 Lightning impulse voltage – Test 2A (Corona ring type 1)

For this experiment a *distance between the conductor and the lower guy wire of 2.35 m* has been simulated. Thereby the $U_{90\%}$ -voltage with a value of 1476 kV under testing conditions was chosen as testing voltage. The calculation of this $U_{90\%}$ -value is described in section 6.1. The main target of this test was to determine in which sector of the tower window the flashover occur.

Results

Table 6.5 shows the summary of the results of the Lightning impulse voltage – Test 2A for corona ring type 1.

Table 6.5: Summary of results: LI – Test 2A (Corona ring type 1)

Lightning impulse voltage – Test 2A (Corona ring type 1)				
Voltage level		flashover	Area of flashover in tower window	No flashover
Charging voltage [kV]	Load voltage [kV]			
127.2	1478	✓	5	
	1477	✓	5	
	1479	✓	5	
	1478	✓	5	
	1477	✓	5	
	1477	✓	5	
	1478	✓	5	
	1478	✓	5	
	1478	✓	5	
	1478	✓	5	
	1477	✓	5	
	1477	✓	5	
	1477	✓	5	
	1478	✓	5	
	1479	✓	5	
	1478	✓	5	
	1477	✓	5	
	1478	✓	5	
	1475	✓	5	
	1477	✓	5	

Table 6.6 shows the measured values of atmospheric conditions at the time of the Lightning impulse voltage – Test 2A for corona ring type 1.

Table 6.6: Atmospheric conditions at the time of LI – Test 2A (Corona ring type 1)

Atmospheric conditions: LI – Test 2A (Corona ring type 1)	
Temperature [°C]	21.0
Air pressure [mbar]	967.0
Air humidity [%]	56.4
Air humidity [g/m^3]	10.8

As it can be seen in Table 6.5 all the flashovers occur in area 5, which means that went to the lower guy wire.

Representing result

In Figure 6.5 a flashover to the lower guy wire during Lightning impulse voltage – Test 2A is shown.

**Figure 6.5:** Flashover to the lower guy wire: LI – Test 2A

6.2.4 Lightning impulse voltage – Test 2B (Corona ring type 1)

For this experiment a *distance between the conductor and the lower guy wire of 2.44 m* has been simulated. Thereby the $U_{90\%}$ -voltage with a value of 1476 kV under testing conditions was chosen as testing voltage. The calculation of this $U_{90\%}$ -value is described in section 6.1. The main target of this test was to determine in which sector of the tower window the flashover occur.

Results

Table 6.7 shows the summary of the results of the Lightning impulse voltage – Test 2B for corona type 1.

Table 6.7: Summary of results: LI – Test 2B (Corona ring type 1)

Lightning impulse voltage – Test 2B (Corona ring type 1)				
Voltage level		flashover	Area of flashover in tower window	No flashover
Charging voltage	Load voltage			
[kV]	[kV]			
127.2	1477	✓	3	
	1477	✓	3	
	1478	✓	5	
	1477	✓	3	
	1479	✓	5	
	1479	✓	5	
	1479	✓	3	
	1480	✓	5	
	1480	✓	5	
	1478	✓	5	
	1478	✓	5	
	1480	✓	5	
	1479	✓	5	
	1479	✓	5	
	1479	✓	5	
	1475	✓	5	
	1479	✓	5	
	1480	✓	5	
	1479	✓	5	
	1478	✓	5	

Table 6.8 shows the measured values of atmospheric conditions at the time of the Lightning impulse voltage – Test 2B for corona ring type 1.

Table 6.8: Atmospheric conditions at the time of LI – Test 2B (Corona ring type 1)

Atmospheric conditions: LI – Test 2B (Corona ring type 1)	
Temperature [°C]	21.0
Air pressure [mbar]	967.0
Air humidity [%]	56.4
Air humidity [g/m^3]	10.8

As it can be seen in Table 6.7, 20 % of the flashovers occur in the area 3 which means that they occur along the insulator. The remaining 80 % went to the lower guy wire.

6.2.5 Lightning impulse voltage – Test 2C (Corona ring type 1)

For this experiment a *distance between the conductor and the lower guy wire of 2.50 m* has been simulated. Thereby the $U_{90\%}$ -voltage with a value of 1476 kV under testing conditions was chosen as testing voltage. The calculation of this $U_{90\%}$ -value is described in section 6.1. The main target of this test was to determine in which sector of the tower window the flashover occur.

Results

Table 6.9 shows the summary of the results of the Lightning impulse voltage – Test 2C for corona type 1.

Table 6.9: Summary of results: LI – Test 2C (Corona ring type 1)

Lightning impulse voltage – Test 2C (Corona ring type 1)				
Voltage level		flashover	Area of flashover in tower window	No flashover
Charging voltage [kV]	Load voltage [kV]			
127.2	1479	✓	3	
	1480	✓	3	
	1479	✓	3	
	1480	✓	3	
	1480	✓	3	
	1482	✓	3	
	1480	✓	5	
	1476	✓	3	
	1475	✓	3	
	1476	✓	3	
	1478	✓	5	
	1475	✓	3	
	1473	✓	5	
	1476	✓	5	
	1470	✓	3	
	1473	✓	5	
	1476	✓	5	
	1479	✓	3	
	1479	✓	3	
	1475	✓	3	

Table 6.10 shows the measured values of atmospheric conditions at the time of the Lightning impulse voltage – Test 2C for corona ring type 1.

Table 6.10: Atmospheric conditions at the time of LI – Test 2C (Corona ring type 1)

Atmospheric conditions: LI – Test 2C (Corona ring type 1)	
Temperature [°C]	22.0
Air pressure [mbar]	967.0
Air humidity [%]	56.4
Air humidity [g/m^3]	10.8

As it can be seen in Table 6.9, 70% of the flashovers occur in the area 3 which means that they occur along the insulator. The remaining 30% went to the lower guy wire.

Representing result

In Figure 6.6 a flashover to the lower guy wire during Lightning impulse voltage – Test 2C is shown.

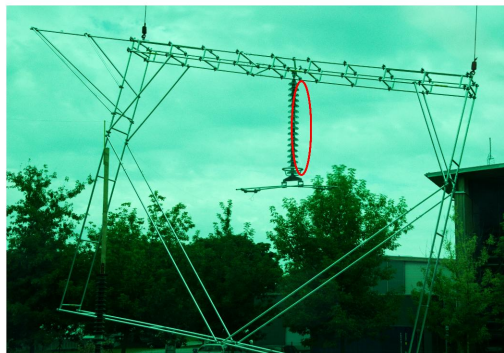


Figure 6.6: Flashover along the insulator: LI – Test 2C

6.2.6 Lightning impulse voltage – Additional Test 1 (Damper loop + Corona ring type 1)

Additional to the tests only with a corona ring, lightning impulse voltage tests using a damper loop mounted underneath one of the two conductor tubes have been carried out. The main function of this damper loop mounted at the conductor wires inside the tower window is the reduction of corona losses. Due to their position underneath the conductor tubes they also influence the electrical distances inside the tower window in reality. In Figure 6.7 a drawing of the damper loop and in Figure 6.8 a picture of the damper loop in reality is shown. Figure 6.9 shows a picture of the mounted damper loop in the testing setup. The damper loop was realized in form of a conductor wire with a diameter of 34.5 mm.

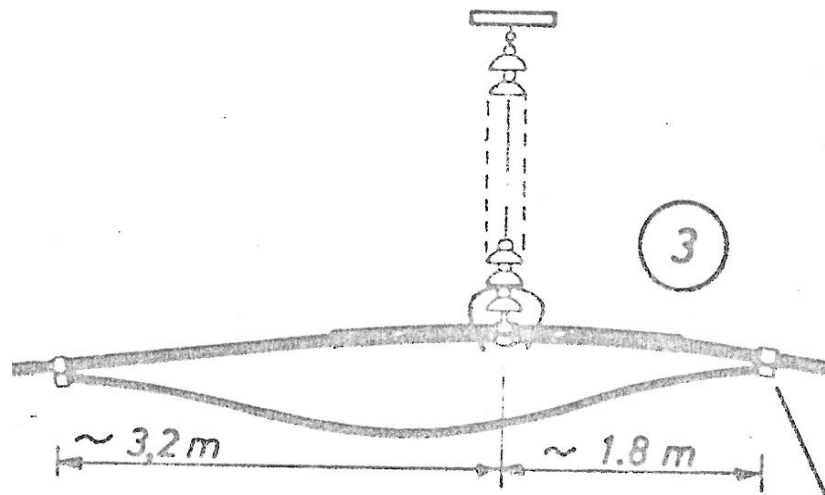


Figure 6.7: Drawing of damper loop

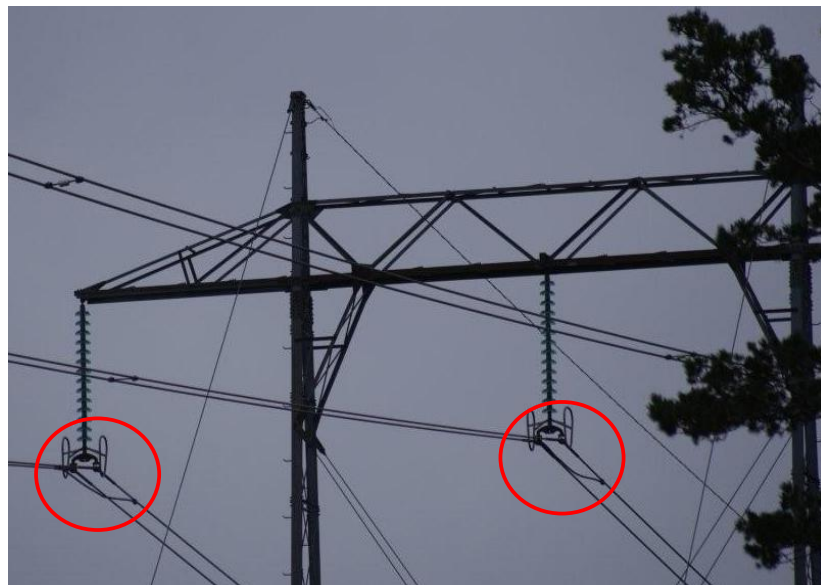


Figure 6.8: Damper loop in reality

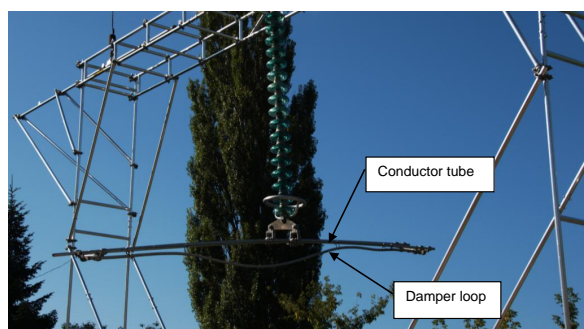


Figure 6.9: Damper loop in testing setup

At the first experiment using a damper loop a *distance between the damper loop and the lower guy wire of 2.45 m and between the conductor and the lower guy wire of 2.63 m* has been

simulated. Thereby the $U_{90\%}$ -voltage with a value of 1476 kV under testing conditions was chosen as testing voltage. The calculation of this $U_{90\%}$ -value is described in section 6.1. The main target of this test was to determine in which sector of the tower window the flashover occur.

Results

Table 6.11 shows the summary of the results of the Lightning impulse voltage – Additional Test 1 for damper loop plus corona type 1.

Table 6.11: Summary of results: LI – Additional Test 1 (Damper loop + Corona ring type 1)

Lightning impulse voltage – Additional test 1 (Damper loop + Corona ring type 1)				
Voltage level		flashover	Area of flashover in tower window	No flashover
Charging voltage	Load voltage			
[kV]	[kV]			
125.9	1474	✓	2	
	1471	✓	5	
	1471	✓	5	
	1473	✓	5	
	1472	✓	5	
	1473	✓	2	
	1474	✓	2	
	1471			✓
	1477	✓	5	
	1477	✓	5	
	1475	✓	2	
	1479	✓	2	
	1473	✓	5	
	1472	✓	2	
	1471	✓	5	
	1476	✓	2	
	1474	✓	5	
	1475	✓	2	
	1474	✓	5	
	1479	✓	5	
1479	✓	2		

Table 6.12 shows the measured values of atmospheric conditions at the time of the Lightning impulse voltage – Additional Test 1 for damper loop plus corona ring type 1.

As it can be seen in Table 6.11, 45 % of the flashovers occur in the area 2 which means that they occur along the insulator string. The remaining 55 % went to the lower guy wire.

Table 6.12: Atmospheric conditions at the time of LI – Additional Test 1 (Damper loop + Corona ring type 1)

Atmospheric conditions: LI – Additional Test 1 (Damper loop + Corona ring type 1)	
Temperature [°C]	20.0
Air pressure [mbar]	976.4
Air humidity [%]	76.0
Air humidity [g/m^3]	13.2

Representing result

In Figure 6.10 a flashover to the lower guy wire in case of Lightning impulse voltage – Additional Test 1 is shown.

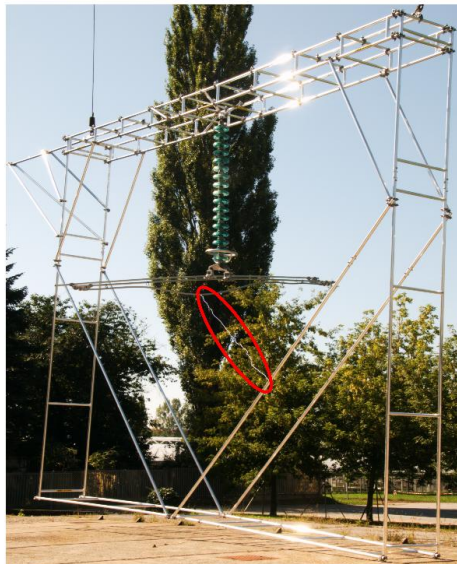


Figure 6.10: Flashover to the lower guy wire: LI – Additional Test 1

6.2.7 Lightning impulse voltage – Additional Test 2 (Damper loop + Corona ring type 1)

At this experiment using a damper loop a *distance between the damper loop and the lower guy wire of 2.27 m and between the conductor and the lower guy wire of 2.45 m* has been simulated. Thereby the $U_{90\%}$ -voltage with a value of 1476 kV under testing conditions was chosen as testing voltage. The calculation of this $U_{90\%}$ -value is described in section 6.1. The main target of this test was to determine in which sector of the tower window the flashover occur.

Results

Table 6.13 shows the summary of the results of the Lightning impulse voltage – Additional Test 2 for damper loop plus corona type 1.

Table 6.13: Summary of results: LI – Additional Test 2 (Damper loop + Corona ring type 1)

LI – Additional test 2 (Damper loop + Corona ring type 1)				
Voltage level		flashover	Area of flashover in tower window	No flashover
Charging voltage	Load voltage			
[kV]	[kV]			
125.9	1479	✓	5	
	1471	✓	5	
	1474	✓	5	
	1475	✓	5	
	1478	✓	5	
	1475	✓	5	
	1477	✓	5	
	1473	✓	5	
	1474	✓	5	
	1474	✓	5	
	1474	✓	5	
	1473	✓	5	
	1471	✓	5	
	1473	✓	5	
	1473	✓	5	
	1473	✓	5	
	1474	✓	5	
	1475	✓	5	
	1472	✓	5	
1476	✓	5		

Table 6.14 shows the measured values of atmospheric conditions at the time of the Lightning impulse voltage – Additional Test 2 for damper loop plus corona ring type 1.

Table 6.14: Atmospheric conditions at the time of LI – Additional Test 2 (Damper loop + Corona ring type 1)

Atmospheric conditions: LI – Additional Test 2 (Damper loop + Corona ring type 1)	
Temperature [°C]	21.0
Air pressure [mbar]	976.4
Air humidity [%]	70.7
Air humidity [g/m^3]	12.9

As it can be seen in Table 6.13, all the flashovers occur in the area 5 which means that they occur along the lower guy wire.

Representing result

Figure 6.11 shows a flashover to the lower guy wire during Lightning impulse voltage – Additional Test 2.

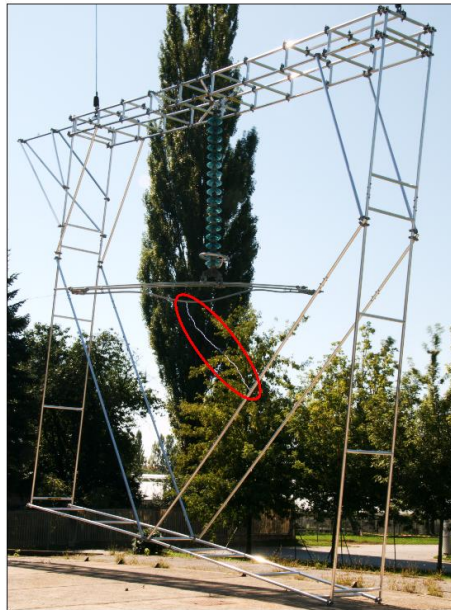


Figure 6.11: Flashover to the lower guy wire: LI – Additional Test 2

6.2.8 Lightning impulse voltage – Additional Test 3 (Damper loop + Corona ring type 1)

At this experiment using a damper loop a *distance between the damper loop and the lower guy wire of 2.27 m and between the conductor and the lower guy wire of 2.40 m* has been simulated. Thereby the $U_{90\%}$ -voltage with a value of 1476 kV under testing conditions was chosen as testing voltage. The calculation of this $U_{90\%}$ -value is described in section 6.1. The main target of this test was to determine in which sector of the tower window the flashover occur.

Results

Table 6.15 shows the summary of the results of the Lightning impulse voltage – Additional Test 3 for damper loop plus corona type 1.

Table 6.15: Summary of results: LI – Additional Test 3 (Damper loop + Corona ring type 1)

LI – Additional test 3 (Damper loop + Corona ring type 1)				
Voltage level		flashover	Area of flashover in tower window	No flashover
Charging voltage	Load voltage			
[kV]	[kV]			
125.9	1471	✓	2	
	1474	✓	2	
	1471	✓	2	
	1471	✓	2	
	1473	✓	2	
	1470	✓	2	
	1473	✓	2	
	1473	✓	2	
	1478	✓	5	
	1474	✓	2	
	1477	✓	2	
	1474	✓	5	
	1479	✓	2	
	1478	✓	2	
	1477	✓	2	
	1477	✓	2	
	1476	✓	2	
	1474	✓	2	
	1475	✓	2	
	1476	✓	5	

Table 6.16 shows the measured values of atmospheric conditions at the time of the Lightning impulse voltage – Additional Test 3 for damper loop plus corona ring type 1.

Table 6.16: Atmospheric conditions at the time of LI – Additional Test 3

Atmospheric conditions: LI – Additional Test 3 (Damper loop + Corona ring type 1)	
Temperature [°C]	24.0
Air pressure [mbar]	975.3
Air humidity [%]	60.7
Air humidity [g/m^3]	13.0

As it can be seen in Table 6.15, 85 % of the flashovers occur in the area 2 which means that they occur along the insulator string. The remaining 15 % went to the lower guy wire.

Representing result

In Figure 6.12 a flashover to the lower guy wire in case of Lightning impulse voltage – Additional Test 3 is shown.

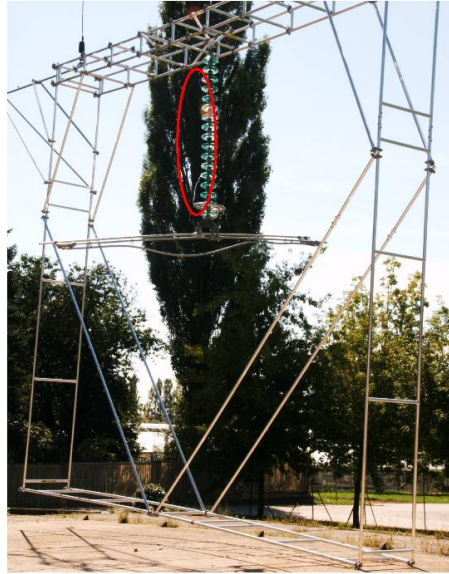


Figure 6.12: Flashover along the insulator: LI – Additional Test 3

6.2.9 Discussion of test results

As shown in section 6.2.1, in case of corona ring type 1 and lightning impulse voltage, for a swing angle of 0° a withstand voltage $U_{10\%}$ of 1457 kV has been measured under standard basic reference atmosphere. In Table 3.1 the required withstand voltage values given in the international standard IEC 60071 – Part 1 [25] for several operating voltage levels are shown. A comparison of the value from the practical test with these values shows, that the measured result is higher than the applicable withstand voltage range (1050 ÷ 1425 kV).

6.3 Lightning impulse voltage Tests – Corona ring type 2

Figure 6.14 shows the total testing plan for the lightning impulse voltage tests in case of the type 2 of corona ring (2-ring corona ring, see also Figure 6.13)

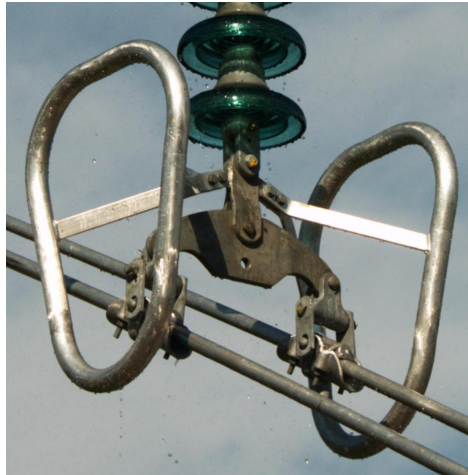


Figure 6.13: Corona ring type 2

INTRODUCTION TEST II

- # insulators = 16
- corona ring type 2
- Swing angle = 0°
- Distance to guy wire $a = 2.70$ m
- Up-and-down-method (40 enhancement, 20 flashovers)
- Determination $U_{50\%}$
- Classification of tower window in 6 areas
- Photography of flashover (where does flashover occur?)



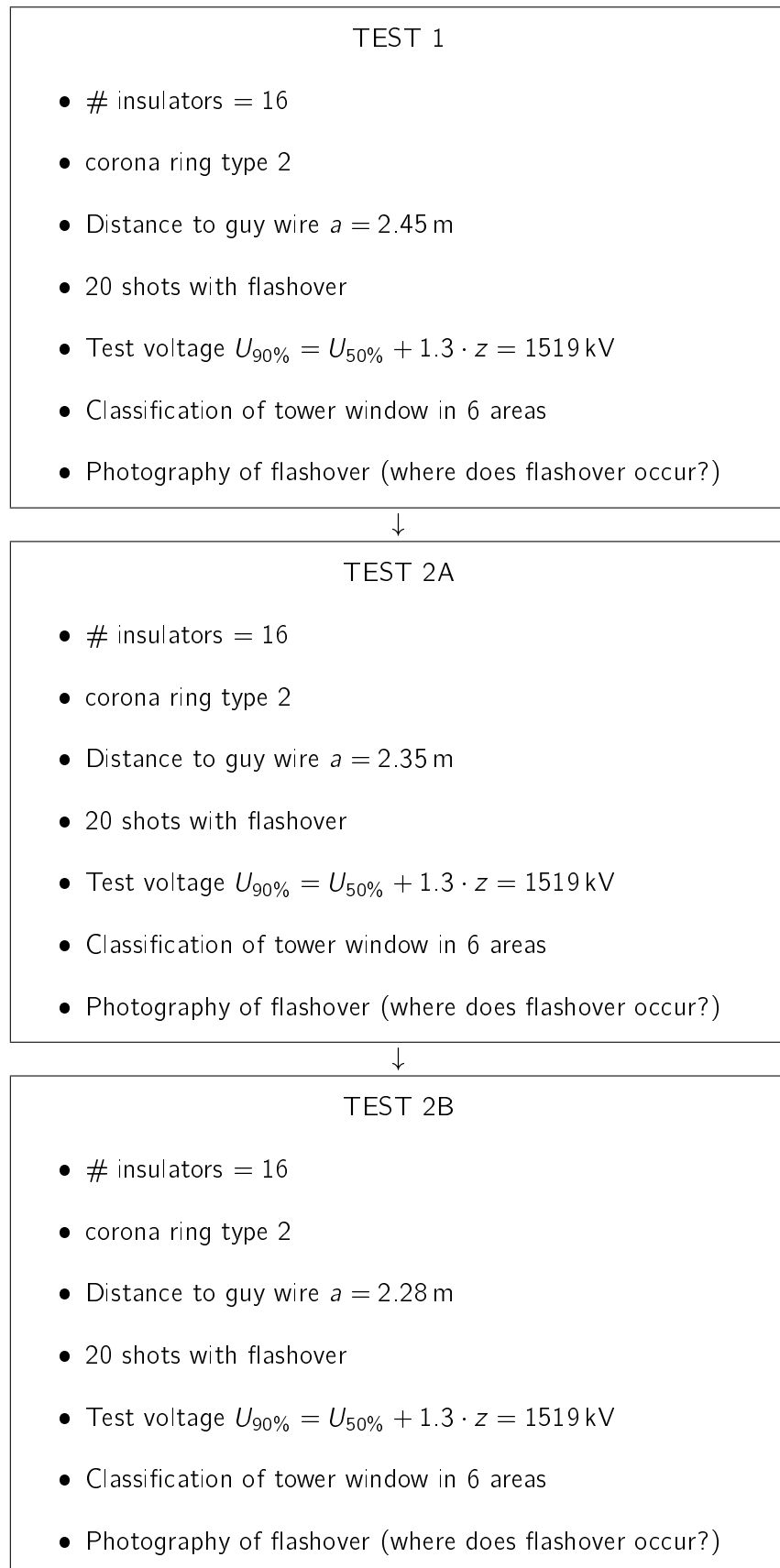


Figure 6.14: Testing plan: Lightning impulse voltage Tests – Corona ring type 2

6.3.1 Lightning impulse voltage – Introduction Test II (Corona ring type 2)

Thereby a *swing angle* of 0° has been simulated and a *distance* of 2.70 m between conductor and the lower guy wire has been measured. As mentioned before the main target of this test was to determine the $U_{50\%}$ -voltage and the calculation of the $U_{90\%}$ -voltage.

Results

Table 6.17 shows a summary of the results of the Introduction Test II for corona ring type 2 using the up-and-down method.

Table 6.17: Summary of results: LI – Introduction Test II (Corona ring type 2)

Lightning impulse voltage – Introduction Test II (Corona ring type 2)				
Voltage level		flashover	Area of flashover in tower window	No flashover
Charging voltage [kV]	Load voltage [kV]			
124	1449			✓
127	1483	✓	3	
124	1449			✓
127	1484	✓	2	
124	1447			✓
127	1483	✓	2	
124	1448			✓
127	1484	✓	2	
124	1448			✓
127	1483	✓	2	
124	1448			✓
127	1483			✓
130	1517	✓	2	
127	1480	✓	2	
124	1447			✓
127	1483	✓	3	
124	1448			✓
127	1483	✓	3	
124	1448			✓
127	1483	✓	2	
124	1446			✓
127	1482	✓	2	
124	1449			✓
127	1483	✓	3	

Continued on next page

Table 6.17 – continued from previous page

124	1449			✓
127	1483	✓	3	
124	1449			✓
127	1484	✓	3	
124	1450			✓
127	1484	✓	2	
124	1449			✓
127	1483	✓	3	
124	1449			✓
127	1483	✓	2	
124	1447			✓
127	1485	✓	3	
124	1448			✓
127	1484	✓	2	
124	1450			✓
127	1483	✓	2	

Table 6.18 shows the measured values of atmospheric conditions at the time of the Introduction Test II for corona ring type 2 using the up-and-down method.

Table 6.18: Atmospheric conditions at the time of LI – Introduction Test II (Corona ring type 2)

Atmospheric conditions: LI – Introduction Test II (Corona ring type 2)	
Temperature [°C]	21.0
Air pressure [mbar]	969.3
Air humidity [%]	73.6
Air humidity [g/m^3]	13.7

Calculation

$U_{50\%}$ under testing conditions:

$$U_p^* = \sum \frac{k_i \cdot U_i}{n} \Rightarrow U_{50\%test} = \sum \frac{U_i}{n} = \frac{58489}{40} = 1462 \text{ kV}$$

Conversion to $U_{50\%}$ under standard basic reference atmosphere:

$$K_t = 0.9857 \Rightarrow U_{50\%basicref} = 1483 \text{ kV}$$

Calculation of $U_{90\%}$ under testing condition:

$$U_{90\%test} = U_{50\%test} \cdot (1 + 1.3 \cdot 0.03) = 1462 \text{ kV} \cdot (1 + 1.3 \cdot 0.03) = 1519 \text{ kV}$$

Conversion to $U_{90\%}$ under standard basic reference atmosphere:

$$K_t = 0.9857 \Rightarrow U_{90\%basicref} = 1541 \text{ kV}$$

Calculation of $U_{10\%}$ under testing condition:

$$U_{10\%test} = U_{50\%test} \cdot (1 - 1.3 \cdot 0.03) = 1462 \text{ kV} \cdot (1 - 1.3 \cdot 0.03) = 1405 \text{ kV}$$

Conversion to $U_{10\%}$ under standard basic reference atmosphere:

$$K_t = 0.9857 \Rightarrow U_{10\%basicref} = 1426 \text{ kV}$$

6.3.2 Lightning impulse voltage – Test 1 (Corona ring type 2)

For this experiment a *distance between the corona ring and the lower guy wire of 2.45 m* has been simulated. Thereby the $U_{90\%}$ -voltage with a value of 1519 kV under testing conditions was chosen as testing voltage. The calculation of this $U_{90\%}$ -value is described in section 6.1. The main target of this test was to determine in which sector of the tower window the flashover occur.

Results

Table 6.19 shows the summary of the results of the Lightning impulse voltage – Test 1 for corona type 2.

Table 6.19: Summary of results: LI – Test 1 (Corona ring type 2)

Lightning impulse voltage – Test 1 (Corona ring type 2)				
Voltage level		flashover	Area of flashover in tower window	No flashover
Charging voltage [kV]	Load voltage [kV]			
131	1518	✓	2	
	1520	✓	2	
	1518	✓	2	
	1518	✓	2	
	1519	✓	2	
	1519	✓	2	
	1519	✓	2	
	1520	✓	2	
	1520	✓	2	
	1521	✓	2	
	1520	✓	2	
	1519	✓	3	
	1519	✓	3	
	1520	✓	2	

Continued on next page

Table 6.19 – continued from previous page

131	1519	✓	2	
	1518	✓	2	
	1519	✓	2	
	1518	✓	3	
	1518	✓	2	
	1518	✓	2	

Table 6.20 shows the measured values of atmospheric conditions at the time of the Lightning impulse voltage – Test 1 for corona ring type 2.

Table 6.20: Atmospheric conditions at the time of LI – Test 1 (Corona ring type 2)

Atmospheric conditions: LI – Test 1 (Corona ring type 2)	
Temperature [°C]	21.0
Air pressure [mbar]	971.1
Air humidity [%]	53.8
Air humidity [g/m^3]	9.8

As it can be seen in Table 6.19 all the flashovers occur in area 2 and area 3, which means that they occur along the insulator.

6.3.3 Lightning impulse voltage – Test 2A (Corona ring type 2)

For this experiment a *distance between the corona ring and the lower guy wire of 2.35 m* has been simulated. Thereby the $U_{90\%}$ -voltage with a value of 1519 kV under testing conditions was chosen as testing voltage. The calculation of this $U_{90\%}$ -value is described in section 6.1. The main target of this test was to determine in which sector of the tower window the flashover occur.

Results

Table 6.21 shows the summary of the results of the Lightning impulse voltage – Test 2A for corona type 2.

Table 6.21: Summary of results: LI – Test 2A (Corona ring type 2)

Lightning impulse voltage – Test 2A (Corona ring type 2)				
Voltage level		flashover	Area of flashover in tower window	No flashover
Charging voltage	Load voltage			
[kV]	[kV]			
131	1522	✓	2	
	1522	✓	2	

Continued on next page

Table 6.21 – continued from previous page

131	1522	✓	2	
	1522	✓	2	
	1523	✓	2	
	1519	✓	2	
	1520	✓	2	
	1522	✓	5	
	1521	✓	2	
	1521	✓	2	
	1520	✓	2	
	1518	✓	2	
	1518	✓	2	
	1518	✓	2	
	1519	✓	2	
	1519	✓	2	
	1520	✓	2	
	1520	✓	2	
	1519	✓	2	
1518	✓	2		

Table 6.22 shows the measured values of atmospheric conditions at the time of the Lightning impulse voltage – Test 2A for corona ring type 2.

Table 6.22: Atmospheric conditions at the time of LI – Test 2A (Corona ring type 2)

Atmospheric conditions: LI – Test 2A (Corona ring type 2)	
Temperature [°C]	21.0
Air pressure [mbar]	971.0
Air humidity [%]	53.4
Air humidity [g/m^3]	9.6

As it can be seen in Table 6.21, 95 % of the flashovers occur in area 2, which means that they occur along the insulator. The remaining 5 % of the flashovers went to the lower guy wire.

6.3.4 Lightning impulse voltage – Test 2B (Corona ring type 2)

For this experiment a *distance between the corona ring and the lower guy wire of 2.28 m* has been simulated. Thereby the $U_{90\%}$ -voltage with a value of 1519 kV under testing conditions was chosen as testing voltage. The calculation of this $U_{90\%}$ -value is described in section 6.1. The main target of this test was to determine in which sector of the tower window the flashover occur.

Results

Table 6.23 shows the summary of the results of the Lightning impulse voltage – Test 2B for corona ring type 2.

Table 6.23: Summary of results: LI – Test 2B (Corona ring type 2)

Lightning impulse voltage – Test 2B (Corona ring type 2)				
Voltage level		flashover	Area of flashover in tower window	No flashover
Charging voltage	Load voltage			
[kV]	[kV]			
131	1518	✓	5	
	1518	✓	5	
	1519	✓	5	
	1517	✓	5	
	1516	✓	5	
	1514	✓	5	
	1517	✓	5	
	1515	✓	5	
	1516	✓	5	
	1518	✓	5	
	1516	✓	5	
	1515	✓	5	
	1517	✓	5	
	1515	✓	5	
	1516	✓	5	
	1514	✓	5	
	1514	✓	5	
	1514	✓	5	
	1516	✓	5	
1514	✓	5		

Table 6.24 shows the measured values of atmospheric conditions at the time of the Lightning impulse voltage – Test 2B for corona ring type 2.

Table 6.24: Atmospheric conditions at the time of LI – Test 2B (Corona ring type 2)

Atmospheric conditions: LI – Test 2B (Corona ring type 2)	
Temperature [°C]	21.0
Air pressure [mbar]	968.0
Air humidity [%]	52.8
Air humidity [g/m^3]	9.3

As it can be seen in Table 6.21, all the flashovers occur in area 5, which means that they went to the lower guy wire.

6.3.5 Discussion of test results

As shown in section 6.3.1, in case of corona ring type 2 and lightning impulse voltage, for a swing angle of 0° a withstand voltage $U_{10\%}$ of 1426 kV has been measured under basic reference atmosphere. In Table 3.1 the required withstand voltage values given in the international standard IEC 60071 – Part 1 [25] for several operating voltage levels are shown. A comparison of the value from the practical test with these values shows, that the measured result is higher than the applicable withstand voltage range (1050 ÷ 1425 kV).

6.4 Basics – Switching impulse voltage Tests

In contrast to the lightning impulse voltage tests the main goal of the tests with switching impulse voltage was to find out the value of the $U_{50\%}$ -voltage and arising thereby the $U_{90\%}$ -voltage and the $U_{10\%}$ -voltage. Similar to the lightning impulse voltage tests the tests have been carried out with the two different types of corona rings as they are described in section 5.3 to make a point concerning the voltage behaviour of the corona ring additional to the voltage behaviour of specified swing angles and distances, respectively. The equation for the calculation of the $U_{90\%}$ -voltage in case of switching impulse voltage is equal to lightning impulse voltage (see Equation (6.1) in section 6.1), whereby $z = 0.06$ in case of switching impulse voltage [32]. Using Equation (6.2) (section 6.1) the $U_{10\%}$ -voltage, can be calculated similar to lightning impulse voltage.

Similar to lightning impulse voltage the $U_{50\%}$ -voltage is necessary for the calculation of the $U_{90\%}$ -voltage and the $U_{10\%}$ -voltage, respectively. Also the calculation of the $U_{50\%}$ -withstand-voltage using the up-and-down method as well as the conversion in values under standard basic reference atmosphere is equal to lightning impulse voltage tests (see Equation (6.3) (6.4) (6.5) in section 6.1).

To calculate the atmospheric correction factor respectively the given flashover voltage under standard basic reference atmosphere, the atmospheric outdoor conditions have been measured during the tests by use of the measuring device mounted at the High Voltage Laboratory. Specifically, the following three values of atmospheric outdoor conditions have been measured:

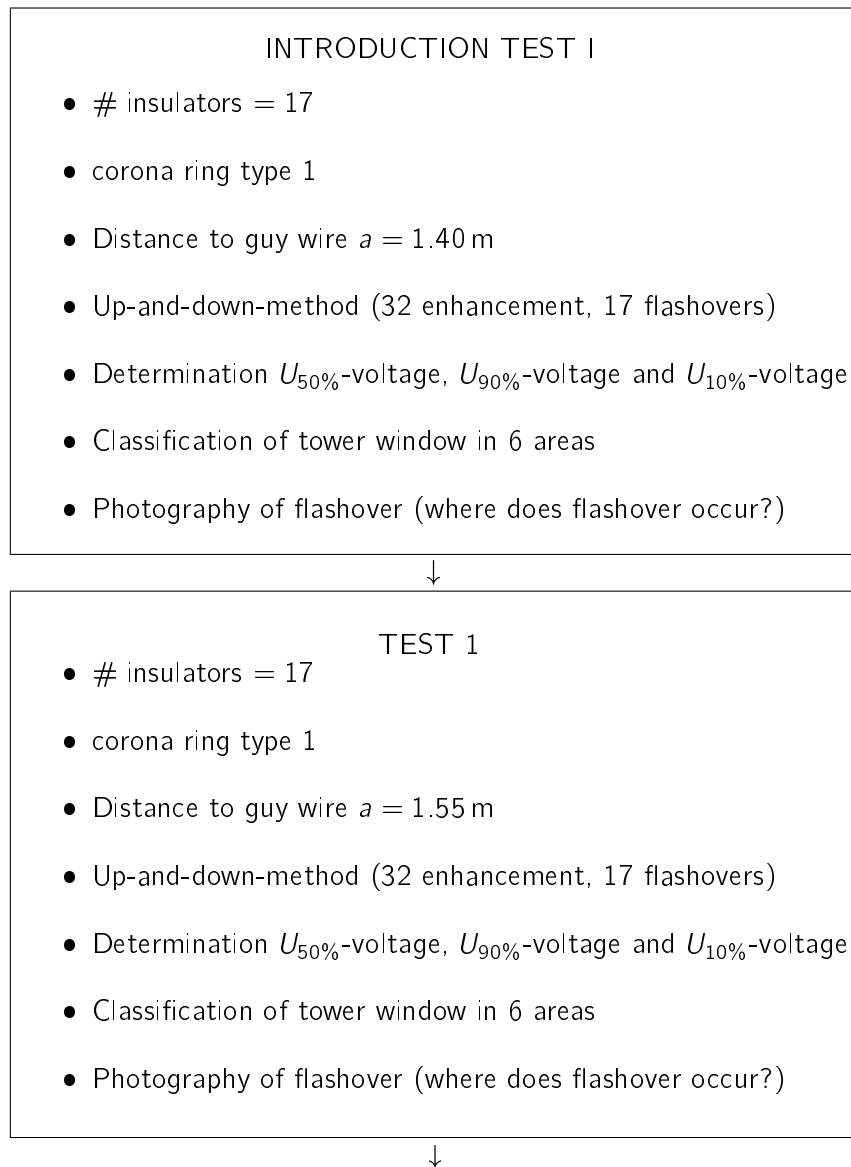
1. Temperature in [°C]
2. Air pressure in [mbar]
3. Air humidity in [%] and [g/m^3]

The correction factor K_t arising from this measured atmospheric outdoor conditions have been calculated by use of an excel-sheet. Additional to the estimation of the $U_{50\%}$ -voltage and arising thereby the calculation of the $U_{90\%}$ -voltage and the $U_{10\%}$ -voltage, an evaluation, where the flashover occur inside the model, has been carried out. Therefore similar to the lightning impulse voltage the tower window has been classified in 6 areas (see also Figure 6.1) and all flashovers had been photographed to assign to the appropriate area. Concerning the results of the tests it must be mentioned that the impulse voltage generator of the High Voltage Laboratory consists of 13 stages, which are charged parallel and discharged in series by use of spark gaps. The first value of the voltage level in all tables of results is the charging voltage (per stage) and the second value of the measured load voltage which arise from the series connection of the capacitances. The variation of the voltage level has been accomplished by variation of the charging voltage of the capacitances. Attention should be paid to the fact that in case of a flashover the load voltage break down before peak value. The values given in the table in that case are calculated by the ratio of the charging voltages.

Between the impulses an waiting time of 1 minute was chosen in all tests. The value in the column "area of flashover in tower window" of the tables in case of flashover denotes the area of the tower window in which the flashover occur according to Figure 6.1.

6.5 Switching impulse voltage Tests – Corona ring type 1

Figure 6.15 shows the total testing plan for the switching impulse voltage tests in case of the type 1 of corona ring (1-ring corona ring, see also Figure 6.2).



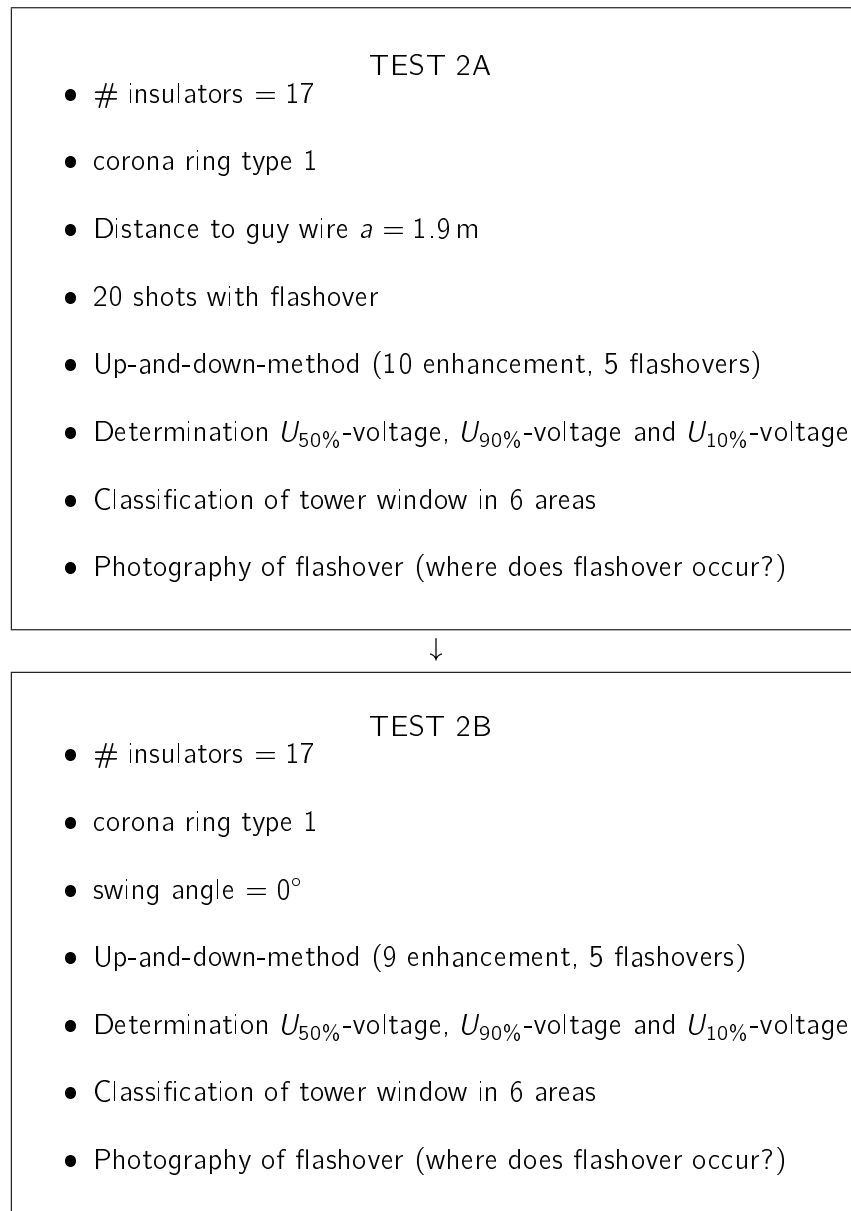


Figure 6.15: Testing plan: Switching impulse voltage Tests – Corona ring type 1

6.5.1 Switching impulse voltage – Introduction Test I (Corona ring type 1)

At the first experiment a *distance of 1.55 m between conductor and the lower guy wire* has been simulated. As mentioned before the main target of this test was to determine the $U_{50\%}$ -voltage and the calculation of the $U_{90\%}$ -voltage and $U_{10\%}$ -voltage, respectively.

Results

Table 6.25 shows a summary of the results of the Introduction Test I for corona ring type 1 using the up-and-down method.

Table 6.25: Summary of results: SI – Introduction Test I (Corona ring type 1)

Switching impulse voltage – Introduction Test I (Corona ring type 1)				
Voltage level		flashover	Area of flashover in tower window	No flashover
Charging voltage	Load voltage			
[kV]	[kV]			
86	846			✓
89	875	✓	5	
86	846	✓	5	
83	814			✓
86	845			✓
89	875			✓
92	904	✓	5	
89	875	✓	5	
86	845	✓	5	
83	815			✓
86	847			✓
89	875	✓	5	
86	845			✓
89	878			✓
92	904	✓	5	
89	875	✓	5	
86	845	✓	5	
83	815			✓
86	845	✓	5	

Table 6.26 shows the measured values of atmospheric conditions at the time of the Introduction Test I for corona ring type 1 using the up-and-down method.

Table 6.26: Atmospheric conditions at the time of SI – Introduction Test I (Corona ring type 1)

Atmospheric conditions: SI – Introduction Test I (Corona ring type 1)	
Temperature [°C]	19.0
Air pressure [mbar]	967.4
Air humidity [%]	83.5
Air humidity [g/m^3]	13.0

Calculation

$U_{50\%}$ under testing conditions:

$$U_p^* = \sum \frac{k_i \cdot U_i}{n} \Rightarrow U_{50\%test} = \sum \frac{U_i}{n} = \frac{16269}{19} = 856 \text{ kV}$$

Conversion to $U_{50\%}$ under standard basic reference atmosphere:

$$K_t = 0.9828 \Rightarrow U_{50\%basicref} = 871 \text{ kV}$$

Calculation of $U_{90\%}$ under testing condition:

$$U_{90\%test} = U_{50\%test} \cdot (1 + 1.3 \cdot 0.06) = 856 \text{ kV} \cdot (1 + 1.3 \cdot 0.06) = 923 \text{ kV}$$

Conversion to $U_{90\%}$ under standard basic reference atmosphere:

$$K_t = 0.9828 \Rightarrow U_{90\%basicref} = 939 \text{ kV}$$

Calculation of $U_{10\%}$ under testing condition:

$$U_{10\%test} = U_{50\%test} \cdot (1 - 1.3 \cdot 0.06) = 856 \text{ kV} \cdot (1 - 1.3 \cdot 0.06) = 789 \text{ kV}$$

Conversion to $U_{10\%}$ under standard basic reference atmosphere:

$$K_t = 0.9828 \Rightarrow U_{10\%basicref} = 803 \text{ kV}$$

Representing result

In Figure 6.16 a standard impulse voltage due to a non-flashover during Introduction Test I is shown.

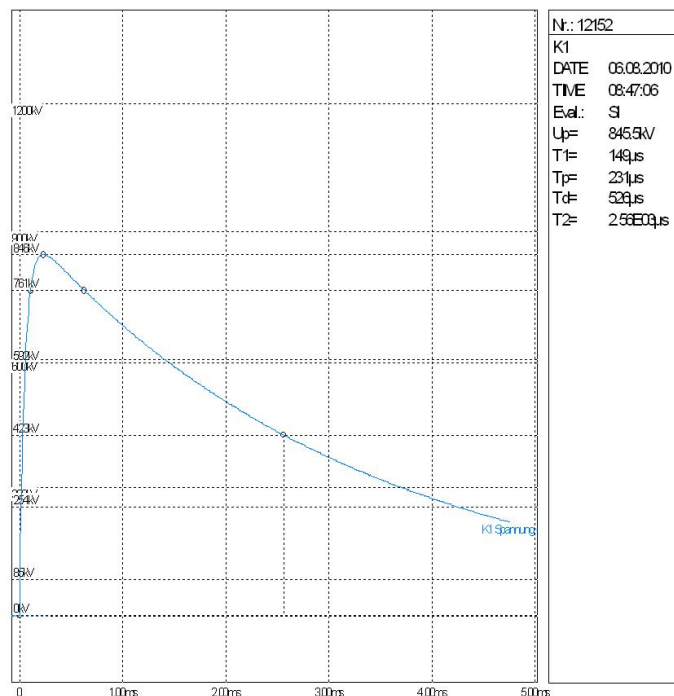


Figure 6.16: Standard impulse voltage (250/2500 μ s) in case of non-flashover: SI – Introduction Test I

6.5.2 Switching impulse voltage – Test 1 (Corona ring type 1)

At this experiment a *distance of 1.40 m between conductor and the lower guy wire* has been simulated. As mentioned before the main target of this test was to determine the $U_{50\%}$ -voltage and the calculation of the $U_{90\%}$ -voltage and $U_{10\%}$ -voltage, respectively.

Results

Table 6.27 shows the summary of the results of the Switching impulse voltage – Test 1 for corona type 1.

Table 6.27: Summary of results: SI – Test 1 (Corona ring type 1)

Switching impulse voltage – Test 1 (Corona ring type 1)				
Voltage level		flashover	Area of flashover in tower window	No flashover
Charging voltage [kV]	Load voltage [kV]			
81	795			✓
84	824	✓	5	
81	795			✓
84	824	✓	5	
81	794			✓
84	824	✓	5	
81	794	✓	5	
78	763			✓
81	794	✓	5	
78	763	✓	5	
75	734			✓
78	763			✓
81	796	✓	5	
78	763	✓	5	
75	734			✓
78	763	✓	5	
75	734			✓
78	763			✓
81	795			✓
84	824			✓
87	853	✓	5	
84	825			✓
87	853	✓	5	
84	825	✓	5	

Continued on next page

Table 6.27 – continued from previous page

81	795	✓	5	
78	765			✓
81	795	✓	5	
78	765	✓	5	
75	734			✓
78	765	✓	5	
75	734	✓	5	
72	701			✓

Table 6.28 shows the measured values of atmospheric conditions at the time of the Switching impulse voltage – Test 1 for corona ring type 1 using the up-and-down method.

Table 6.28: Atmospheric conditions at the time of SI – Test 1 (Corona ring type 1)

Atmospheric conditions: SI – Test 1 (Corona ring type 1)	
Temperature [°C]	21.0
Air pressure [mbar]	968.4
Air humidity [%]	74.6
Air humidity [g/m^3]	13.5

Calculation

$U_{50\%}$ under testing conditions:

$$U_p^* = \sum \frac{k_i \cdot U_i}{n} \Rightarrow U_{50\%test} = \sum \frac{U_i}{n} = \frac{25049}{32} = 783 \text{ kV}$$

Conversion to $U_{50\%}$ under standard basic reference atmosphere:

$$K_t = 0.9829 \Rightarrow U_{50\%basicref} = 796 \text{ kV}$$

Calculation of $U_{90\%}$ under testing condition:

$$U_{90\%test} = U_{50\%test} \cdot (1 + 1.3 \cdot 0.06) = 783 \text{ kV} \cdot (1 + 1.3 \cdot 0.06) = 844 \text{ kV}$$

Conversion to $U_{90\%}$ under standard basic reference atmosphere:

$$K_t = 0.9829 \Rightarrow U_{90\%basicref} = 859 \text{ kV}$$

Calculation of $U_{10\%}$ under testing condition:

$$U_{10\%test} = U_{50\%test} \cdot (1 - 1.3 \cdot 0.06) = 783 \text{ kV} \cdot (1 - 1.3 \cdot 0.06) = 722 \text{ kV}$$

Conversion to $U_{10\%}$ under standard basic reference atmosphere:

$$K_t = 0.9829 \Rightarrow U_{10\%basicref} = 734 \text{ kV}$$

Representing result

In Figure 6.17 a flashover to the lower guy wire during Switching impulse voltage – Test 1 can be seen.

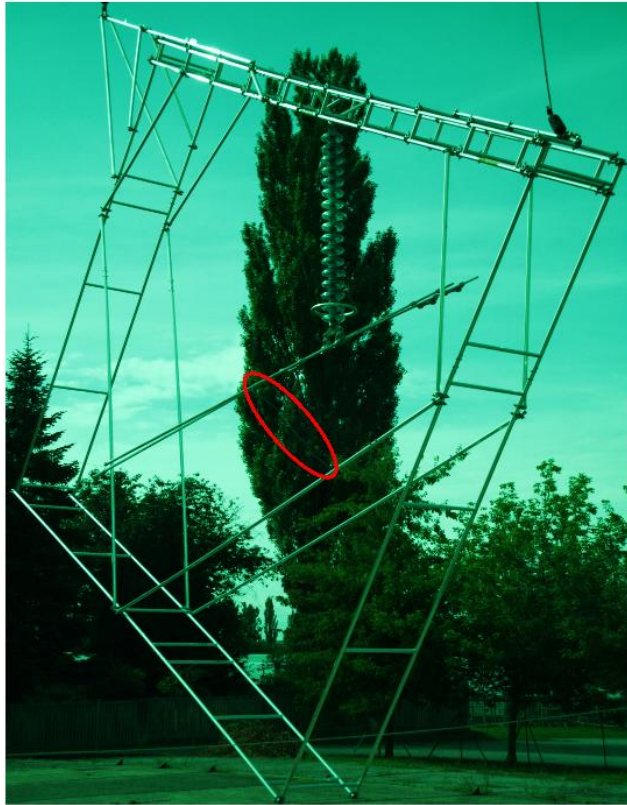


Figure 6.17: Flashover to the lower guy wire: SI – Test 1

6.5.3 Switching impulse voltage – Test 2A (Corona ring type 1)

At this experiment a *distance of 1.90 m between conductor and the lower guy wire* has been simulated. As mentioned before the main target of this test was to determine the $U_{50\%}$ -voltage and the calculation of the $U_{90\%}$ -voltage and $U_{10\%}$ -voltage, respectively.

Results

Table 6.29 shows the summary of the results of the Switching impulse voltage – Test 2A for corona type 1 using the up-and-down method.

Table 6.29: Summary of results: SI – Test 2A (Corona ring type 1)

Switching impulse voltage – Test 2A (Corona ring type 1)				
Voltage level		flashover	Area of flashover in tower window	No flashover
Charging voltage [kV]	Load voltage [kV]			
92	902			✓
95	931	✓	5	
92	903			✓
95	933			✓
98	962	✓	5	
95	933			✓
98	962	✓	3	
95	933	✓	5	
92	903			✓
95	932	✓	5	

Table 6.30 shows the measured values of atmospheric conditions at the time of the Switching impulse voltage – Test 2A for corona ring type 1 using the up-and-down method.

Table 6.30: Atmospheric conditions at the time of SI – Test 2A (Corona ring type 1)

Atmospheric conditions: SI – Test 2A (Corona ring type 1)	
Temperature [°C]	26.0
Air pressure [mbar]	975.6
Air humidity [%]	53.8
Air humidity [g/m^3]	12.6

Calculation

$U_{50\%}$ under testing conditions:

$$U_p^* = \sum \frac{k_i \cdot U_i}{n} \Rightarrow U_{50\%test} = \sum \frac{U_i}{n} = \frac{9294}{10} = 929 \text{ kV}$$

Conversion to $U_{50\%}$ under standard basic reference atmosphere:

$$K_t = 0.9659 \Rightarrow U_{50\%basicref} = 962 \text{ kV}$$

Calculation of $U_{90\%}$ under testing condition:

$$U_{90\%test} = U_{50\%test} \cdot (1 + 1.3 \cdot 0.06) = 929 \text{ kV} \cdot (1 + 1.3 \cdot 0.06) = 1002 \text{ kV}$$

Conversion to $U_{90\%}$ under standard basic reference atmosphere:

$$K_t = 0.9659 \Rightarrow U_{90\%basicref} = 1037 \text{ kV}$$

Calculation of $U_{10\%}$ under testing condition:

$$U_{10\%test} = U_{50\%test} \cdot (1 - 1.3 \cdot 0.06) = 929 \text{ kV} \cdot (1 - 1.3 \cdot 0.06) = 857 \text{ kV}$$

Conversion to $U_{10\%}$ under standard basic reference atmosphere:

$$K_t = 0.9659 \Rightarrow U_{10\%basicref} = 887 \text{ kV}$$

Representing result

Figure 6.18 shows a plot of a voltage breakdown due to a flashover during Switching impulse voltage – Test 2A.

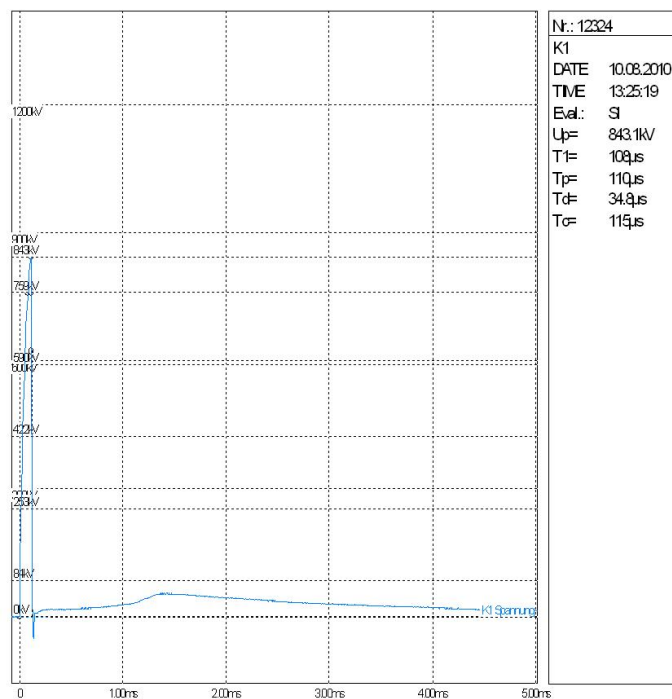


Figure 6.18: Voltage breakdown in case of flashover – Switching impulse voltage – Test 2A

6.5.4 Switching impulse voltage – Test 2B (Corona ring type 1)

At this experiment a *swing angle* of 0° has been simulated and a *distance* of 2,87m between conductor and the lower guy wire has been measured. As mentioned before the main target of this test was to determine the $U_{50\%}$ -voltage and the calculation of the $U_{90\%}$ -voltage and $U_{10\%}$ -voltage, respectively.

Results

Table 6.31 shows a summary of the results of the Switching impulse voltage – Test 2B for corona ring type 1 using the up-and-down method.

Table 6.31: Summary of results: SI – Test 2B (Corona ring type 1)

Switching impulse voltage – Test 2B (Corona ring type 1)				
Voltage level		flashover	Area of flashover in tower window	No flashover
Charging voltage [kV]	Load voltage [kV]			
110	1093			✓
115	1143	✓	2	
110	1093	✓	2	
105	1042			✓
110	1093	✓	2	
105	1042			✓
110	1093	✓	2	
105	1045			✓
110	1093	✓	2	

Table 6.32 shows the measured values of atmospheric conditions at the time of the Switching impulse voltage – Test 2B for corona ring type 1 using the up-and-down method.

Table 6.32: Atmospheric conditions at the time of SI – Test 2B (Corona ring type 1)

Atmospheric conditions: SI – Test 2B (Corona ring type 1)	
Temperature [°C]	21.0
Air pressure [mbar]	977.6
Air humidity [%]	67.8
Air humidity [g/m^3]	11.6

Calculation

$U_{50\%}$ under testing conditions:

$$U_p^* = \sum \frac{k_i \cdot U_i}{n} \Rightarrow U_{50\%test} = \sum \frac{U_i}{n} = \frac{9739}{9} = 1082 \text{ kV}$$

Conversion to $U_{50\%}$ under standard basic reference atmosphere:

$$K_t = 0.9853 \Rightarrow U_{50\%basicref} = 1098 \text{ kV}$$

Calculation of $U_{90\%}$ under testing condition:

$$U_{90\%test} = U_{50\%test} \cdot (1 + 1.3 \cdot 0.06) = 1082 \text{ kV} \cdot (1 + 1.3 \cdot 0.06) = 1167 \text{ kV}$$

Conversion to $U_{90\%}$ under standard basic reference atmosphere:

$$K_t = 0.9853 \Rightarrow U_{90\%basicref} = 1184 \text{ kV}$$

Calculation of $U_{10\%}$ under testing condition:

$$U_{10\%test} = U_{50\%test} \cdot (1 - 1.3 \cdot 0.06) = 1082 \text{ kV} \cdot (1 - 1.3 \cdot 0.06) = 998 \text{ kV}$$

Conversion to $U_{10\%}$ under standard basic reference atmosphere:

$$K_t = 0.9853 \Rightarrow U_{10\%basicref} = 1013 \text{ kV}$$

6.5.5 Discussion of test results

As shown in section 6.5.4, in case of corona ring type 1 and switching impulse voltage, for a swing angle of 0° a withstand voltage $U_{10\%}$ of 1013 kV has been measured under standard basic reference atmosphere. In Table 3.1 the required withstand voltage values given in the international standard IEC 60071 – Part 1 [25] for several operating voltage levels are shown. A comparison of the value from the practical test with these values shows, that the measured result is within the applicable withstand voltage range (850 ÷ 1050 kV).

6.6 Switching impulse voltage Tests – Corona ring type 2

Figure 6.19 shows the total testing plan for the Switching impulse voltage tests in case of the type 2 of corona ring (2-ring corona ring, see also Figure 6.13).

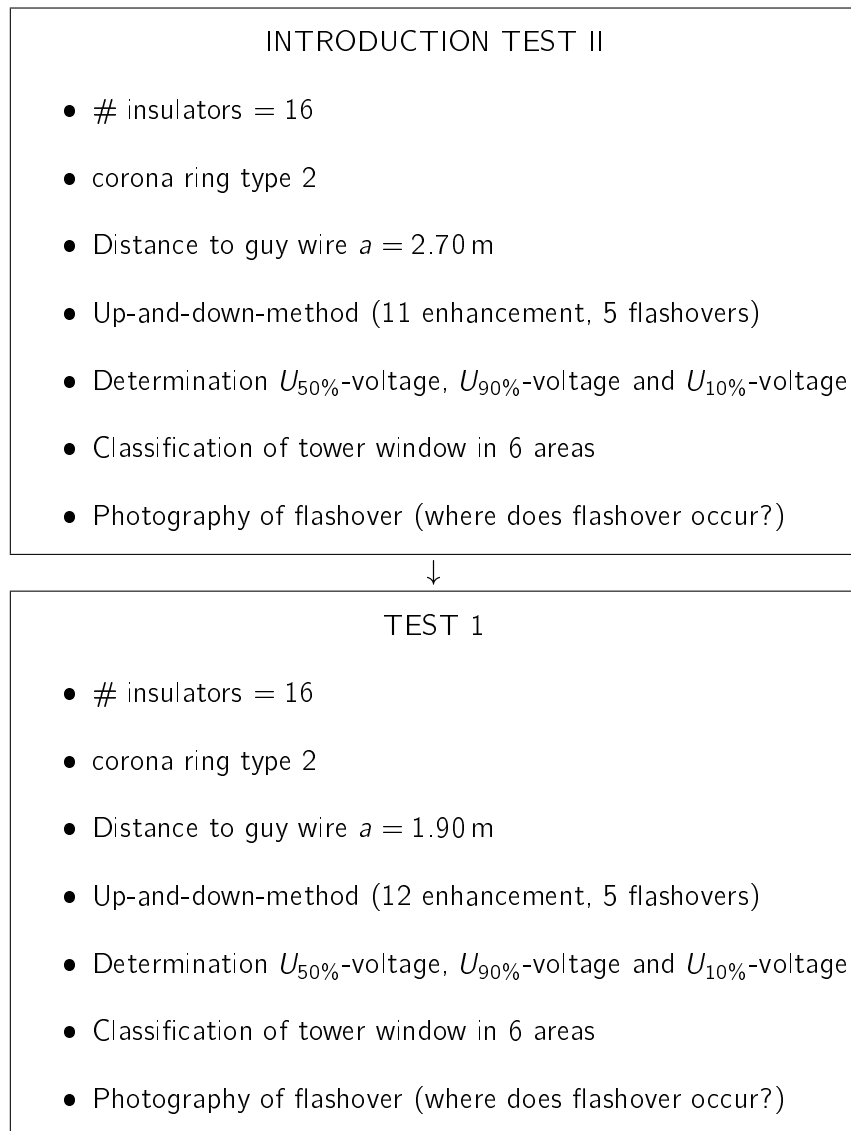


Figure 6.19: Testing plan: Switching impulse voltage Tests – Corona ring type 2

6.6.1 Switching impulse voltage – Introduction Test II (Corona ring type 2)

At the first experiment a *swing angle* of 0° has been simulated and a *distance* of 2.70 m between *corona ring* and the *lower guy wire* has been measured. As mentioned before the main target of this test was to determine the $U_{50\%}$ -voltage and the calculation of the $U_{90\%}$ -voltage and $U_{10\%}$ -voltage, respectively.

Results

Table 6.33 shows a summary of the results of the Introduction Test II of corona ring type 2 using the up-and-down method.

Table 6.33: Summary of results: SI – Introduction Test II (Corona ring type 2)

Switching impulse voltage - Introduction Test II (Corona ring type 2)				
Voltage level		flashover	Area of flashover in tower window	No flashover
Charging voltage	Load voltage			
[kV]	[kV]			
100	987			✓
105	1036	✓	2	
100	990			✓
105	1035			✓
110	1088			✓
115	1137	✓	2	
110	1089			✓
115	1137	✓	2	
110	1089	✓	2	
105	1040			✓
110	1090	✓	2	

Table 6.34 shows the measured values of atmospheric conditions at the time of the Introduction Test II for corona ring type 2 using the up-and-down method.

Table 6.34: Atmospheric conditions at the time of SI – Introduction Test II (Corona ring type 2)

Atmospheric conditions: SI – Introduction Test II (Corona ring type 2)	
Temperature [°C]	26.0
Air pressure [mbar]	976.2
Air humidity [%]	51.5
Air humidity [g/m^3]	10.8

Calculation

$U_{50\%}$ under testing conditions:

$$U_p^* = \sum \frac{k_i \cdot U_i}{n} \Rightarrow U_{50\%test} = \sum \frac{U_i}{n} = \frac{11718}{11} = 1065 \text{ kV}$$

Conversion to $U_{50\%}$ under standard basic reference atmosphere:

$$K_t = 0.9671 \Rightarrow U_{50\%basicref} = 1102 \text{ kV}$$

Calculation of $U_{90\%}$ under testing condition:

$$U_{90\%test} = U_{50\%test} \cdot (1 + 1.3 \cdot 0.06) = 1065 \text{ kV} \cdot (1 + 1.3 \cdot 0.06) = 1148 \text{ kV}$$

Conversion to $U_{90\%}$ under standard basic reference atmosphere:

$$K_t = 0.9671 \Rightarrow U_{90\%basicref} = 1187 \text{ kV}$$

Calculation of $U_{10\%}$ under testing condition:

$$U_{10\%test} = U_{50\%test} \cdot (1 - 1.3 \cdot 0.06) = 1065 \text{ kV} \cdot (1 - 1.3 \cdot 0.06) = 982 \text{ kV}$$

Conversion to $U_{10\%}$ under standard basic reference atmosphere:

$$K_t = 0.9671 \Rightarrow U_{10\%basicref} = 1016 \text{ kV}$$

6.6.2 Switching impulse voltage – Test 1 (Corona ring type 2)

At this experiment a *distance of 1.90 m between corona ring and the lower guy wire* has been simulated. As mentioned before the main target of this test was to determine the $U_{50\%}$ -voltage and the calculation of the $U_{90\%}$ -voltage and $U_{10\%}$ -voltage, respectively.

Results

Table 6.35 shows the summary of the results of the Switching impulse voltage – Test 1 for corona type 2 using the up-and-down method.

Table 6.35: Summary of results: SI – Test 1 (Corona ring type 2)

Switching impulse voltage – Test 1 (Corona ring type 2)				
Voltage level		flashover	Area of flashover in tower window	No flashover
Charging voltage [kV]	Load voltage [kV]			
86	840			✓
89	869	✓	5	
86	838			✓
89	867	✓	3	
86	839			✓
89	870			✓
92	899	✓	5	
89	870			✓
92	899	✓	5	
89	870			✓
92	900			✓
95	929	✓	5	

Table 6.36 shows the measured values of atmospheric conditions at the time of the Switching impulse voltage – Test 1 for corona ring type 2 using the up-and-down method.

Table 6.36: Atmospheric conditions at the time of SI – Test 1 (Corona ring type 2)

Atmospheric conditions: SI – Test 1 (Corona ring type 2)	
Temperature [°C]	28.0
Air pressure [mbar]	975.0
Air humidity [%]	44.4
Air humidity [g/m^3]	12.4

Calculation

$U_{50\%}$ under testing conditions:

$$U_p^* = \sum \frac{k_i \cdot U_i}{n} \Rightarrow U_{50\%test} = \sum \frac{U_i}{n} = \frac{10490}{12} = 874 \text{ kV}$$

Conversion to $U_{50\%}$ under standard basic reference atmosphere:

$$K_t = 0.9594 \Rightarrow U_{50\%basicref} = 911 \text{ kV}$$

Calculation of $U_{90\%}$ under testing condition:

$$U_{90\%test} = U_{50\%test} \cdot (1 + 1.3 \cdot 0.06) = 874 \text{ kV} \cdot (1 + 1.3 \cdot 0.06) = 942 \text{ kV}$$

Conversion to $U_{90\%}$ under standard basic reference atmosphere:

$$K_t = 0.9594 \Rightarrow U_{90\%basicref} = 982 \text{ kV}$$

Calculation of $U_{10\%}$ under testing condition:

$$U_{10\%test} = U_{50\%test} \cdot (1 - 1.3 \cdot 0.06) = 874 \text{ kV} \cdot (1 - 1.3 \cdot 0.06) = 806 \text{ kV}$$

Conversion to $U_{10\%}$ under standard basic reference atmosphere:

$$K_t = 0.9594 \Rightarrow U_{10\%basicref} = 840 \text{ kV}$$

Representing result

Figure 6.20 shows a flashover to the lower guy wire during Switching impulse voltage – Test 1.



Figure 6.20: Flashover to the lower guy wire: SI – Test 1

6.6.3 Discussion of test results

As shown in section 6.6.1, in case of corona ring type 2 and switching impulse voltage, for a swing angle of 0° a withstand voltage $U_{10\%}$ of 1016 kV has been measured under testing conditions. In Table 3.1 the required withstand voltage values given in the international standard IEC 60071 – Part 1 [25] for several operating voltage levels are shown. A comparison of the value from the practical test with these values shows, that the measured result is within the applicable withstand voltage range (850 ÷ 1050 kV).

6.7 Switching impulse voltage Tests – Rain Tests

The rain test as defined in [32] should simulate the effect of natural rain on external insulations. To accomplish this effect the testing object must be sprayed with water, which has a defined conductivity and temperature. The required conditions are specified in detail in [32] and the actual parameters are shown in Table 6.37. Relating to the horizontal amount of rain it must be mentioned, that it should be approximately identically to the vertical part.

Table 6.37: Actual parameters of rain test [32]

Parameter	Horizontal amount [mm/min]	Vertical amount [mm/min]	Water temperature [°C]	Specific resistance [Ωm]
Required	1 – 2	1 – 2	ambient \pm 15	100 \pm 15
Measured	1.1	1.2	20	93

In Figure 6.21 a picture of the testing setup including the raining device is shown and Figure 6.22 shows the testing plan for rain tests concerning switching impulse voltage. All the rain tests with switching impulse voltage have been carried out with corona ring type 2 and 16 insulator caps. The variation of the voltage level for the up-and-down method has been accomplished by variation of the charging voltage of the capacitances. Attention should be paid to the fact that in case of a flashover the load voltage break down before peak value. The values given in the table in that case are calculated by the ratio of the charging voltages. Similar to the previous tests a waiting time between the impulses of 1 minute was chosen in the rain tests.

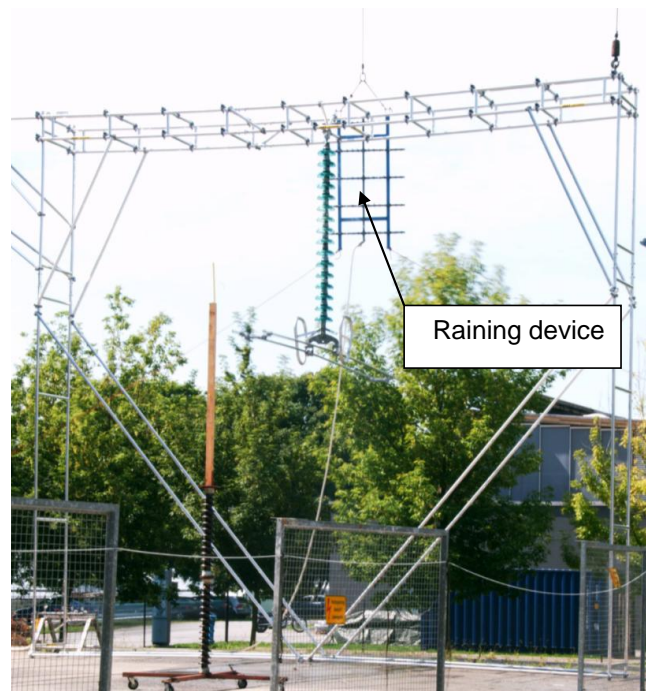


Figure 6.21: Testing setup: Switching impulse voltage – Rain test

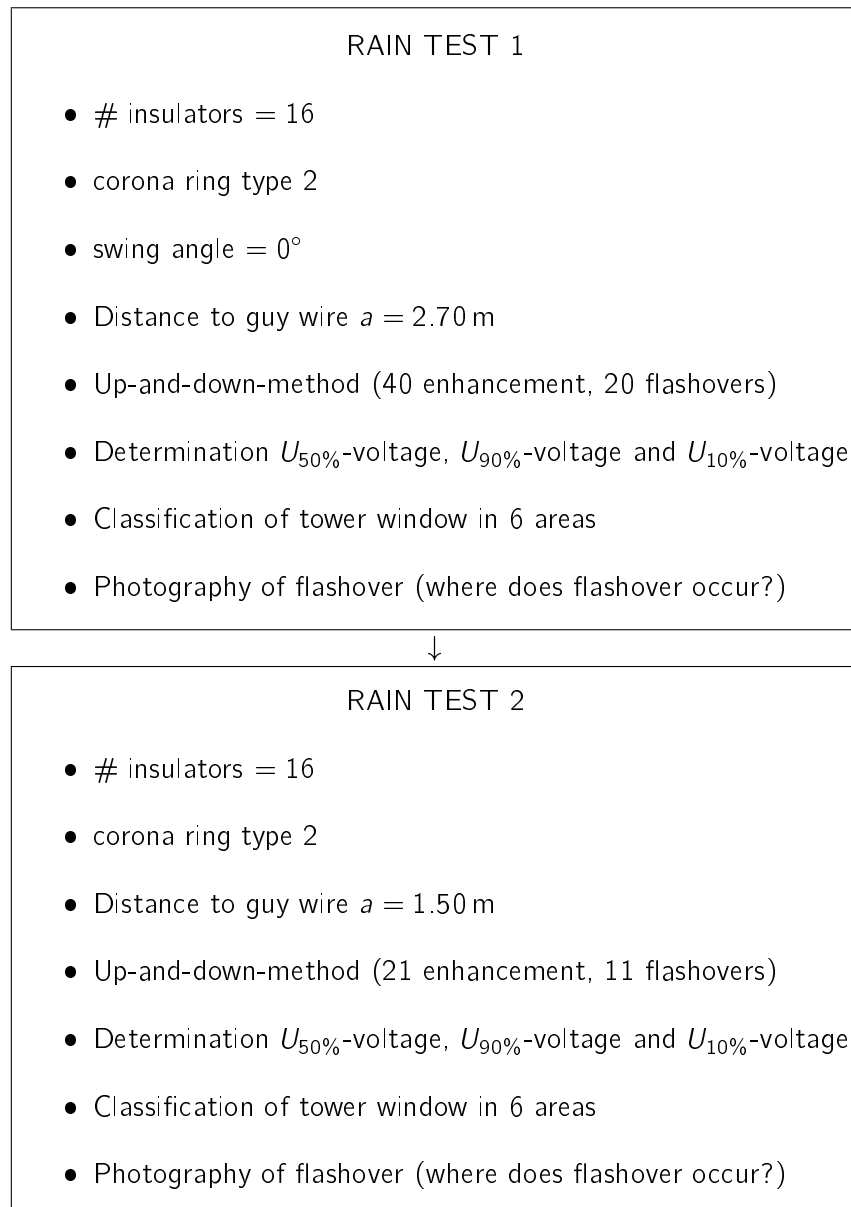


Figure 6.22: Testing plan: Switching impulse voltage – Rain test

6.7.1 Switching impulse voltage – Rain Test 1 (Corona ring type 2)

At the first experiment a *swing angle of 0° has been simulated and a distance of 2.70 m between corona ring and the lower guy wire* has been measured. As mentioned before the main target of this test was to determine the $U_{50\%}$ -voltage and the calculation of the $U_{90\%}$ -voltage and $U_{10\%}$ -voltage, respectively.

Results

Table 6.38 shows a summary of the results of the Switching impulse voltage – Rain Test 1 of corona ring type 2 using the up-and-down method.

Table 6.38: Summary of results: SI – Rain test 1 (Corona ring type 2)

Switching impulse voltage - Rain test 1 (Corona ring type 2)				
Voltage level		flashover	Area of flashover in tower window	No flashover
Charging voltage [kV]	Load voltage [kV]			
110	1088			✓
115	1137	✓	2	
110	1088	✓	2	
105	1036			✓
110	1085	✓	6	
105	1035	✓	2	
100	985	✓	2	
95	934			✓
100	976			✓
105	1034			✓
110	1083	✓	2	
105	1037			✓
110	1086	✓	2	
105	1037			✓
110	1086	✓	2	
105	1037	✓	2	
100	987			✓
105	1036	✓	2	
100	986			✓
105	1035	✓	2	
100	985			✓

Table 6.39 shows the measured values of atmospheric conditions at the time of the Switching impulse voltage – Rain Test 1 for corona ring type 2 using the up-and-down method.

Table 6.39: Atmospheric conditions at the time of SI – Rain test 1 (Corona ring type 2)

Atmospheric conditions: SI – Rain test 1 (Corona ring type 2)	
Temperature [°C]	25.0
Air pressure [mbar]	974.6
Air humidity [%]	63.1
Air humidity [g/m^3]	13.7

Calculation

$U_{50\%}$ under testing conditions:

$$U_p^* = \sum \frac{k_i \cdot U_i}{n} \Rightarrow U_{50\%test} = \sum \frac{U_i}{n} = \frac{21793}{21} = 1038 \text{ kV}$$

Conversion to $U_{50\%}$ under standard basic reference atmosphere:

$$K_t = 0.9887 \Rightarrow U_{50\%basicref} = 1050 \text{ kV}$$

Calculation of $U_{90\%}$ under testing condition:

$$U_{90\%test} = U_{50\%test} \cdot (1 + 1.3 \cdot 0.06) = 1038 \text{ kV} \cdot (1 + 1.3 \cdot 0.06) = 1119 \text{ kV}$$

Conversion to $U_{90\%}$ under standard basic reference atmosphere:

$$K_t = 0.9887 \Rightarrow U_{90\%basicref} = 1132 \text{ kV}$$

Calculation of $U_{10\%}$ under testing condition:

$$U_{10\%test} = U_{50\%test} \cdot (1 - 1.3 \cdot 0.06) = 1038 \text{ kV} \cdot (1 - 1.3 \cdot 0.06) = 957 \text{ kV}$$

Conversion to $U_{10\%}$ under standard basic reference atmosphere:

$$K_t = 0.9887 \Rightarrow U_{10\%basicref} = 968 \text{ kV}$$

Representing result

Figure 6.23 shows a flashover to the lower guy wire during Switching impulse voltage – Rain Test 1.

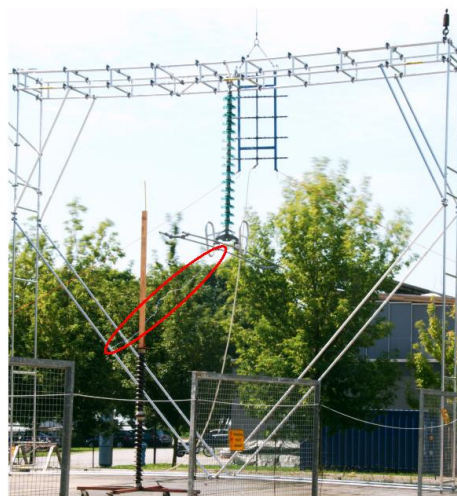


Figure 6.23: Flashover to the lower guy wire: SI – Rain tests 1

6.7.2 Switching impulse voltage – Rain Test 2 (Corona ring type 2)

At the first experiment a *distance of 1.50 m between conductor and the lower guy wire* has been measured. As mentioned before the main target of this test was to determine the $U_{50\%}$ -voltage and the calculation of the $U_{90\%}$ -voltage and $U_{10\%}$ -voltage, respectively.

Results

Table 6.40 shows a summary of the results of the Switching impulse voltage – Rain Test 2 of corona ring type 2 using the up-and-down method.

Table 6.40: Summary of results: SI – Rain test 2 (Corona ring type 2)

Switching impulse voltage – Rain test 2 (Corona ring type 2)				
Voltage level		flashover	Area of flashover in tower window	No flashover
Charging voltage [kV]	Load voltage [kV]			
83	814			✓
86	843	✓	5	
83	814	✓	5	
80	785	✓	5	
77	748			✓
80	785	✓	5	
77	750			✓
80	780			✓
83	810			✓
86	839	✓	5	
83	815			✓
86	844	✓	5	
83	814			✓
86	843	✓	5	
83	814	✓	5	
80	780			✓
83	811			✓
86	840	✓	5	
83	817			✓
86	846	✓	5	
83	810			✓
86	839	✓	5	
83	811			✓
86	840	✓	5	

Continued on next page

Table 6.40 – continued from previous page

83	811			✓
86	840	✓	5	
83	812			✓
86	841	✓	5	
83	812			✓
86	841	✓	5	
83	811	✓	5	
80	780			✓
83	813			✓
86	844			✓
89	873	✓	5	
86	844	✓	5	
83	815	✓	5	
80	795			✓
83	812			✓
86	841	✓	5	

Table 6.41 shows the measured values of atmospheric conditions at the time of the Switching impulse voltage – Rain Test 2 for corona ring type 2 using the up-and-down method.

Table 6.41: Atmospheric conditions at the time of SI – Rain test 2 (Corona ring type 2)

Atmospheric conditions: SI – Rain test 2 (Corona ring type 2)	
Temperature [°C]	21.0
Air pressure [mbar]	974.8
Air humidity [%]	76.0
Air humidity [g/m^3]	13.8

Calculation

$U_{50\%}$ under testing conditions:

$$U_p^* = \sum \frac{k_i \cdot U_i}{n} \Rightarrow U_{50\%test} = \sum \frac{U_i}{n} = \frac{32677}{40} = 817 \text{ kV}$$

Conversion to $U_{50\%}$ under standard basic reference atmosphere:

$$K_t = 0.9915 \Rightarrow U_{50\%basicref} = 824 \text{ kV}$$

Calculation of $U_{90\%}$ under testing condition:

$$U_{90\%test} = U_{50\%test} \cdot (1 + 1.3 \cdot 0.06) = 817 \text{ kV} \cdot (1 + 1.3 \cdot 0.06) = 881 \text{ kV}$$

Conversion to $U_{90\%}$ under standard basic reference atmosphere:

$$K_t = 0.9915 \Rightarrow U_{90\%basicref} = 888 \text{ kV}$$

Calculation of $U_{10\%}$ under testing condition:

$$U_{10\%test} = U_{50\%test} \cdot (1 - 1.3 \cdot 0.06) = 817 \text{ kV} \cdot (1 - 1.3 \cdot 0.06) = 753 \text{ kV}$$

Conversion to $U_{10\%}$ under standard basic reference atmosphere:

$$K_t = 0.9915 \Rightarrow U_{10\%basicref} = 760 \text{ kV}$$

Representing result

Figure 6.24 shows a flashover to the lower guy wire during Switching impulse voltage – Rain Test 2.

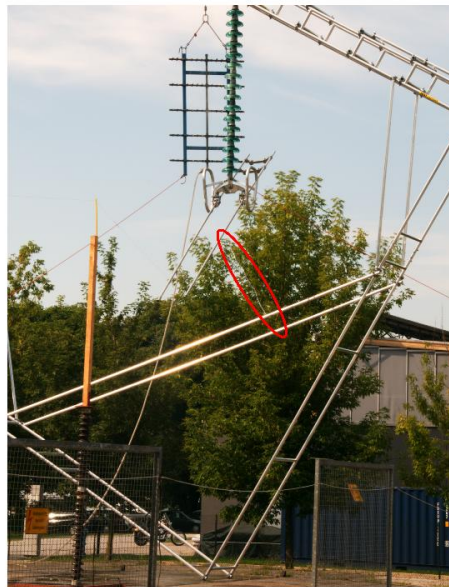


Figure 6.24: Flashover to the lower guy wire: SI – Rain tests 2

6.7.3 Discussion of test results

As shown in section 6.7.1, in case of corona ring type 2 and switching impulse voltage under rain conditions, for a swing angle of 0° a withstand voltage $U_{10\%}$ of 968 kV has been measured under testing conditions. In Table 3.1 the required withstand voltage values given in the international standard IEC 60071 – Part 1 [25] for several operating voltage levels are shown. A comparison of the value from the practical test with these values shows, that the measured result is within the applicable withstand voltage range ($850 \div 1050 \text{ kV}$).

6.8 Switching impulse voltage Tests – Bare insulator string

To evaluate the voltage behaviour of the bare insulator string without corona rings, the two vertical rings of corona ring type 2 have been dismantled and tests with switching impulse voltage have been carried out. Figure 6.25 shows a picture of the bare insulator string without the corona ring and in Figure 6.26 the testing plan for switching impulse voltage by use of the bare insulator string can be seen.



Figure 6.25: Insulator plus conductor without corona ring

INTRODUCTION TEST I

- # insulators = 16
- No corona ring
- Swing angle = 0°
- Up-and-down-method (12 enhancement, 5 flashovers)
- Determination $U_{50\%}$ -voltage, $U_{90\%}$ -voltage and $U_{10\%}$ -voltage
- Classification of tower window in 6 areas
- Photography of flashover (where does flashover occur?)



TEST 1	
•	# insulators = 16
•	No corona ring
•	Distance to guy wire $a = 2.00$ m
•	Up-and-down-method (8 enhancement, 5 flashovers)
•	Determination $U_{50\%}$ -voltage, $U_{90\%}$ -voltage and $U_{10\%}$ -voltage
•	Classification of tower window in 6 areas
•	Photography of flashover (where does flashover occur?)

Figure 6.26: Testing plan: Switching impulse voltage – Bare insulator string

6.8.1 Switching impulse voltage – Introduction Test I (Bare insulator string)

At the first experiment a *swing angle* of 0° has been simulated and a *distance* of 2.86 m between conductor and the lower guy wire has been measured. As mentioned before the main target of this test was to determine the $U_{50\%}$ -voltage and the calculation of the $U_{90\%}$ -voltage and $U_{10\%}$ -voltage, respectively.

Results

Table 6.42 shows a summary of the results of the Introduction Test I of the bare insulator string using the up-and-down method.

Table 6.42: Summary of results: SI – Introduction Test I (Bare insulator string)

Switching impulse voltage – Introduction Test I (Bare insulator string)				
Voltage level		flashover	Area of flashover in tower window	No flashover
Charging voltage [kV]	Load voltage [kV]			
105	1036			✓
110	1085	✓	2	
105	1036			✓
110	1086			✓
115	1138			✓
120	1187	✓	2	
115	1137	✓	2	
110	1084			✓
115	1133	✓	2	

Continued on next page

Table 6.42 – continued from previous page

110	1085			✓
115	1139			✓
120	1188	✓	2	

Table 6.43 shows the measured values of atmospheric conditions at the time of the Introduction Test I of the bare insulator string using the up-and-down method.

Table 6.43: Atmospheric conditions at the time of SI – Introduction Test I (Bare insulator string)

Atmospheric conditions: SI – Introduction Test I (Bare insulator string)	
Temperature [°C]	25.0
Air pressure [mbar]	974.8
Air humidity [%]	59.4
Air humidity [g/m^3]	14.0

Calculation

$U_{50\%}$ under testing conditions:

$$U_p^* = \sum \frac{k_i \cdot U_i}{n} \Rightarrow U_{50\%test} = \sum \frac{U_i}{n} = \frac{13334}{12} = 1111 \text{ kV}$$

Conversion to $U_{50\%}$ under standard basic reference atmosphere:

$$K_t = 0.9897 \Rightarrow U_{50\%basicref} = 1123 \text{ kV}$$

Calculation of $U_{90\%}$ under testing condition:

$$U_{90\%test} = U_{50\%test} \cdot (1 + 1.3 \cdot 0.06) = 1111 \text{ kV} \cdot (1 + 1.3 \cdot 0.06) = 1198 \text{ kV}$$

Conversion to $U_{90\%}$ under standard basic reference atmosphere:

$$K_t = 0.9897 \Rightarrow U_{90\%basicref} = 1210 \text{ kV}$$

Calculation of $U_{10\%}$ under testing condition:

$$U_{10\%test} = U_{50\%test} \cdot (1 - 1.3 \cdot 0.06) = 1111 \text{ kV} \cdot (1 - 1.3 \cdot 0.06) = 1025 \text{ kV}$$

Conversion to $U_{10\%}$ under standard basic reference atmosphere:

$$K_t = 0.9897 \Rightarrow U_{10\%basicref} = 1035 \text{ kV}$$

Representing result

Figure 6.27 shows a flashover along the insulator during Switching impulse voltage – Introduction Test I.

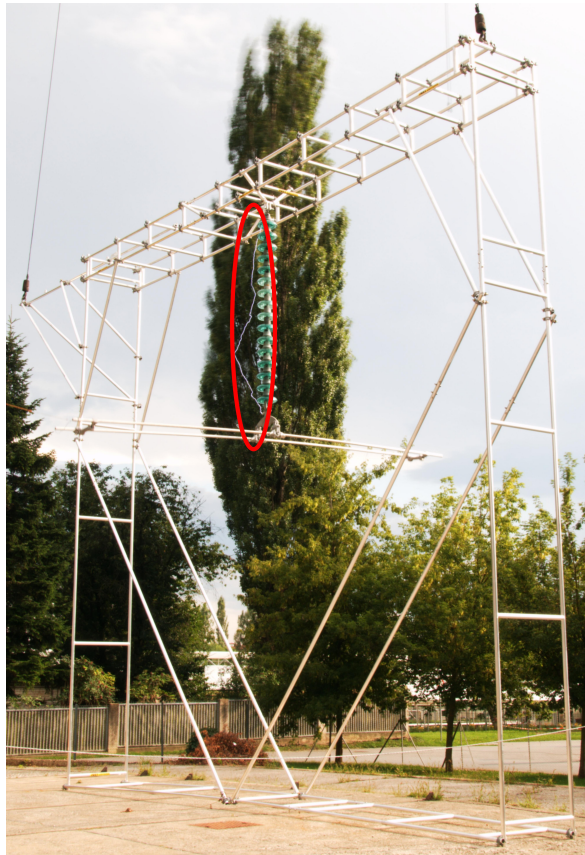


Figure 6.27: Flashover over the insulator string: SI – Introduction Test I (Bare insulator string)

6.8.2 Switching impulse voltage – Test 1 (Bare insulator string)

At this experiment a *distance of 2.00 m between conductor and the lower guy wire* has been simulated. As mentioned before the main target of this test was to determine the $U_{50\%}$ -voltage and the calculation of the $U_{90\%}$ -voltage and $U_{10\%}$ -voltage, respectively.

Results

Table 6.44 shows the summary of the results of the Switching impulse voltage – Test 1 of the bare insulator string using the up-and-down method.

Table 6.44: Summary of results: SI – Test 1 (Bare insulator string)

Switching impulse voltage – Test 1 (Bare insulator string)				
Voltage level		flashover	Area of flashover in tower window	No flashover
Charging voltage [kV]	Load voltage [kV]			
98	966			✓
101	995	✓	5	
98	966			✓

Continued on next page

Table 6.44 – continued from previous page

101	995	✓	5	
98	966	✓	5	
95	935			✓
98	966	✓	5	
95	935	✓	5	

Table 6.43 shows the measured values of atmospheric conditions at the time of the Switching impulse voltage – Test 1 of the bare insulator string using the up-and-down method.

Table 6.45: Atmospheric conditions at the time of SI – Test 1 (Bare insulator string)

Atmospheric conditions: SI – Test 1 (Bare insulator string)	
Temperature [°C]	25.0
Air pressure [mbar]	947.7
Air humidity [%]	59.7
Air humidity [g/m^3]	13.9

Calculation

$U_{50\%}$ under testing conditions:

$$U_p^* = \sum \frac{k_i \cdot U_i}{n} \Rightarrow U_{50\%test} = \sum \frac{U_i}{n} = \frac{7724}{8} = 966 \text{ kV}$$

Conversion to $U_{50\%}$ under standard basic reference atmosphere:

$$K_t = 0.9810 \Rightarrow U_{50\%basicref} = 984 \text{ kV}$$

Calculation of $U_{90\%}$ under testing condition:

$$U_{90\%test} = U_{50\%test} \cdot (1 + 1.3 \cdot 0.06) = 966 \text{ kV} \cdot (1 + 1.3 \cdot 0.06) = 1041 \text{ kV}$$

Conversion to $U_{90\%}$ under standard basic reference atmosphere:

$$K_t = 0.9810 \Rightarrow U_{90\%basicref} = 1061 \text{ kV}$$

Calculation of $U_{10\%}$ under testing condition:

$$U_{10\%test} = U_{50\%test} \cdot (1 - 1.3 \cdot 0.06) = 966 \text{ kV} \cdot (1 - 1.3 \cdot 0.06) = 890 \text{ kV}$$

Conversion to $U_{10\%}$ under standard basic reference atmosphere:

$$K_t = 0.9897 \Rightarrow U_{10\%basicref} = 907 \text{ kV}$$

Representing result

Figure 6.28 shows a flashover to the lower guy wire during Switching impulse voltage – Test 1.



Figure 6.28: Flashover to the lower guy wire: SI – Test 1 (Bare insulator string)

6.8.3 Discussion of test results

As shown in section 6.8.1, in case of switching impulse voltage using no corona ring, for a swing angle of 0° a withstand voltage $U_{10\%}$ of 1035 kV has been measured under testing conditions. In Table 3.1 the required withstand voltage values given in the international standard IEC 60071 – Part 1 [25] for several operating voltage levels are shown. A comparison of the value from the practical test with these values shows, that the measured result is within the applicable withstand voltage range ($850 \div 1050$ kV). In comparison with the measured value using corona ring type 2 (1016 kV), this value is higher, which can be explained by the influence of the electrical field due to resulting changes in geometry based on the missing corona ring.

Chapter 7

Results

Using the results from the practical impulse voltage tests, the gap factors and minimum required distances under upgraded conditions have been calculated, which is covered below.

7.1 Lightning impulse voltage

A comparison of the $U_{50\%}$ -voltage of the two tested corona ring types in case of lightning impulse voltage for a swing angle of 0° shows, that corona ring type 1 has a $U_{50\%}$ -withstand voltage of 1516 kV and corona ring type 2 a $U_{50\%}$ -withstand voltage of 1483 kV, both under standard basic reference condition. By use of these two voltage values, the applicable shortest striking distance of the corona ring (2.73 m for type 1; 2.60 m for type 2) and the correct altitude factor K_a from Table 2.2, the gap factor K_g for the insulator string can be calculated using Equation (2.8) and (2.9) (see section 2.1.3). In Table 7.1 the calculated values using the results of the practical tests are compared with the values given in the standards [21][16] and the values given in the literature [22][23] (see also section 2.3.2).

Table 7.1: Comparison of gap factors for insulator string in case of lightning impulse voltage

Type of corona ring	Gap factor test TU Graz	Gap factor Standard ^{1,2}	Gap factor Literature ^{3,4}
1	1.052	1.07 (1.12)	0.96 (1.30) ³ ; 1.10 ⁴
2	1.081		

¹ Standard EN 50341 - Part 1 [16]

² Standard IEC 60071 - Part 2 [21]

³ See [22]

⁴ See [23]

As mentioned in section 2.3.2, the values of the gap factor for the insulator string given in the standard [21][16] are ambiguous, because in contrast to the value for the air gap, where the factor for the configuration conductor - tower window can be chosen, for the insulator string two values are possible. On the one hand the value for the configuration conductor - tower window ($K_g = 1.07$) and on the other hand for the conductor - tower construction ($K_g = 1.12$) can be

chosen. As it can be seen in Table 7.1, the gap factor in case of corona ring type 1 is up to 6 % lower depending on the chosen value in the standard. In case of corona ring type 2 the gap factor is either 1 % higher or 3 % lower depending on the chosen value in the standard. As mentioned in section 6.1, the main goal of the lightning impulse voltage tests was the determination of the percentages of the flashover occurrence inside the tower window. These results are the basis for the calculation of the gap factor of the air gap. Table 7.2 shows a summary of the percentage of flashover occurrence inside the tower window for the lightning impulse voltage tests of corona ring type 1 without use of a damper loop (chosen testing voltage $U = U_{90\%} = 1476$ kV).

Table 7.2: Summary of results – Lightning impulse voltage Tests (Corona ring type 1 without damper loop)

Lightning impulse voltage Tests – Corona ring type 1 (without damper loop)		
Distance conductor – guy wire [m]	Percentage of flashovers	
	Insulator string	Lower guy wire
2.35	0 %	100 %
2.44	20 %	80 %
2.50	70 %	30 %
2.60	100 %	0 %

Table 7.3 shows a summary of percentage of flashover occurrence inside the tower window for the lightning impulse voltage tests of corona ring type 1 using a damper loop (chosen testing voltage $U = U_{90\%} = 1476$ kV).

Table 7.3: Summary of results – Lightning impulse voltage Tests (Corona ring type 1 with damper loop)

Lightning impulse voltage Tests – Corona ring type 1 (with damper loop)			
Distance conductor – guy wire [m]	Distance damper loop – guy wire [m]	Percentage of flashovers	
		Insulator string	Lower guy wire
2.45	2.27	0 %	100 %
2.60	2.40	85 %	15 %
2.63	2.45	45 %	55 %

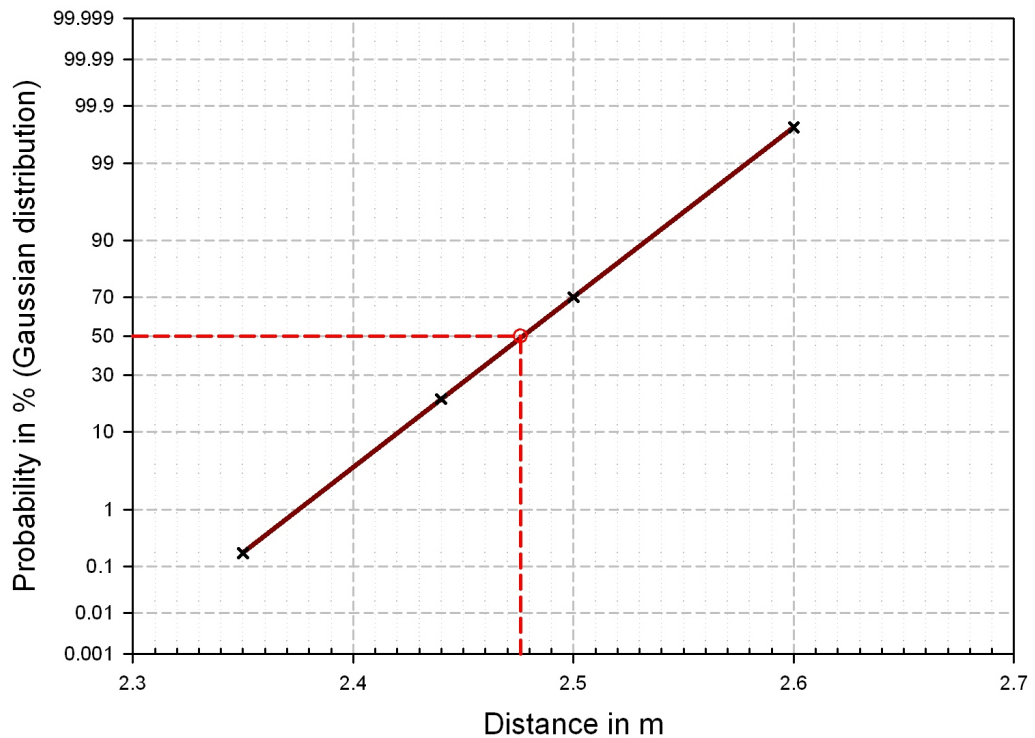
Table 7.4 shows a summary of percentage of flashover occurrence inside the tower window for the lightning impulse voltage tests of corona ring type 2 (chosen testing voltage $U = U_{90\%} = 1519$ kV).

For the calculation of the gap factor for the air gap, the distance of the 50%-flashover occurrence along the insulator and the 50%-flashover occurrence to the guy wire is needed, because thereby the $U_{50\%}$ -withstand voltage of the insulator and of the air gap is equal. There are a lot of theoretical distribution functions established for engineering. In high voltage engineering two typical distribution functions are applicable: Weibull-distribution and Gaussian distribution [33]. The Gaussian distribution is particularly applicable for description of random processes.

Table 7.4: Summary of results – Lightning impulse voltage Tests (Corona ring type 2)

Lightning impulse voltage Tests – Corona ring type 2		
Distance conductor – guy wire [m]	Percentage of flashovers	
	Insulator string	Lower guy wire
2.28	0 %	100 %
2.35	95 %	5 %
2.45	100 %	0 %

They are arising very often in high voltage engineering especially at flashovers in air, flashovers along insulators as well as other types of insulation. In comparison to the Gaussian distribution the Weibull-distribution is geared particularly for questions of lifetime [34]. Figure 7.1 shows the distribution of the results of the lightning impulse voltage test of corona ring type 1 in form of a line according to a Gaussian distribution function (results see also Table 7.2). Thereby the linear equation results due to the both value of results in the middle (20 % and 70 %). Arising thereby the outer two points (0 % and 100 % in the tests) have been determined, whereby these two values (0.18 % and 99.75 %)⁵ fit quite well to the test values. That means that the results from these practical tests can be looked upon as normally distributed. Based on this knowledge, also the remaining testing results can be assumed as normally distributed. To determine a more precise linear equation of the Gaussian distribution, tests with additional distances would be necessary, which was not possible in this thesis due to limited resources.

**Figure 7.1:** Distribution of Lightning impulse voltage test results of Corona ring type 1

⁵ values result from the distribution given by 2.44 m and 2.50 m

Based on the previous considerations, the $U_{50\%}$ -withstand voltage can be determined by an interpolation of the striking distance based on the determined percentages of flashovers. As shown in Table 7.2 a difference of 50 % of the flashovers is adequate to a distance of 0.06 m, which means that a difference of 10 % is equivalent to 0.012 m. Due to these considerations the missing distance for the $U_{50\%}$ -withstand voltage of the air gap can be calculated. As it can be seen in Figure 7.1, the calculated interpolated value of 2.476 m (see also Table 7.5) fits quite well with the value due to the distribution function in form of the linear equation (see red line in Figure 7.1). By use of an equalisation of Equation (2.8) of the insulator string and the air gap (including the calculated values K_g for the insulator string, see Table 7.1), the unknown gap factor K_g of the air gap can be calculated. Table 7.5 shows a comparison of the calculated gap factors due to results of the practical tests and the values given in the standard [21][16].

Table 7.5: Comparison of gap factors for air gap in case of lightning impulse voltage

Type of Corona ring	Interpolation striking distance in [m]	Gap factor – Test TU Graz	Gap factor – Standard ^{6,7}
1	2.476	1.15	1.07
2	2.317	1.21	

⁶ Standard EN 50341 - Part 1 [16]

⁷ Standard IEC 60071 - Part 2 [21]

As it can be seen in Table 7.5, the calculated gap factor of the air gap is up to 13 % higher than the value in the standard depending on the chosen type of corona ring. Based on the results of the gap factor of the air gap (see Table 7.5) and the results of Table 7.1 the minimum required distances can be calculated using Equation (2.12). A comparison of these values and the results based on the given values in the standard [21][16] are summarized in Table 7.6. Thereby it must be mentioned, that in case of corona ring type 2 the striking distance is the same as for corona ring type 1. That is due to the fact, that for both cases 17 insulator caps have been assumed and in that case the two striking distances are equal.

Table 7.6: Comparison of required distances in case of lightning impulse voltage

Type of Corona ring	Nr. of insulator caps	Shortest striking distance in [m]	Required distances – Test TU Graz [m]	Required distances – Standard [m] ^{8,9}	Empirical distance – Standard [m] ¹⁰
1	17	2.73	2.51	2.74 (2.87)	2.80
2	17	2.73	2.45	2.74 (2.87)	
2	17	2.60	2.34	2.62 (2.74)	

⁸ Standard EN 50341 - Part 1 [16]

⁹ Standard IEC 60071 - Part 2 [21]

¹⁰ Standard EN 50341 - Part 1 [16] (see also Table 2.5)

As it can be seen in Table 7.6, the required distance in case of corona ring type 1 is up to 12.5 % lower depending on the chosen value in the standard. In case of corona ring type 2 it is up to 16.4 % lower. In that case, the reduction is depending on the chosen standard value as well as the chosen number of insulator caps.

7.2 Switching impulse voltage

A comparison of the $U_{50\%}$ -voltage of the two tested types of corona rings in case of switching impulse voltage for a swing angle of 0° shows, that corona ring type 1 has a $U_{50\%}$ -withstand voltage of 1098 kV under standard basic reference condition and corona ring type 2 a $U_{50\%}$ -withstand voltage of 1102 kV under standard basic reference condition. By use of these two voltage values, the applicable shortest striking distance of the corona ring (2.73 m for type 1; 2.60 m for type 2) and the correct altitude factor K_a from Table 2.2, the gap factor K_g for the insulator string can be calculated using Equation (2.8) and (2.10) (see section 2.1.3). In Table 7.7 the calculated values of results of the practical tests are compared with the values given in the standards [21][16] (see also section 2.3.2).

Table 7.7: Comparison of gap factors for insulator string in case of switching impulse voltage

Type of Corona ring	Gap factor – Test TU Graz	Gap factor – Standard ^{11,12}
1	1.26	1.25 (1.45)
2	1.31	

¹¹ Standard EN 50341 - Part 1 [16]

¹² Standard IEC 60071 - Part 2 [21]

Similar to lightning impulse voltage, in case of switching impulse voltage the values of the gap factor for the insulator string given in the standard [21][16] are ambiguous, because in contrast to the value for the air gap, where the factor for the configuration conductor - tower window can be chosen, for the insulator string two value are possible. On the one hand the value for the configuration conductor - tower window ($K_g = 1.25$) and on the other hand for the conductor - tower construction ($K_g = 1.45$) can be chosen.

Table 7.8 shows a summary of the $U_{50\%}$ -, $U_{90\%}$ - and $U_{10\%}$ -voltages under testing conditions for the switching impulse voltage tests of corona ring type 1. Table 7.9 shows a summary of the same values under standard basic reference atmosphere.

Table 7.10 shows a summary of the $U_{50\%}$ -, $U_{90\%}$ - and $U_{10\%}$ -voltages under testing conditions for the dry tests with switching impulse voltage of corona ring type 2. Table 7.11 shows a summary of the same values under standard basic reference atmosphere.

Table 7.12 shows a summary of the $U_{50\%}$ -, $U_{90\%}$ - and $U_{10\%}$ -voltages for the rain tests with switching impulse voltage of corona ring type 2. Table 7.13 shows a summary of the same values under standard basic reference atmosphere.

Table 7.8: Results under testing conditions: SI – Tests (Corona ring type 1)

Switching impulse voltage Tests – Corona ring type 1			
Shortest striking distance in [m]	$U_{50\%}$ (testing conditions)	$U_{90\%}$ (testing conditions)	$U_{10\%}$ (testing conditions)
	[kV]	[kV]	[kV]
1.40	796	859	734
1.55	871	939	803
1.90	962	1037	887
2.73 (swing angle= 0°)	1098	1184	1013

Table 7.9: Results under standard basic reference atmosphere: SI – Tests (Corona ring type 1)

Switching impulse voltage Tests – Corona ring type 1			
Shortest striking distance in [m]	$U_{50\%}$ (s.b.r.a.)¹³	$U_{90\%}$ (s.b.r.a.)¹³	$U_{10\%}$ (s.b.r.a.)¹³
	[kV]	[kV]	[kV]
1.40	783	844	722
1.55	856	923	789
1.90	929	1002	857
2.73 (swing angle= 0°)	1082	1167	998

¹³ s. b. r. a. = standard basic reference atmosphere

Table 7.10: Results under testing conditions: SI – Tests dry (Corona ring type 2)

Switching impulse voltage Tests (dry) – Corona ring type 2			
Shortest striking distance in [m]	$U_{50\%}$ (testing conditions)	$U_{90\%}$ (testing conditions)	$U_{10\%}$ (testing conditions)
	[kV]	[kV]	[kV]
1.90	874	942	806
2.60 (swing angle= 0°)	1065	1148	982

Table 7.11: Results under standard basic reference atmosphere: SI – Tests dry (Corona ring type 2)

Switching impulse voltage Tests (dry) – Corona ring type 2			
Shortest striking distance in [m]	$U_{50\%}$ (s.b.r.a.)¹⁴	$U_{90\%}$ (s.b.r.a.)¹⁴	$U_{10\%}$ (s.b.r.a.)¹⁴
	[kV]	[kV]	[kV]
1.90	911	982	840
2.60 (swing angle= 0°)	1102	1187	1016

¹⁴ s. b. r. a. = standard basic reference atmosphere

Using the results of the $U_{50\%}$ -withstand voltage in Table 7.9, Table 7.11 and Table 7.13 (except of the results for a swing angle of 0°), Equation (2.8) and (2.10) as well as the correct altitude factor K_a , the gap factor K_g for the air gap can be calculated. Table 7.14 shows a comparison of the calculated gap factors due to results of the practical tests and the values given in the standard [21][16].

As it can be seen in Table 7.14, the calculated gap factor of the air gap in case of corona ring type 1 is up to 20 % higher than the value in the standard. In case of corona ring type 2 and rain test conditions the gap factor is 16.8 % higher than the standard value. Using these calculated values the minimum distance for a required $U_{50\%}$ -withstand voltage of 780.9 kV (demand by Statnett SF) can be reduced from 1.70 m to 1.36 m, which is a reduction of 20 %. For switching impulse tests using no corona ring a $U_{50\%}$ -voltage of 1111 kV has been calculated in case of a swing angle of 0° and for a distance of 2.00 m between conductor and the lower guy wire a $U_{50\%}$ -voltage of 966 kV.

Table 7.12: Results under testing conditions: SI – Rain Tests (Corona ring type 2)

Switching impulse voltage Tests (rain) – Corona ring type 2			
Shortest striking distance in [m]	$U_{50\%}$ (testing conditions)	$U_{90\%}$ (testing conditions)	$U_{10\%}$ (testing conditions)
	[kV]	[kV]	[kV]
1.50	817	881	753
2.60 (swing angle= 0°)	1038	1119	957

Table 7.13: Results under standard basic reference atmosphere: SI – Rain Tests (Corona ring type 2)

Switching impulse voltage Tests (rain) – Corona ring type 2			
Shortest striking distance in [m]	$U_{50\%}$ (s.b.r.a.)¹⁵	$U_{90\%}$ (s.b.r.a.)¹⁵	$U_{10\%}$ (s.b.r.a.)¹⁵
	[kV]	[kV]	[kV]
1.50	824	888	760
2.60 (swing angle= 0°)	1050	1132	968

¹⁵ s. b. r. a. = standard basic reference atmosphere

Table 7.14: Comparison of gap factors for air gap in case of switching impulse voltage

Type of Corona ring	Shortest striking distance in [m]	Gap factor – Test TU Graz	Gap factor – Standard^{16,17}
1	1.55	1.50	1.25
1	1.40	1.48	
2 (rain test)	1.50	1.46	

¹⁶ Standard EN 50341 - Part 1 [16]

¹⁷ Standard IEC 60071 - Part 2 [21]

Chapter 8

Conclusion

8.1 Survey

The method of upgrading an existing overhead line involves several advantages such as the fact that it is a fast and economic way to increase capacity and/or to improve the reliability of the system. This reduction of costs is based on the fact, that the existing towers are used and no new towers need to be constructed. On the other hand this topic raises some issues in terms of insulation coordination. Especially the dimensioning of the required clearances at the upgraded overhead line tower has to be accomplished exactly to guarantee the reliability of the electricity transmission. These distances are influenced by factors like the longer insulators which are necessary due to the higher operating voltage, but also due to environmental factors like snow and ice. In this context, the correct determination of the gap factor which influences the withstand voltages and arising thereby the required distances are of particular interest. The international standards and guidelines concerning the gap factor seem to be very conservative. Statnett SF (Norway's Transmission System Operator) is planning to upgrade approximately 5000 km of its 300 kV overhead transmission line network to an operating voltage of 420 kV by lengthen the existing cap-and-pin insulators. Within the frame of this work the correct gap factors respectively the minimum required distances under upgraded conditions have been determined. Therefore a practical full-scale model of the upper tower section of an affected suspension tower has been developed and constructed. Using this model, impulse voltage tests with lightning as well as switching impulse voltage (dry and rain) have been carried out at the High Voltage Laboratory of the Graz University of Technology. For the impulse voltage tests a specific testing plan has been developed, which covers swing angles respectively distances occurring on-site in Norway on the one hand and an efficient design and realization of experiment on the other hand. Based on the results from these practical tests the gap factors respectively the minimum required distances under upgraded conditions have been evaluated and compared with the values given in the international standards [21][16].

8.2 Summary

A practical full-scale model of the upper tower section of an affected suspension tower has been developed and constructed and impulse voltage tests have been carried out for several defined distances using this model. Thereby in case of lightning impulse voltage tests a gap factor has been investigated, which is up to 13 % higher than the given value in the standard, depending on the chosen type of corona ring. Arising thereby the required distance is up to 12.5 % (corona ring type 1) and 16.4 % (corona ring type 2) lower than the values in the standard. Thereby the reduction is depending on the chosen value in the standard, the chosen number of insulator caps as well as the chosen type of corona ring. In case of switching impulse voltage the gap factor is up to 20 % (corona ring type 1) respectively up to 16.8 % (corona ring type 2, rain conditions) higher than the value in the standard. Due to the required withstand voltage on the part of Statnett SF, the distance in case of switching impulse voltage can be reduced by about 20 %.

8.3 Relevance of the work

The topic of voltage upgrading is getting more and more interesting for transmission system operators as well as distribution grid operators. This is due to the fact that the demand of energy is growing continuously, which requires an expansion of the existing grids. However, the installation of new overhead lines is getting more and more problematic concerning social obstacles, environmental protection issues and long project durations. Due to these considerations, system operators trend towards upgrading their grids. Unfortunately, there have been little investigations concerning the topics of gap factor and minimum required distances in the last two decades. For these reasons this thesis has been carried in cooperation with Statnett SF. Due to the determined results the reduction of costs in running upgrading voltage projects of Statnett SF is currently approximately 35 Mio. € [11]. Furthermore, the outcome of these investigations have been published and presented at several conferences [35][36][37].

8.4 Outlook

This work describes the investigations of the gap factor in case of voltage upgrading for a mono layer suspension tower of Statnett SF. To investigate this topic in every detail, a comprehensive study of insulation coordination would be necessary, which is a process in stages and could not be covered within the scope of this work. Additional outstanding tests, which could not be carried out in this work for temporal reasons, are planned for spring 2011. Thereby the investigation of the influence of the damper loop to the gap factors as well as the evaluation of the interpolated striking distance of the $U_{50\%}$ -withstand voltage are of particular interest. Based on this work also similar investigations and testing for corresponding tension towers are planned in autumn 2011. Furthermore, the developed model can also be used on the one hand for further tests

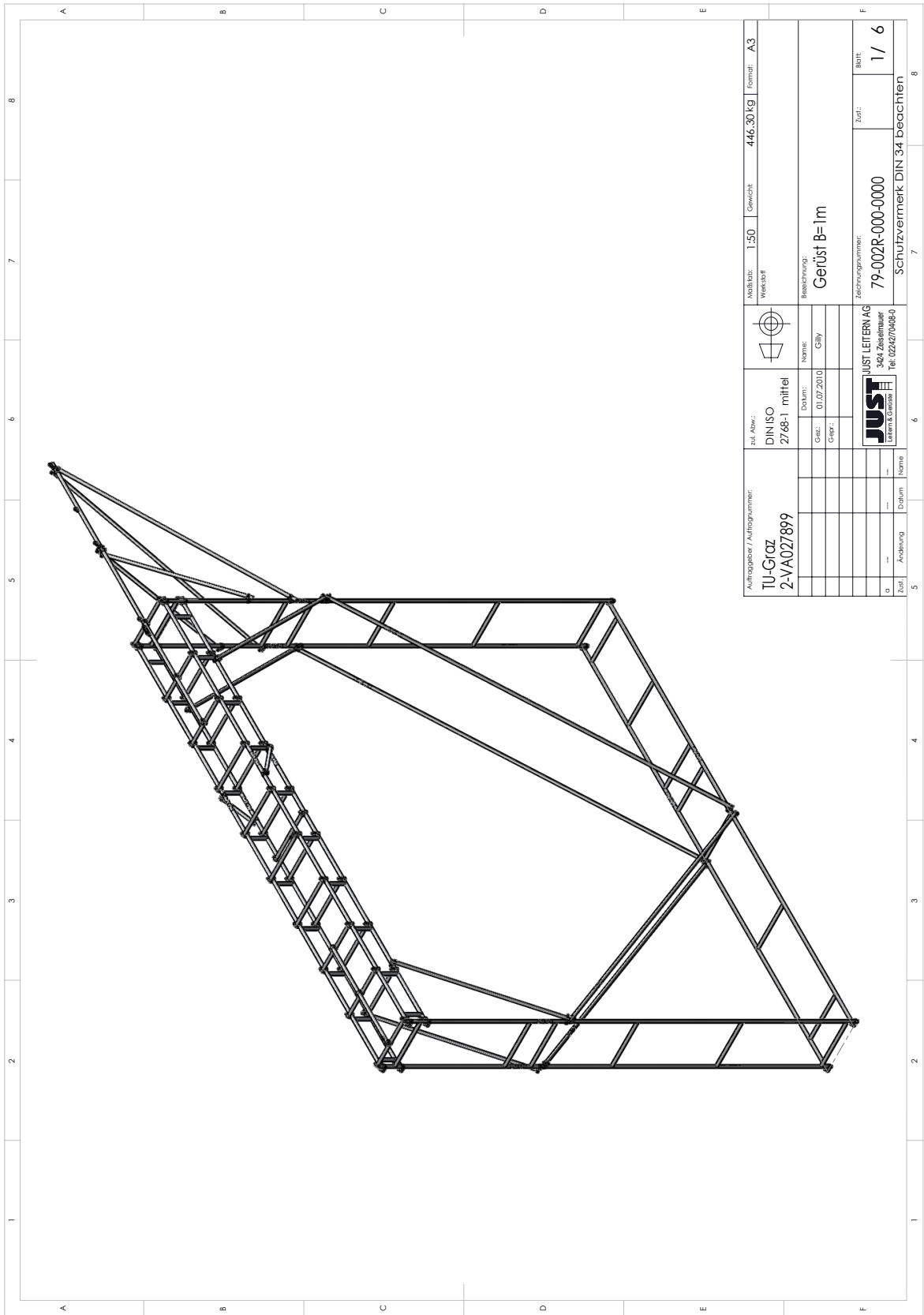
concerning operating conditions and influence of ice and wind load and on the other hand for additional tests of the insulator string and corona rings.

Chapter 9

Appendix

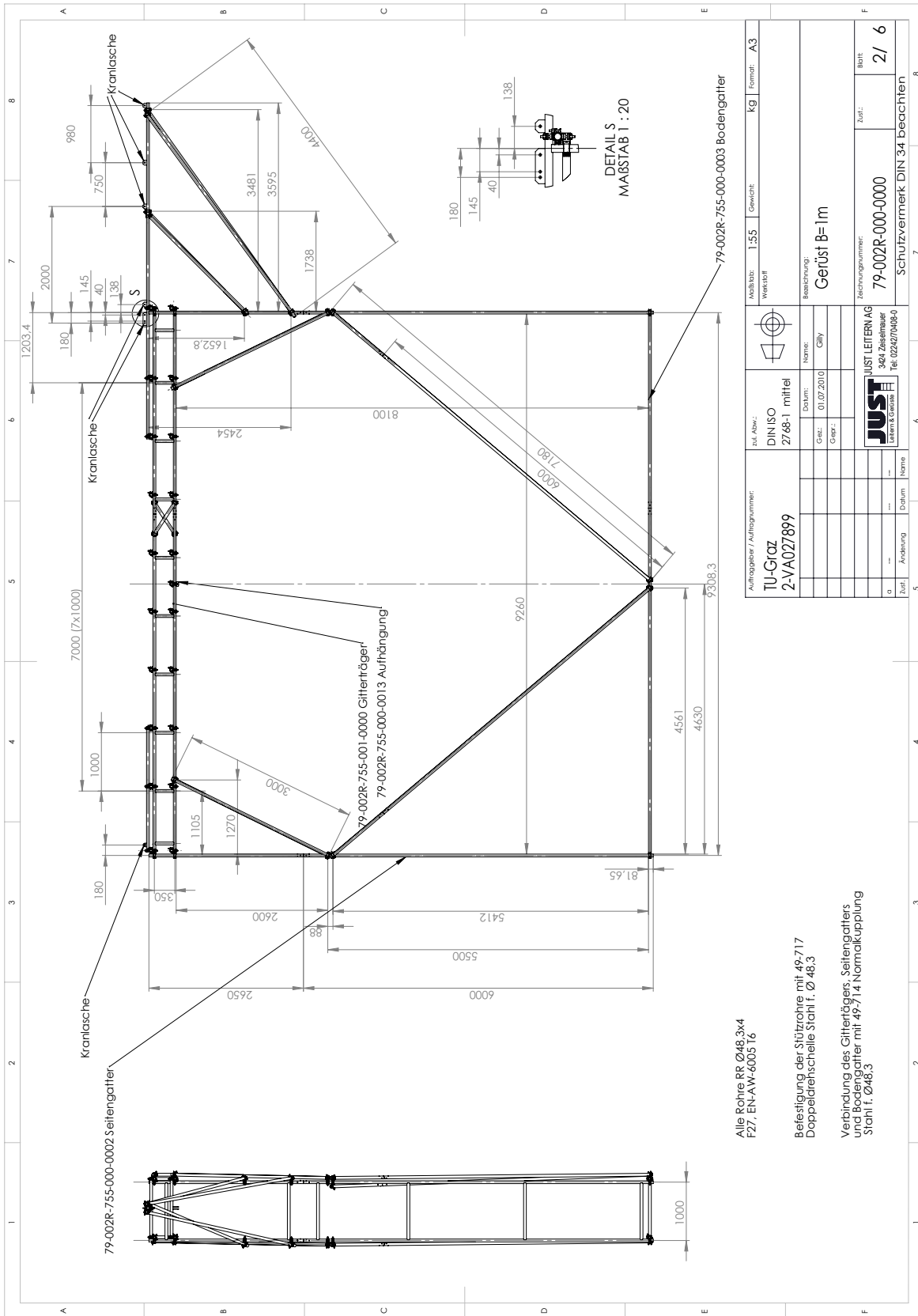
The appendix consist of the following datasheets:

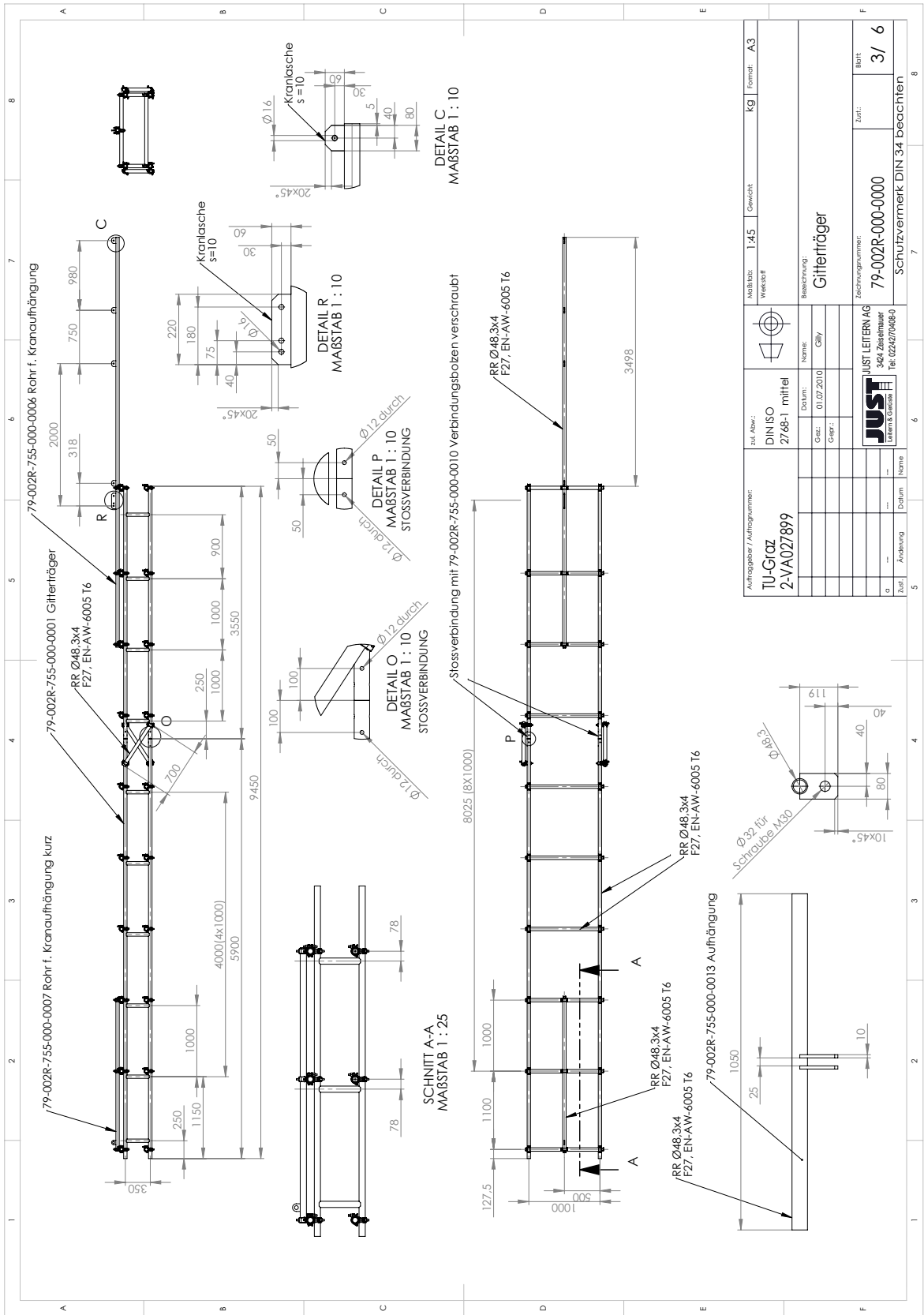
- Tower model - Assembly drawing (3D)
- Tower model - Assembly drawing (2D), front view
- Tower model - Assembly drawing of top part (2D)
- Tower model - Assembly drawing of side part (2D)
- Tower model - Assembly drawing (2D), details
- Tower model - List of parts



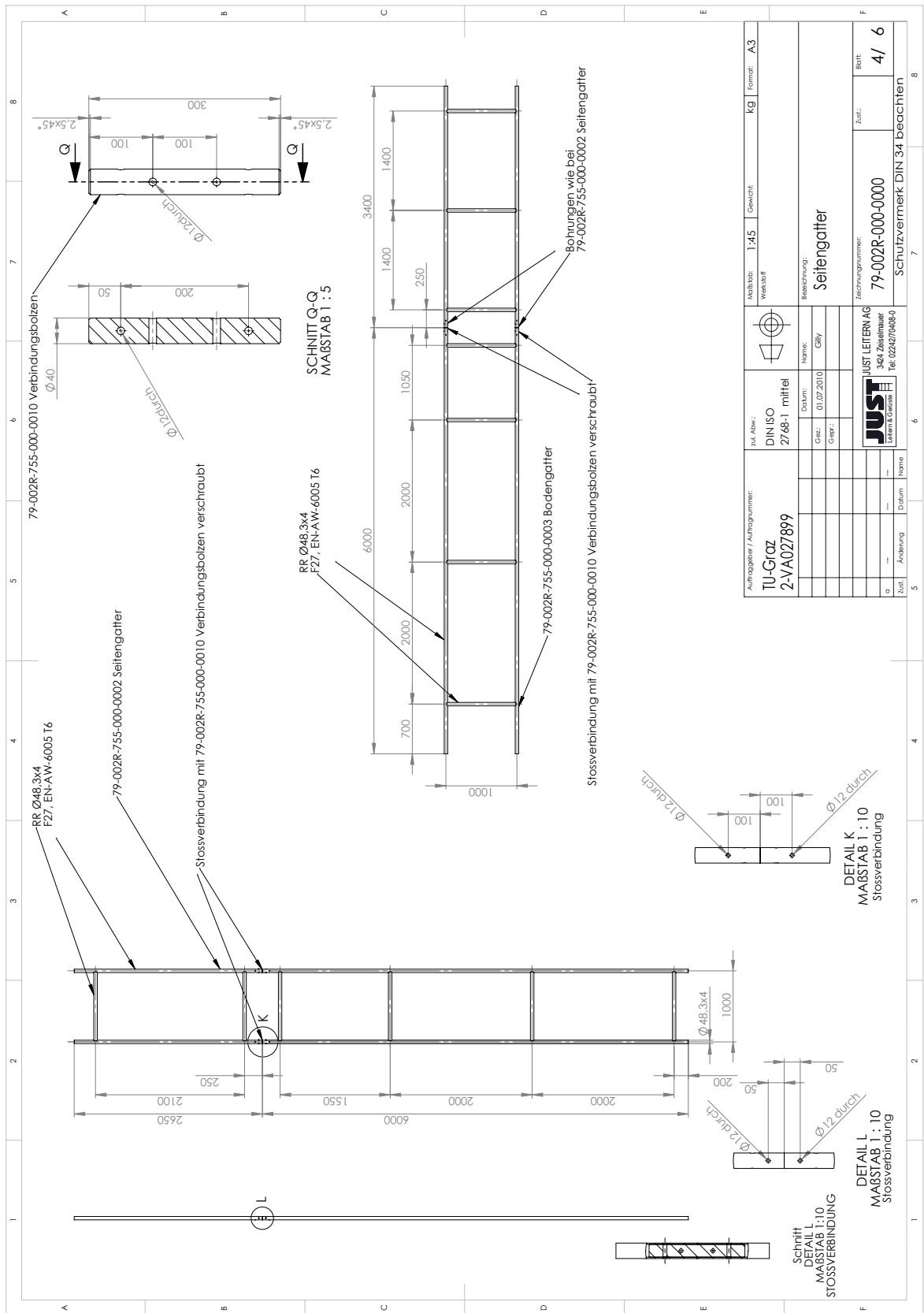
Auftraggeber / Auftragsnummer: TU-GIaZ 2-VA027899		Zu: Abw.: DIN ISO 2768-1 mittel		Maststab: Maßstab: 1:50 Gewicht: 446,30 KG Format: A3	
		Datum: 01.07.2010		Weichholz	
		Gez.: <input type="checkbox"/>		Bezeichnung: Gerüst B=1m	
		Gepr.: <input type="checkbox"/>			
		Name: <input type="text"/>			
		Gib: <input type="text"/>			
				Zeichnungsnummer: 79-002R-000-0000	
				Zur: <input type="text"/>	
				Blatt: 1 / 6	
				Schutzvermerk DIN 34 beachten	
Zur: <input type="text"/>		Datum: <input type="text"/>		Name: <input type="text"/>	
Änderung: <input type="text"/>		Datum: <input type="text"/>		Name: <input type="text"/>	
...		
...		
...		
...		
...		
...		
...		
...		
...		
...		
...		
...		
...		

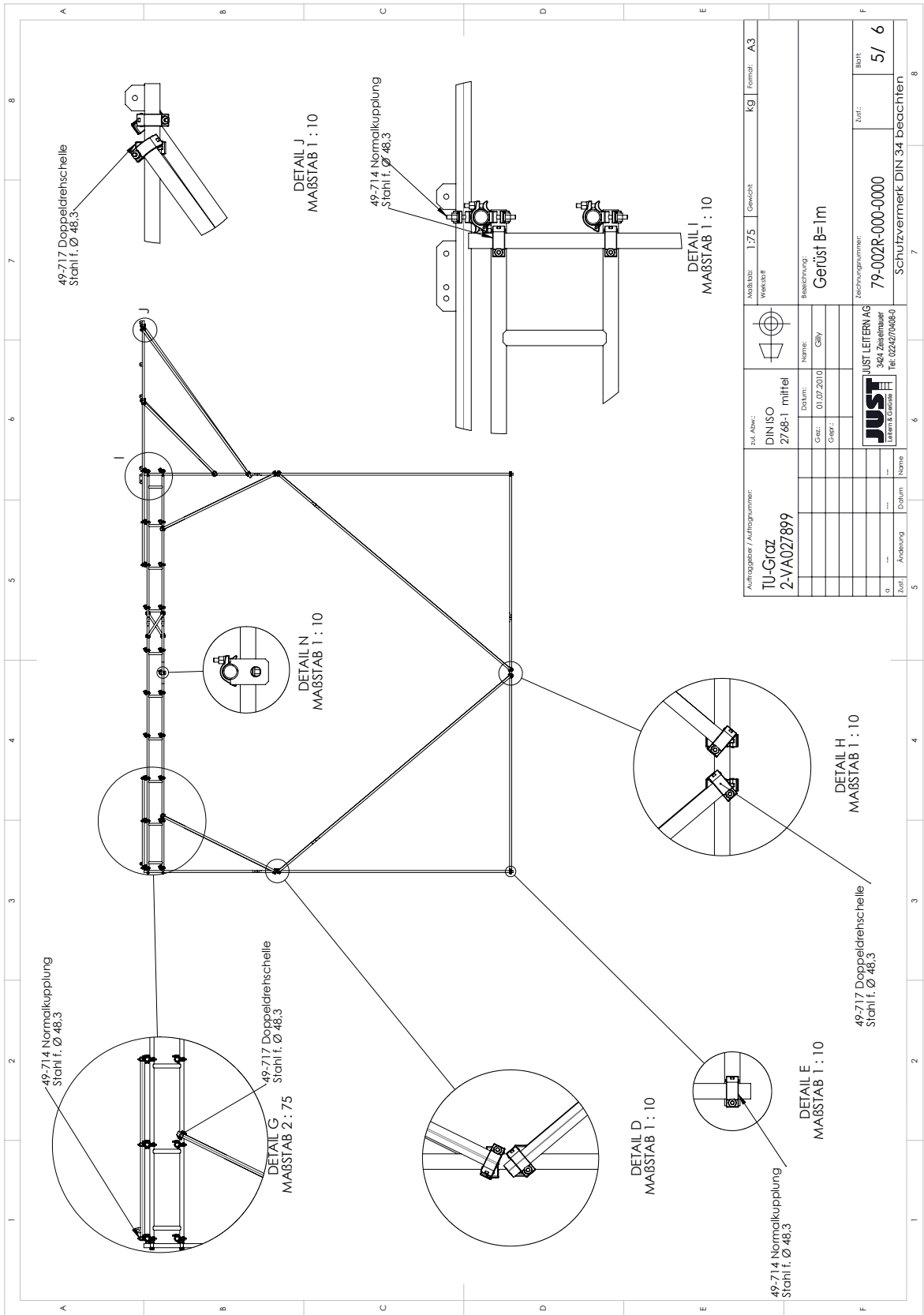


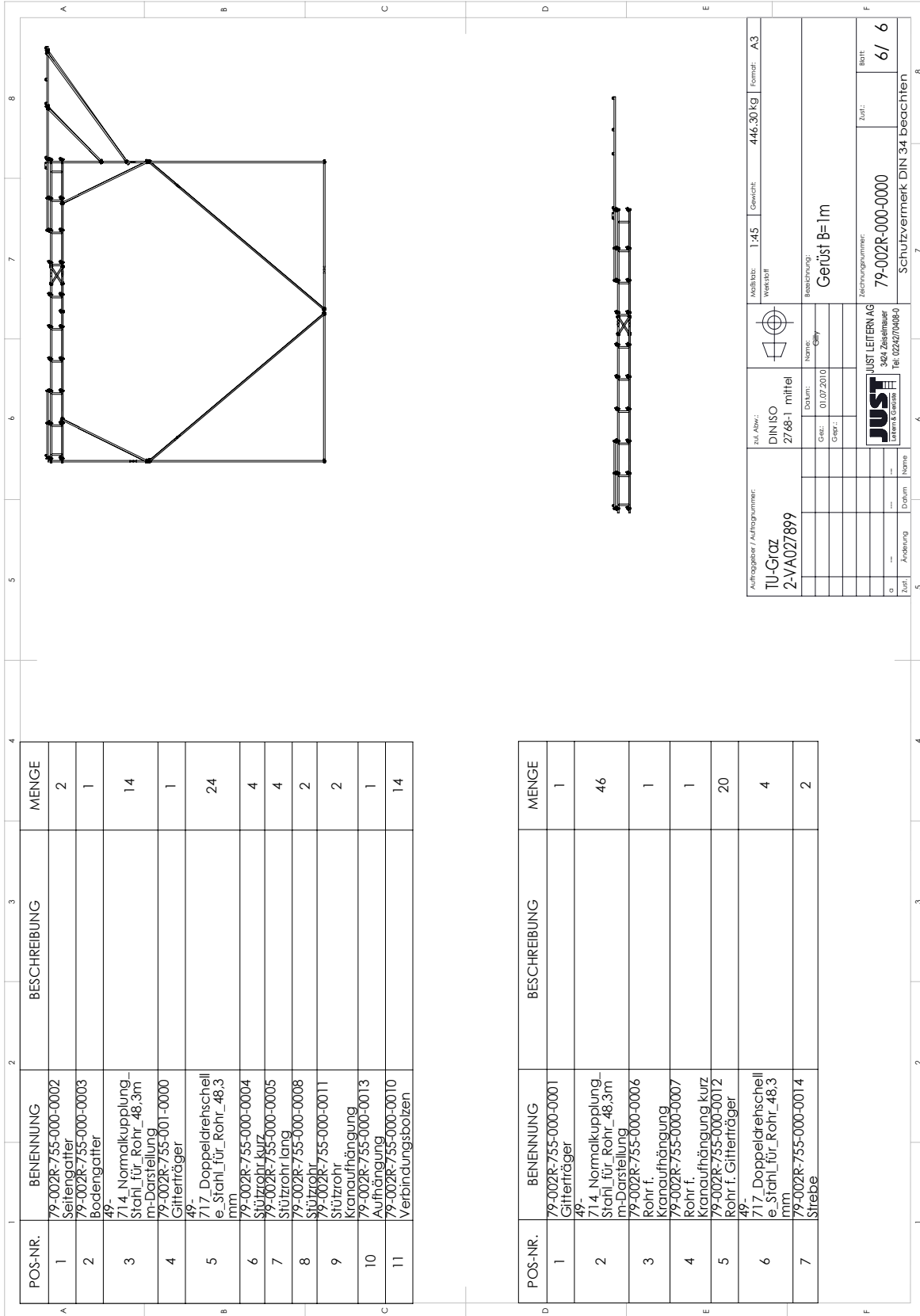




Auftraggeber / Auftragsnummer: TU-Graz 2-VA027899		Zucl. Abw.: DIN ISO 2768-1 mittel		Menge: 1.45		Gewicht: KG		Format: A3	
Datum: 01.07.2010		Name: Gilly		Rechenprogramm: Gitterträger					
Gez.: ---		Gepr.: ---		Zeichnungsnummer: 79-002R-000-0000		Blatt: 3/ 6			
a: ---		b: ---		c: ---		d: ---		e: ---	
f: ---		g: ---		h: ---		i: ---		j: ---	
k: ---		l: ---		m: ---		n: ---		o: ---	
p: ---		q: ---		r: ---		s: ---		t: ---	
u: ---		v: ---		w: ---		x: ---		y: ---	
z: ---		aa: ---		ab: ---		ac: ---		ad: ---	
ae: ---		af: ---		ag: ---		ah: ---		ai: ---	
aj: ---		ak: ---		al: ---		am: ---		an: ---	
ao: ---		ap: ---		aq: ---		ar: ---		as: ---	
at: ---		au: ---		av: ---		aw: ---		ax: ---	
ay: ---		az: ---		ba: ---		bb: ---		bc: ---	
bd: ---		be: ---		bf: ---		bg: ---		bh: ---	
bi: ---		bj: ---		bk: ---		bl: ---		bm: ---	
bn: ---		bo: ---		bp: ---		bq: ---		br: ---	
bs: ---		bt: ---		bu: ---		bv: ---		bw: ---	
bx: ---		by: ---		bz: ---		ca: ---		cb: ---	
cc: ---		cd: ---		ce: ---		cf: ---		cg: ---	
ch: ---		ci: ---		cj: ---		ck: ---		cl: ---	
cm: ---		cn: ---		co: ---		cp: ---		cq: ---	
cr: ---		cs: ---		ct: ---		cu: ---		cv: ---	
cw: ---		cx: ---		cy: ---		cz: ---		da: ---	
db: ---		dc: ---		dd: ---		de: ---		df: ---	
dg: ---		dh: ---		di: ---		dj: ---		dk: ---	
dl: ---		dm: ---		dn: ---		do: ---		dp: ---	
dq: ---		dr: ---		ds: ---		dt: ---		du: ---	
dv: ---		dw: ---		dx: ---		dy: ---		dz: ---	
ea: ---		eb: ---		ec: ---		ed: ---		ee: ---	
ef: ---		eg: ---		eh: ---		ei: ---		ej: ---	
ek: ---		el: ---		em: ---		en: ---		eo: ---	
ep: ---		eq: ---		er: ---		es: ---		et: ---	
eu: ---		ev: ---		ew: ---		ex: ---		ey: ---	
ez: ---		fa: ---		fb: ---		fc: ---		fd: ---	
fe: ---		ff: ---		fg: ---		fh: ---		fi: ---	
fj: ---		fk: ---		fl: ---		fm: ---		fn: ---	
fo: ---		fp: ---		fq: ---		fr: ---		fs: ---	
ft: ---		fu: ---		fv: ---		fw: ---		fx: ---	
fy: ---		fz: ---		ga: ---		gb: ---		gc: ---	
gd: ---		ge: ---		gf: ---		gg: ---		gh: ---	
gi: ---		gj: ---		gk: ---		gl: ---		gm: ---	
gn: ---		go: ---		gp: ---		gq: ---		gr: ---	
gs: ---		gt: ---		gu: ---		gv: ---		gw: ---	
gx: ---		gy: ---		gz: ---		ha: ---		hb: ---	
hc: ---		hd: ---		he: ---		hf: ---		hg: ---	
hh: ---		hi: ---		hj: ---		hk: ---		hl: ---	
hm: ---		hn: ---		ho: ---		hp: ---		hq: ---	
hr: ---		hs: ---		ht: ---		hu: ---		hv: ---	
hw: ---		hx: ---		hy: ---		hz: ---		ia: ---	
ib: ---		ic: ---		id: ---		ie: ---		if: ---	
ig: ---		ih: ---		ii: ---		ij: ---		ik: ---	
il: ---		im: ---		in: ---		io: ---		ip: ---	
iq: ---		ir: ---		is: ---		it: ---		iu: ---	
iv: ---		iv: ---		iv: ---		iv: ---		iv: ---	







Bibliography

- [1] Homepage European Commission Energy; visited on November 22nd 2009. [Online]. Available: http://ec.europa.eu/energy/publications/statistics/statistics_en.htm
- [2] EIA-Energy Information Administration, International Energy Annual 2006; visited on November 22nd 2009. [Online]. Available: <http://www.eia.doe.gov/iea/elec.html>
- [3] Homepage European Commission Energy; visited on November 22nd 2009. [Online]. Available: http://ec.europa.eu/energy/energy_policy/doc/06_progress_report_renewable_electricity_en.pdf
- [4] Austrian Energy Report 2003 of the Austrian government; visited on November 22nd 2009. [Online]. Available: <http://www.bmwfj.gv.at/BMWA/Schwerpunkte/Energie/InfoPublikation/Energiebericht/default.htm>
- [5] Homepage E-Control Austria; visited on November 22nd 2009. [Online]. Available: <http://www.e-control.at/de/publikationen/marktberichte>
- [6] I. Albizu, A. Mazon, and I. Zamora, "Methods for Increasing the Rating of Overhead Lines," *Power Tech, IEEE Russia*, 2005.
- [7] "Data of europe-eurostat annual," 2009, Homepage European Commission Eurostat; visited on November 22nd 2009. [Online]. Available: http://epp.eurostat.ec.europa.eu/portal/page/portal/publications/eurostat_yearbook
- [8] R. Rashedin, H. Griffiths, N. Harid, and A. Haddad, "Uprating the electrical capacity of an existing transmission line- 275 kV to 400 kV," in *Proceedings of the 16th Symposium of High Voltage Engineering*, School of Engineering, Cardiff University, UK, 2009, high Voltage Energy Systems Group.
- [9] W. Hafner, "Styria line: Closing the gap in the Austrian 380 kV Ring ," i-Tagung Mosdorfer Company, Weiz, Styria, Tech. Rep., October 1st and 2nd, technical lecture.
- [10] CIGRE Working Group B2-12, "Conductors for the uprating of overhead lines," 2003.
- [11] Information on behalf of Statnett SF, Telephone conference with Dr. Sonja Berlijn, Electromechanical section – Transmission line dept., Statnett SF, Date: 10th of May, 2011.

- [12] J. Hanson, "Upgrading transmission lines," in *Proceeding of the 1991 IEEE Power Engineering Society*, 1991, Transmission and Distribution Conference.
- [13] S. Venkatesan, A. Haddad, H. Griffiths, and N. H. M. Albano, "Reducing Air Clearance Requirements for Voltage Uprating of Overhead Line by use of Line Surge Arrester," Cardiff University, 2009, High Voltage Energy Systems Group.
- [14] M. Sanaye-Pasand, M. Dadashzadeh, and M. Khodayar, "Limitation of Transmission Line Switching Overvoltages using Switchsync Relays IPST05-087-16b," ISPT Conference Papers 2005, Homepage of the ISPT Conference, visited on 28th of November. [Online]. Available: http://www.ipst.org/TechPapers/2005/IPST05_Paper087.pdf
- [15] F. Kießling, P. Nefzger, and U. Kaintzyk, *Freileitungen – Planung, Berechnung, Ausführung*, 5th ed. Berlin: Springer, 2001, no. ISBN: 3-540-42255-2.
- [16] "Overhead lines exceeding 45 kV," Standard DIN EN 50341-1, 2001.
- [17] Overhead electrical lines exceeding 45 kV - Supplement 1 General Requirements and Normative Aspects for Germany (NNA), Standard DIN EN 50341, 2007.
- [18] "Overhead electrical lines exceeding 45 kV," Austrian Standard ÖVE/ÖNORM EN 50341, September 2002.
- [19] CIGRE Working Group 072 of Study Committee 33, "Guidelines for the evaluation of the dielectric strength of external insulation," 1992, CIGRE 072.
- [20] "Working under electrical voltage- minimum working distances- calculation procedure," Standard IEC 61472, 2004.
- [21] "Insulation co-ordination Part 2 - Application Guide," International standard IEC 60071-2, 1993.
- [22] A. Hileman, *Insulation Coordination for Power Systems*. New York: Marcel Dekker Inc., 1999, no. ISBN: 0-8247-9957-7.
- [23] A. T. Olsen, "Voltage Upgrading of Overhead Lines," Master Thesis, NTNU Trondheim, June 2010, Department of Electric Power Engineering.
- [24] M. Yasui and M. Murooka, "Practical design of AC 1000 kV insulator assemblies," in *IEEE Transactions on Power Delivery*, vol. 3, 1988.
- [25] "Insulation co-ordination Part 1 - Definitions, principles and rules," International standard IEC 60071-1, 1993.
- [26] W. Vosloo, R. E. Macey, and C. de Toureil, *The practical guide to Outdoor High Voltage Insulators*, 2nd ed. Crown Publications cc, September 2006, no. ISBN: 0-620-31074-X.
- [27] W. Lick, "Analyseverfahren der Isolierstoffe," Graz University of Technology, Documents to lecture, Winter term 2009/10, Lecture at Graz University of Technology.

- [28] "Insulators for overhead lines with a nominal voltage above 1 kV: Part 1 - Ceramic or glass insulator units for a.c. systems- Definitions, test methods and acceptance criteria," Standard DIN EN 60383-1, 1996, German version EN 60383-1.
- [29] *The fundamentals and practice of Overhead Line Maintenance*, 2nd ed. Crown Publications cc, September 2006, no. ISBN: 0-620- 30906-7.
- [30] CIGRE Working Group B2-03, "Use of corona rings to control the electrical field along transmission line composite insulator," 2005, CIGRE 284.
- [31] R. Woschitz, "Hochspannungstechnologie und Systemtechnik," Graz University of Technology, Documents to lecture, Winter term 2009/10, Lecture at Graz University of Technology.
- [32] High voltage test techniques - Part 1: General definitions and test requirements, International standard IEC 60060-1.
- [33] A. Küchler, *Hochspannungstechnik*, 3rd ed. Berlin: Springer, 2009, no. ISBN: 978-3-540-78412-8.
- [34] W. Hauschild and W. Mosch, *Statistik für Elektrotechniker*. Berlin: VEB Verlag Technik, 1984.
- [35] M. Hinteregger, T. Judendorfer, M. Muhr, S. Berlijn, and A. Olsen, "Voltage Withstand Tests on a Full Scale Overhead Line Tower Model for Line Upgrading," *Electrical Insulation Conference 2011, Annapolis, Maryland*, June 2011.
- [36] S. Berlijn, A. Olsen, M. Muhr, T. Judendorfer, M. Hinteregger, and M. Runde, "Voltage upgrading of overhead lines – An insulation coordination challenge," *17th International Symposium of High Voltage Engineering, Hannover, Germany*, August 2011.
- [37] S. Berlijn, A. Olsen, K. Halsan, M. Hinteregger, T. Judendorfer, and M. Muhr, "Voltage upgrading – An insulation coordination challenge," *IEEE PES Trondheim PowerTech 2011, Trondheim*, June 2011.

List of Figures

1.1	Gross Electricity Consumption 1990 – 2006 (adapted from [1])	2
1.2	World Total Net Electricity Consumption 1980 – 2006 (adapted from [2]) . . .	2
1.3	Electricity generation from wind 1990 – 2005 [3]	3
2.1	Statistical method	6
2.2	Density function of overvoltage	7
2.3	Cumulative frequency of impulse withstand voltage	8
2.4	Position of conductor 2 to vertical conductor 1 regarding Table	23
2.5	Typical Construction of a suspension insulator string assembly and detailed figure of suspension insulator assembly	28
3.1	Cap-and-pin disc insulator	31
3.2	Suspension insulator assembly of a 1000 kV AC UHV transmission line	32
3.3	Tension insulator assembly of a 1000 kV AC UHV transmission line	33
3.4	Field distribution of insulator profile 1	36
3.5	Field distribution of insulator profile 2	36
3.6	Plot – Clearance D as a function of the swing angle ϕ	38
3.7	Plot – Gap factor K_S as a function of the swing angle ϕ	38
4.1	Affected tower of Statnett SF	39
4.2	Tower window with guy wires	40
4.3	Drawing of an affected suspension tower	40
4.4	Replication of the upper tower section including tower window and centre phase	41
5.1	Normative shape form 1.2/50 μs (left) and 250/2500 μs (right)	43
5.2	Testing setup with testing portal	44
5.3	Schematic of the testing setup	45
5.4	Insulator, corona ring and metal tubes (replication of conductor wire)	45
5.5	Simulation of swing angle and distances, respectively	46
5.6	Straight model	46
5.7	Model in angle	47
5.8	Drawing of insulators	47
5.9	Drawing of corona ring type 1	48

5.10	Corona ring type 1	48
5.11	Drawing of corona ring type 2	49
5.12	Corona ring type 2	49
6.1	Classification of tower window for evaluation of flashover occurrence	52
6.2	Corona ring type 1	53
6.3	Testing plan: Lightning impulse voltage Tests – Corona ring type 1	56
6.4	Voltage breakdown in case of flashover - Introduction Test I	59
6.5	Flashover to the lower guy wire: LI – Test 2A	62
6.6	Flashover along the insulator: LI – Test 2C	65
6.7	Drawing of damper loop	66
6.8	Damper loop in reality	66
6.9	Damper loop in testing setup	66
6.10	Flashover to the lower guy wire: LI – Additional Test 1	68
6.11	Flashover to the lower guy wire: LI – Additional Test 2	70
6.12	Flashover along the insulator: LI – Additional Test 3	72
6.13	Corona ring type 2	73
6.14	Testing plan: Lightning impulse voltage Tests – Corona ring type 2	74
6.15	Testing plan: Switching impulse voltage Tests – Corona ring type 1	85
6.16	Standard impulse voltage (250/2500 μ s) in case of non-flashover: SI – Introduction Test I	87
6.17	Flashover to the lower guy wire: SI – Test 1	90
6.18	Voltage breakdown in case of flashover – Switching impulse voltage – Test 2A	92
6.19	Testing plan: Switching impulse voltage Tests – Corona ring type 2	95
6.20	Flashover to the lower guy wire: SI – Test 1	99
6.21	Testing setup: Switching impulse voltage – Rain test	100
6.22	Testing plan: Switching impulse voltage – Rain test	101
6.23	Flashover to the lower guy wire: SI – Rain tests 1	103
6.24	Flashover to the lower guy wire: SI – Rain tests 2	106
6.25	Insulator plus conductor without corona ring	107
6.26	Testing plan: Switching impulse voltage – Bare insulator string	108
6.27	Flashover over the insulator string: SI – Introduction Test I (Bare insulator string)	110
6.28	Flashover to the lower guy wire: SI – Test 1 (Bare insulator string)	112
7.1	Distribution of Lightning impulse voltage test results of Corona ring type 1	115

List of Tables

2.1	Typical values for ν_u and K_z	9
2.2	Typical values for K_a depending on the coordination withstand voltage	10
2.3	Typical values for D_{el} and D_{pp} for fast front overvoltages	12
2.4	Typical values for D_{el} and D_{pp} for slow front overvoltages	13
2.5	Empirical values of D_{el} and D_{pp}	13
2.6	Typical values for coefficient k	23
2.7	Typical values for coefficient k	24
2.8	Equations and value of typical configurations	24
2.9	Typical values for K_g	26
3.1	Standard insulation level for range II ($U_m > 245$ kV)	34
3.2	Example of calculation	37
6.1	Summary of results: LI – Introduction Test I (Corona ring type 1)	57
6.2	Atmospheric conditions at the time of LI – Introduction Test I (Corona ring type 1)	58
6.3	Summary of results: LI – Test 1 (Corona ring type 1)	60
6.4	Atmospheric conditions at the time of LI – Test 1 (Corona ring type 1)	60
6.5	Summary of results: LI – Test 2A (Corona ring type 1)	61
6.6	Atmospheric conditions at the time of LI – Test 2A (Corona ring type 1)	62
6.7	Summary of results: LI – Test 2B (Corona ring type 1)	63
6.8	Atmospheric conditions at the time of LI – Test 2B (Corona ring type 1)	63
6.9	Summary of results: LI – Test 2C (Corona ring type 1)	64
6.10	Atmospheric conditions at the time of LI – Test 2C (Corona ring type 1)	65
6.11	Summary of results: LI – Additional Test 1 (Damper loop + Corona ring type 1)	67
6.12	Atmospheric conditions at the time of LI – Additional Test 1 (Damper loop + Corona ring type 1)	68
6.13	Summary of results: LI – Additional Test 2 (Damper loop + Corona ring type 1)	69
6.14	Atmospheric conditions at the time of LI – Additional Test 2 (Damper loop + Corona ring type 1)	69
6.15	Summary of results: LI – Additional Test 3 (Damper loop + Corona ring type 1)	71
6.16	Atmospheric conditions at the time of LI – Additional Test 3	71
6.17	Summary of results: LI – Introduction Test II (Corona ring type 2)	75

6.18 Atmospheric conditions at the time of LI – Introduction Test II (Corona ring type 2)	76
6.19 Summary of results: LI – Test 1 (Corona ring type 2)	77
6.20 Atmospheric conditions at the time of LI – Test 1 (Corona ring type 2)	78
6.21 Summary of results: LI – Test 2A (Corona ring type 2)	78
6.22 Atmospheric conditions at the time of LI – Test 2A (Corona ring type 2)	79
6.23 Summary of results: LI – Test 2B (Corona ring type 2)	80
6.24 Atmospheric conditions at the time of LI – Test 2B (Corona ring type 2)	80
6.25 Summary of results: SI – Introduction Test I (Corona ring type 1)	86
6.26 Atmospheric conditions at the time of SI – Introduction Test I (Corona ring type 1)	86
6.27 Summary of results: SI – Test 1 (Corona ring type 1)	88
6.28 Atmospheric conditions at the time of SI – Test 1 (Corona ring type 1)	89
6.29 Summary of results: SI – Test 2A (Corona ring type 1)	91
6.30 Atmospheric conditions at the time of SI – Test 2A (Corona ring type 1)	91
6.31 Summary of results: SI – Test 2B (Corona ring type 1)	93
6.32 Atmospheric conditions at the time of SI – Test 2B (Corona ring type 1)	93
6.33 Summary of results: SI – Introduction Test II (Corona ring type 2)	96
6.34 Atmospheric conditions at the time of SI – Introduction Test II (Corona ring type 2)	96
6.35 Summary of results: SI – Test 1 (Corona ring type 2)	97
6.36 Atmospheric conditions at the time of SI – Test 1 (Corona ring type 2)	98
6.37 Actual parameters of rain test [32]	100
6.38 Summary of results: SI – Rain test 1 (Corona ring type 2)	102
6.39 Atmospheric conditions at the time of SI – Rain test 1 (Corona ring type 2)	102
6.40 Summary of results: SI – Rain test 2 (Corona ring type 2)	104
6.41 Atmospheric conditions at the time of SI – Rain test 2 (Corona ring type 2)	105
6.42 Summary of results: SI – Introduction Test I (Bare insulator string)	108
6.43 Atmospheric conditions at the time of SI – Introduction Test I (Bare insulator string)	109
6.44 Summary of results: SI – Test 1 (Bare insulator string)	110
6.45 Atmospheric conditions at the time of SI – Test 1 (Bare insulator string)	111
7.1 Comparison of gap factors for insulator string in case of lightning impulse voltage	113
7.2 Summary of results – Lightning impulse voltage Tests (Corona ring type 1 without damper loop)	114
7.3 Summary of results – Lightning impulse voltage Tests (Corona ring type 1 with damper loop)	114
7.4 Summary of results – Lightning impulse voltage Tests (Corona ring type 2)	115
7.5 Comparison of gap factors for air gap in case of lightning impulse voltage	116
7.6 Comparison of required distances in case of lightning impulse voltage	116

7.7	Comparison of gap factors for insulator string in case of switching impulse voltage	117
7.8	Results under testing conditions: SI – Tests (Corona ring type 1)	118
7.9	Results under standard basic reference atmosphere: SI – Tests (Corona ring type 1)	118
7.10	Results under testing conditions: SI – Tests dry (Corona ring type 2)	118
7.11	Results under standard basic reference atmosphere: SI – Tests dry (Corona ring type 2)	118
7.12	Results under testing conditions: SI – Rain Tests (Corona ring type 2)	119
7.13	Results under standard basic reference atmosphere: SI – Rain Tests (Corona ring type 2)	119
7.14	Comparison of gap factors for air gap in case of switching impulse voltage . . .	119